

1960

# Ultimate strength of bolted connections, 1960 Ph.D.

J. L. Rumpf

Follow this and additional works at: <http://preserve.lehigh.edu/engr-civil-environmental-fritz-lab-reports>

---

## Recommended Citation

Rumpf, J. L., "Ultimate strength of bolted connections, 1960 Ph.D." (1960). *Fritz Laboratory Reports*. Paper 1730.  
<http://preserve.lehigh.edu/engr-civil-environmental-fritz-lab-reports/1730>

This Technical Report is brought to you for free and open access by the Civil and Environmental Engineering at Lehigh Preserve. It has been accepted for inclusion in Fritz Laboratory Reports by an authorized administrator of Lehigh Preserve. For more information, please contact [preserve@lehigh.edu](mailto:preserve@lehigh.edu).

271.14

THE ULTIMATE STRENGTH

of

BOLTED CONNECTIONS

by

John L. Rumpf

A DISSERTATION

Presented to the Graduate Faculty

of Lehigh University

in Candidacy for the Degree of

Doctor of Philosophy

Lehigh University

1960

ACKNOWLEDGMENTS

The author is particularly indebted to Dr. Lynn S. Beedle for his encouragement and advice during the preparation of this dissertation. The interest of Professors William J. Eney, Roy J. Leonard, and Samuel L. Gulden, Chairman and members of the Special Committee directing the author's doctoral work, is gratefully acknowledged.

The dissertation covers parts of a research project on "Large Bolted Joints" currently being carried out at the Fritz Engineering Laboratory, Lehigh University. Professor William J. Eney is Director of the Laboratory. The project is sponsored financially by the Pennsylvania Department of Highways and the Bureau of Public Roads. Technical guidance has been provided by a committee of the Research Council for Riveted and Bolted Structural Joints. Special acknowledgment is made of the assistance of the following committee members: Messrs. E. F. Ball, T. R. Higgins, E. J. Ruble, and the late J. Jones.

The large test specimens were fabricated by Bethlehem Steel Company and appreciation is expressed to Messrs: E. F. Ball, K. de Vries, J. J. Higgins, and A. Schwartz for their interest and cooperation.

Preparation of testing setups at the Fritz Laboratory was directed by Mr. S. J. Errera and Mr. K. Harpel. Appreciation is due them and the many technicians working under their direction.

Special gratitude is extended to the author's close associates of the past four years, Research Assistants R. T. Foreman, R. A. Bendigo, and R. M. Hansen, for their interest, enthusiasm and cooperation in prosecuting the work of this project.

This manuscript was typed by Mrs. Rita Tall and drawings were made by Mr. R. Kozo. Their help in the last stage of preparing this dissertation has been invaluable.

TABLE OF CONTENTS

	Page
ABSTRACT	viii
1. INTRODUCTION	1
1.1 The Rise of the High Strength Bolt	1
1.2 Description of the A325 Bolt	4
1.3 Behavior of a Bolted Joint	7
1.4 Design Procedure	18
1.5 Previous Theoretical Studies	21
1.6 Objective of Dissertation	29
2. THEORETICAL SOLUTION	31
2.1 Development of Equilibrium Equation	31
2.2 Development of Compatibility Equations	40
2.3 Calibration Procedures	50
2.4 Solution of Equations	61

3. EXPERIMENTAL WORK	67
3.1 Purpose of Tests	67
3.2 Description of Joints	68
3.3 Instrumentation	71
3.4 Calculation of Hole Offsets	74
3.5 Check on Measurements	76
3.6 Results of Tests	77
3.7 Deformation of Joints	78
4. COMPARISON OF THEORY WITH EXPERIMENTAL WORK	84
4.1 Theoretical Bolt Forces	84
4.2 Predicted Ultimate Strength of Joint	88
4.3 Unbuttoning Factor	92
4.4 Hole Offsets	93
4.5 Distribution of Bolt Forces	94
5. EFFECT OF VARIATION IN TENSION-SHEAR RATIO	97
6. SUMMARY AND CONCLUSIONS	106

7. NOMENCLATURE	112
8. TABLES AND FIGURES	115
Figs. 1.1 to 1.3	116
Figs. 2.1 to 2.25	119
Tables 3.1 to 3.3	142
Figs. 3.1 to 3.13	145
Figs. 4.1 to 4.19	156
Figs. 5.1 to 5.5	175
9. REFERENCES	180
VITA	184



ABSTRACT

In recent years the high strength bolt has become the leading fastener for the field connection of structural steel. Bolted connections are divided into two types: friction and bearing. In the latter type the connection is erected with the bolts in bearing or it is considered harmless if the bolts slip into bearing under load. Design of the bearing type connection is made by using an allowable design stress based on the ultimate strength of short test joints and by making the assumption that each bolt carries an equal share of the load. The assumption is in error for long joints in particular, even though plastic yield of the bolts permits some redistribution.

This dissertation has developed a theoretical solution for the unequal distribution of load among the bolts of a double shear splice under static axial load. Attention has been centered on the region from slip load to the ultimate load in which the bolts and the plates are deforming in a non-linear manner.

Determination of the unknown bolt forces has been accomplished by the solution of an equilibrium equation and a set of compatibility equations. The non-linear relationships of force to deformation have been determined experimentally by tests of representative portions of plate and of single bolts. The solution has been used to predict the ultimate strength of the bolts in "balanced design" connections with  $n = 3$  to 10 bolts in a line.

Validation of the theoretical solution has been obtained through tests of eight full-size connections using  $\frac{7}{8}$  inch bolts and A7 steel plate. Results of these tests verified the predicted ultimate load within 4.5%. Nine other test joints with slightly different properties checked within 10%.

The unequal distribution of load among the bolts has been determined. Results show that the longer the joint the greater will be the force on the end bolts. With the bolts and plate used in this study, the end bolt in a 10-bolt connection carries at failure 133% of the equally distributed load commonly assumed by the structural

designer. In a 3-bolt connection the end bolt carries at failure only 102% of that assumed.

Since bolted connections have been designed with proportions other than those of "balanced design", the effect of tension-shear ratio on load partition has been studied. Results show that a surplus of plate material will reduce plate strains and will result in a more uniform distribution of load among the fasteners.

The results of this dissertation could be used to provide a rational design procedure in which the factor of safety against rupture of the long joint will be the same as that for the short joint.

## 1. INTRODUCTION

### 1.1 The Rise of the High Strength Bolt

In the period 1947 to 1960 the structural high strength bolt has advanced from the experimental stage to its present position in the United States as the leading fastener for the field connection of structural steel. The bolt, known as the A325 bolt, has almost completely replaced the field rivet because of a particular set of circumstances that arose during the post World War II era. Because of depressed conditions during the 30's, restrictive apprentice programs of the iron workers unions, and a turn to welding in many areas of construction during the war years, a shortage of trained riveting crews developed. This shortage was coupled with sharp wage increases granted to iron workers so that the cost of a four-man crew consisting of the driver, buckler, forge man, and the thrower is \$140 per day in direct wages.

Contrasted to this, the high strength bolt is installed by two ordinary iron workers requiring no special

training. One man turns the nut with a pneumatically powered impact wrench while the second prevents the bolt from turning by holding the head. In addition to saving daily labor costs a further savings is realized through bolting because it proceeds more rapidly, requires less scaffolding and less equipment.

In all, the saving in field labor more than offsets the greater initial cost of the bolt itself so that an in-place bolt is slightly cheaper than an in-place rivet.<sup>(1)</sup>

In addition to the direct, obvious savings just noted, further savings are realized by a building owner through the shorter erection time required for a bolted job. These accrue through lower overhead charges, speed-up of the general contractor's work, early completion of the job resulting in a saving in financing costs, and the earlier beginning of manufacturing in the plant.

The impetus behind the rapid adoption of the high strength bolt did not derive altogether from the economies of field erection, however. The design engineer had to be sure that the bolt was at least equal in strength to the

rivet and some of the early tests showed this to be true. In fact, these tests showed the bolt to be superior in ultimate strength, a property that is just now being exploited on the basis of the large scale tests made at Lehigh University<sup>(2)</sup> under the auspices of the Research Council for Riveted and Bolted Structural Joints.

In addition to high static strength, railroad engineers discovered that the bolted joint possessed good fatigue strength; and where rivets failed under the working action of stress reversal, the bolts held tightly. Thus, the railroads were able to produce stronger bridge connections and save thousands of dollars each year in replacement costs for rivets that worked loose.

Now, with the recently adopted 1960 Specifications of the Research Council<sup>(3)</sup> that recognizes the greater strength of the high strength bolt, engineers will be able to design connections that are just as safe as riveted ones but that use fewer bolts. Such a decrease in the number of bolts will result in further savings and assure the competitive position of the bolt as the foremost field method of connecting structural steel members. As a matter of fact,

bolts have even proved economical under certain shop conditions so that shop usage of the high strength bolt will be enhanced, too, by this change.

## 1.2 Description of the A325 Bolt

As noted in the preceding paragraph, the high strength bolt is relatively new to the structural field of bridges and buildings. There are various kinds of high strength bolts in use in the field of machine design so one must be sure to designate the specific properties of the bolt under discussion. In the United States the structural high strength bolt is known as the A325 bolt (Fig. 1.1), where A325 is the designation of the American Society for Testing Materials. <sup>(4)</sup> The specified ultimate tensile strength varies somewhat for different size bolts ranging from 120 ksi for small diameter bolts to 105 ksi for 1 1/8" diameter bolts. These properties are derived from basic SAE 1030 steels by quenching and tempering.

Because a full-size bolt test is the customary acceptance test for the ordinary size structural bolts, the

properties of bolts are generally given in terms of a specified proof load and ultimate tensile load. The proof load is a designated tensile load at which no permanent elongation is permitted. It is in effect a lower boundary for the elastic limit. These values are tabulated below for common size structural bolts:

<u>Bolt Size</u> <u>in.</u>	<u>Proof Load</u> <u>lb.</u>	<u>Ultimate Load</u> <u>lb.</u>
3/4	28,400	40,100
7/8	36,050	53,150
1	47,250	69,700
1 1/8	56,450	80,100

Hereafter, in this paper, use of the word "bolt" will imply an A325 bolt together with the heavy semi-finished hexagonal nut and the two hardened washers that go together to make up the assembly (Fig. 1.1).

The bolt is placed in a hole 1/16 inch larger in diameter than the bolt shank and if all the holes in the connected parts are aligned the amount of rigid body slip that is possible is 1/16 inch. This is true regardless of whether the bolt is placed exactly in the center of the hole or is



touching one side of the hole.

The A325 assembly is tightened by long-handled torque wrenches or pneumatically powered impact wrenches and a tensile force at least equal to the proof load is induced in the bolt. This tensile force serves as a clamping force to hold the pieces of connected material together and to develop a sizeable friction force on the contact surfaces. In this respect the A325 bolt is different from the ordinary "black bolt" used in connecting minor structural members such as purlins and girts. The latter cannot develop much friction because its clamping force is limited by its low yield point.

Since the A325 bolt is replacing the hot driven rivet, it is of value to examine the rivet properties. The ordinary hot driven rivet bears the ASTM designation, A141, and the properties of the bar stock from which the rivet is formed are: <sup>(5)</sup>

Yield Point	28 ksi min.
Ultimate Tensile Strength	52-62 ksi

Driving of the rivet improves these properties from

10 to 20 percent<sup>(6)</sup>, depending upon many factors, but it is quite obvious that the rivet is not as strong as the A325 bolt.

### 1.3 Behavior of a Bolted Joint

Since its introduction into practice, the design of bolted connections has been geared to the idea of the bolt as a replacement for the rivet. Concepts of riveted joint design have been carried over despite certain differences in the behavior of the two types of connections. Tests conducted on large bolted joints<sup>(2,7)</sup> have assisted in evaluating the behavior of the bolted connection. It will be valuable to describe that behavior here so that the reader may understand better the scope of this dissertation.

The load transfer mechanism is not the same during the whole loading history of the bolted joint. It must be thought of in phases. Consider a double shear type of splice with all holes aligned.

a. Phase 1. No Slip

During this phase the plates are compressed laterally by the initial clamping force of the bolts. No relative displacement of any two contact points on the faying surfaces takes place and the bolted joint may be considered equivalent to a solid piece of metal of the same shape. In the latter, load is transferred by shear stresses. The plates of the bolted joint also undergo shear deformations but the tangential force that actually transfers load from plate to plate is friction. This can be visualized with the help of Fig. 1.2a.

As a matter of fact, the bolted joint is probably more similar to the solid piece of material than one would first suspect. According to the most recent work, friction is really shearing resistance. As two pieces of metal are brought together, the high points touch and if the normal force is great enough the mill scale surface is overstressed and forced to flow plastically until bare clean metal comes into molecular contact, and a fusion or weld takes place. In order for relative tangential movement to take place the "weld" must be sheared. The force required is determined by

the dimensions of the junction and while the force necessary to shear any tiny weld is very small, there are many, many of these weld points so that the total force required to shear all of them is in the measurable range.

It is known from elastic studies of welded joints (8,9) that high shear stresses exist near the ends of the joint and this leads one to expect a similar situation for the bolted joint. Recently this was shown to be true in both a theoretical and an experimental investigation made in Germany on bolted joints. (10) Because of the piling up of stress at the ends of the joint, it does not take much applied load to overcome the maximum value of static friction. Phase 1 quickly passes into the second stage of partial slip.

b. Phase 2. Partial Slip

In the second phase there is a relative displacement of certain contact points on the faying surfaces. This relative displacement is called, slip. The first points to move are the end points A and A' (Fig. 1.2b) that move as soon as the tangential force exceeds the maximum

static friction force that can be developed on the end differential length. As load on the connection is increased, the slip zone proceeds inward from the ends toward the center of the joint.

c. Phase 3. Complete Slip - (Major Slip)

Eventually, as load is applied, the slip zones of Phase 2 meet and the maximum value of static friction acts over the entire faying surface of the connection. Then, any small increase of load cannot be balanced by the development of more friction, and the plates accelerate. Large relative displacements occur (Fig. 1.2c).

Even though all holes are perfectly aligned at the time of bolting, it is unreasonable to assume that each bolt occupies the same relative position in the hole; at least one bolt will stand out of position. When the center plate moves with respect to the outer ones it will come into contact with the above bolt and if there is sufficient friction beneath the head and nut of that bolt to make it act rigidly with the outer plates, the slip of the joint will be stopped. At the time this additional

increment of friction is called upon to return the joint to a static condition the plates are moving and the friction acting on the faying surfaces is kinetic friction. Thus it is seen that the single bolt must make up the loss in friction - static to kinetic - in addition to providing friction to offset the load increment.

Under these circumstances it would hardly seem probable that one bolt in a 20-bolt connection could stop the slipping, but one bolt in a 4-bolt connection, or 4 or 5 bolts in the 20-bolt connection, might. When this occurs additional load must be applied to the connection to start it slipping again and then the process is repeated as the plates encounter other bolts. In this second slipping the bolt (or bolts) that stopped the initial slip will be forced to slip with respect to the outer plates, i.e., slip will take place beneath the head and nut of the bolt. Eventually, as more increments of load are applied, the center plate will be in contact with all of the bolts. Finally, the center plate, pulling against the bolts, will cause some of these bolts to come into contact with the lap plates on the opposite side of the bolt shank. This

terminates slip.

The above sequence of slips requiring slight increases of load to produce the various steps has been experienced in tests and might be termed a gradual major slip.<sup>(7)</sup> It seems probable that gradual slip will occur when the plate faying surfaces have a low coefficient of friction, as caused by polishing or painting, whereas the outside surfaces, under the washers, are rougher.

A more likely condition is rough mill scale contact surfaces with paint on the outside surfaces. In this case, because of the release of the high load when the static friction is finally overcome, the plate accelerations are so large that the only thing that can stop the slip is for one plate to encounter bolts which are in bearing on the other plate. This situation might be called a sudden major slip. Tests bear out that it is indeed sudden, violent, and occurs with a resounding noise.

d. Phase 4. Partial Bearing and Redistribution

The preceding phase terminated when at least one bolt contacted both plates. The condition in which the

main plate contacts the bolt on one side and the lap plates contact it on the other side of the shank is known as bearing. Not all of the bolts are pulled into bearing simultaneously. The end bolts are the only ones that are truly in bearing because the end pitch distances have had the greatest differential elongations during the previous phases (Fig. 1.2d). When only some of the fasteners are in bearing the condition is called partial bearing.

Up to this time the only force acting on each bolt has been the tensile force that resulted from the initial tightening. A small amount of this tension may have been lost due to the relaxation of the bolt that occurs as the plate decreases in thickness due to the Poisson effect. Now, for the first time, a bolt is loaded transversely and it tends to shear, to bend, and to compress at points of bearing. In addition the bearing sides of the holes are compressed. The overall flexibility of the bolt, its ability to deform under load, is a function of the hole bearing deformation as well as the deformation of the bolt proper. As load is applied the end bolts and holes deform until the next row of bolts comes into bearing. These in



turn deform and the redistribution process continues until all of the bolts are in bearing. Complete bearing then exists.

For the usual joint, slip will take place before yielding of the net section occurs. Thus the differential pitch elongations that have to be matched by bolt deformations are elastic deformations and fairly small. Not much bolt deformation is required in order to effect complete bearing conditions.

When a sudden major slip occurs, observation of tests seems to indicate that the large impact force causes the bolts to deform almost instantaneously bringing more than the end bolts into bearing. This is particularly true for short joints.

e. Phase 5. Complete Bearing and Continued  
Redistribution

With all bolts in bearing further application of load causes each bolt to deform according to the force carried by each one and in adherence to the laws of equilibrium and compatibility. The deformation of a bolt is

dependent on the difference of the pitch elongations of the lap plate and main plate between any two rows. The deformation in turn dictates the force that the bolt carries. If a portion of one of the plates yields, the difference between the pitch elongations is accentuated and the bolt must deform a greater amount. It is possible that the bolt, in deforming this greater amount, will yield also and therefore the additional force it carries will be small. Since the yielding bolt contributes very little additional force to the job of carrying the applied load other bolts must assume a larger portion. Thus, yielding of bolts produces a redistribution of the total load among the fasteners. A general leveling out of bolt forces occurs as shown diagrammatically in Fig. 1.3. It must be understood that this bar graph represents the redistribution process in a general way only. The actual redistribution in any particular joint depends on the properties of the plate and the bolts, and the relative areas of the same. For example, if the plate material is 100 percent rigid and the bolts are of uniform flexibility, each bolt will deform the same amount and each will carry an equal share of the load.

As the bolts undergo shearing deformation they relax their clamping force so that by the time a bolt approaches its ultimate shearing load practically no clamping force exists. As a consequence, negligible frictional resistance acts in the vicinity of that bolt. Tests have shown that regardless of the initial tightening tensions induced in bolts the ultimate shearing resistances are the same. (11)

f. Phase 6. Bolt Shear and Unbuttoning

Eventually the end pitches have such a large differential elongation that the end bolts cannot accommodate to it and so they fail by excessive deformation. This excessive deformation is primarily a shear detrusion and we call the failure a shear failure. When end bolts shear the load that they formerly carried must be redistributed instantaneously to the remaining bolts. At this time either of two things may happen.

If the distribution of forces on the bolts had been fairly uniform prior to the bolt failure, the additional load thrown on the remaining bolts will be enough

to cause them to fail in rapid succession. To the observer this failure appears to be a simultaneous shearing of all the bolts. Tests have shown this is most likely to occur in short joints. (2)

On the other hand, it has been observed in long joints (7) that the remaining bolts may be capable of assuming the additional load without incurring failure themselves. Then, it is necessary to apply more load to the connection in order to cause further bolt failures. This phenomenon of sequential bolt failures has been dubbed "unbuttoning".

g. Joints Erected in Bearing

There are many connections erected with all the bolts in bearing. This occurs because the dead weight of the connected members forces the bolts into bearing prior to tightening. Under this condition the combined action of friction and shear resistance of the bolts exists from the very beginning of loading. Or, in other words, Phase 5 exists initially.

#### 1.4 Design Procedure

There are two types of bolted connections that concern the design engineer: that in which slip into bearing constitutes failure, and that in which shearing of a bolt (or bolts) is considered as failure. The 1960 Specification of the Research Council designates these as "friction type" and "bearing type" connections, respectively.

A rational design procedure is one that recognizes the true behavior of the structural member. However, such a procedure is sometimes too complicated and time consuming for everyday use. Compromise methods are often developed. Presumably the behavior of the member is understood by those engineers and specification writers who develop such methods and safety is achieved by properly chosen allowable design stresses. The design of the two types of bolted connections fall into the compromise method category.

A rational design procedure for the friction type joint<sup>(12)</sup> would recognize directly such important factors as the coefficient of slip, the initial clamping force, and

the factor of safety. It would make the engineer aware of the importance of contact surface condition and preparation, the advantages of high clamping force, and the lower margin of safety that is considered adequate in friction joint design.

The 1960 Specifications <sup>(3)</sup>, however, call for the design of such a connection by considering the bolts as subject to shear stresses despite the fact that this is not true until Phase 5, Complete Bearing, is encountered. This procedure is clearly a concession to simplicity and to the method of rivet design which is thoroughly ingrained in the minds of structural engineers. The allowable shear stress is set to provide safety under probable conditions of surface preparation and bolt tension.

In the case of the bearing type joint, a rational approach that recognizes the unequal distribution of forces on the bolts would also prove too complicated. The common assumption of riveted design is carried along, namely; each bolt carries an equal share of the load. As noted in Para. 1.3e this amounts to the assumption that the plate material

is 100 percent rigid. Fortunately, tests show that bolts possess a reasonable degree of flexibility in the plastic range and this brings about a redistribution of bolt forces. For short joints, the redistribution is such that the common assumption is not too far off. However, working stresses set on the basis of single bolt shear strength, or even on average shear stress in a short joint, will result in reduced factors of safety if applied to long joints. The 1960 Specifications<sup>(3)</sup> accepts this reduced factor of safety without comment, therefore, the engineer may not be aware of the limitations of the design procedure he is using. This same deficiency exists in the current design practice for rivets.

This may be stated in a different way. The philosophy of riveted design, now carried over to bolts, has been to have a balanced design at ultimate load, i.e., to have the plate and fasteners of equal maximum strength. Working stresses have been decided upon by dividing the stresses at the ultimate load of short test joints by a suitable factor of safety. When such stresses are used for designing long joints, an unbalanced design results.

The bolts will be weaker than the plate.

Fortunately the majority of connections are adequately covered by the design methods used. The exception to this is the unusual type of connection requiring engineering judgment. Here, only the engineer's true understanding of joint behavior will carry him through successfully.

### 1.5 Previous Theoretical Studies

In reviewing the literature on the subject of riveted connections one is impressed with the great number of physical tests made to determine breaking strengths. Yet, despite this extensive work, little is recorded on the behavior of connections under load. Many of these investigations did not study deformation characteristics of the component plates and fasteners nor of the entire joint.

A number of theoretical studies of load distribution have been attempted, but some of these have not been related to experiments. For the most part these theoretical



explanations of joint behavior have dealt with the elastic range of behavior and as a result the conclusions drawn are not indicative of the ultimate strength of the connection. Thus they are not particularly useful in establishing working stresses based on the concept of balanced design at ultimate load.

On searching the literature on high strength bolts, concentrated in the last decade, one discovers only one paper on the subject of theoretical load distribution and that deals with pre-slip conditions and the friction type of connection.

To acquaint the reader with some of the work that has been done on the problem of load partition a brief historical review will be given. Unless otherwise noted these analyses have been made for static axial load applied to the double shear type of plate splice using steel rivets.

In 1909, Arnovlevic<sup>(13)</sup> published what appears to be the first theoretical study of this problem. By considering the joint as a statically indeterminate elastic

structure and relating the plate and rivet deformations, he developed equations which yielded the load carried by each rivet.

In 1916, Batho<sup>(14)</sup>, of McGill University, published in the Journal of the Franklin Institute a solution to the problem in the elastic range using the Method of Least Work. In addition he performed experiments and got remarkable agreement with the theory. His results showed that at working load the end rivets of a 5-in-line joint carried about 35-40% of the total load and the middle rivet carried only about 5%. He also showed that the percentage of load carried by the end rivets is practically constant for 5 or more rivets in line. This means that not much is to be gained in the elastic range by adding rivets in a line because each of these receives a lesser and lesser proportion of the load. Those near the middle are practically idle.

In 1920, Findeisen<sup>(15)</sup>, in Germany, made experiments on the distribution of stress in the cover plates of flat bar butt joints. The connectors were cylindrical,

well-fitting pins. His careful measurements were of use to others.

In 1924, Bleich<sup>(16)</sup> included in his book on steel bridge design a theoretical study of the riveted joint. In it he used certain proportionality factors determined from Findeisen's tests. It is interesting to note that one of the latest text books to emerge from the Continent, that by Stüssi<sup>(17)</sup>, devotes considerable space to load partition under elastic conditions. This emphasis in Europe on elastic conditions probably accounts for the statement that no more than five or six rivets in a line should be used.

Batho, moving to England, participated in the extensive review and extension of structural design practice undertaken by the Steel Structures Research Committee in the period 1929 to 1936. In the reports of this Committee<sup>(9)</sup> he republished his original work along with further experimental data. In these same reports he also published the initial investigations on the use of high strength bolts. However, it remained for American engineers to bring about

the use of these bolts following World War II.

In 1934, Hrennikoff<sup>(18)</sup> wrote in the Transactions of the American Society of Civil Engineers on the subject "Work of Rivets in Riveted Joints". This, too, was a theoretical elastic analysis. Being the most readily available English language paper on the subject, it is familiar to many American engineers. The many discussions it invited serve to cover the then existing literature on the subject.

About this time aeronautical engineers became interested in the problem of riveted joints. However, their studies, being made on light gage material with small diameter rivets, are not readily applicable to heavier structural steel splices. A paper by Vogt<sup>(19)</sup>, in 1944, is singled out because, after developing equations for linear conditions, he proposes a modification to cover loads above the limit of proportionality. But, this is restricted because it deals only with non-linear deformations of the bolts and the holes and not of the sections of the plates between the holes. This is not the case in balanced design structural steel joints in the region of ultimate load.

Before passing to a review of studies made in the post World War II era, it is appropriate to mention one of the excellent bibliographies compiled in the field of engineering. In 1945, DeJonge<sup>(20)</sup> published "Riveted Joints: A Critical Review of the Literature Covering Their Development". This book reviews approximately 1200 items on the subject written between the years 1837 to 1945 and as such is an invaluable aid to the research worker in the field.

Following World War II, as the use of aluminum alloys for heavy civil engineering structures was increased, it became apparent that information was needed on aluminum riveted joints using rivets of structural size. The Aluminium Development Association in England undertook an extensive study which culminated in an excellent treatise by Francis<sup>(21)</sup> in 1953. This paper presented theoretical solutions for the elastic and inelastic range, and experiments were made on joints of aluminum plate connected with aluminum or steel rivets. The load carried by each rivet was checked by measuring the tilt of the rivet head as the rivet deformed. Eccentrically loaded joints were considered also. Though dealing with aluminum, this paper has been of

great assistance to the writer in preparing this dissertation.

In 1952, the first specification for assembly of structural joints using high strength bolts was issued by the Research Council for Riveted and Bolted Structural Joints. Design was on the basis of "substitute one bolt for one rivet" and American research was devoted to practical matters of surface preparation, how to tighten bolts, and performance under fatigue loading. (22, 23, 24) No theoretical studies were made of the load partition problem and limited experimental studies (22, 25) made use of SR-4 gages and were therefore restricted to elastic conditions.

In Germany a stronger high strength bolt is used and special surface preparation is made in order to develop high friction forces. In 1955, K. Dörnen (26) wrote a doctoral dissertation on the subject of transfer of load by friction prior to major slip. This dissertation is not readily available and information on it is obtained in a second-hand fashion from the writings of Steinhardt and

Mohler<sup>(10)</sup> of the Karlsruhe Technische Hochschule where the German research in the field is going on.

From the foregoing literature review it is seen that most of the theoretical studies of the problem of partition of load in riveted joints have concentrated on elastic conditions. The main study in the inelastic range concerned aluminum. With the high strength bolt the major work has concentrated on the friction type joint. The topic of the ultimate strength of steel joints connected with bolts has not been studied previously on a theoretical basis.

## 1.6 Objective of Dissertation

The preceding sections have acquainted the reader with the rising importance of the A325 bolt, its properties, and the general behavior of the bolted joint. It was pointed out that present design procedures, though adequate for a majority of cases, are not completely rational and therefore can lead to trouble in some unusual connections such as long ones. It would be desirable to have a theoretical solution for the behavior of bolted joints in order to predict the ultimate strength of long joints in a rational manner. Such a solution would permit the design of a truly balanced joint, one in which the ultimate strength of the bolts equaled that of the plate being connected. It could also show the influence of certain joint proportions on the behavior of the bolts.

Study of the literature showed that this solution is not available, almost all theoretical solutions having been for elastic conditions which do not prevail at ultimate load. The one solution in the inelastic range was for aluminum connections.



This paper will attempt a theoretical analysis of the bearing type bolted connection in the region from slip load up to the maximum load. The double shear type of splice under static axial loads will be considered. The distribution of load among the various bolts and a prediction of the ultimate strength of the connection will be sought. Correlation of the theoretical values with experiment will serve as a check on the validity of the theoretical solution. The influence of the tension-shear ratio on load distribution will be studied.

Item #64

Reference

Receipt

## 2. THEORETICAL SOLUTION

### 2.1 Development of Equilibrium Equation

#### a. Geometry of Joint

The bolted joint to be analyzed is a double shear, plate splice loaded axially (Fig. 2.1). The inner plate, also referred to as the main plate, represents the member being spliced. It has a thickness  $t_1$ . The outer plates are the connecting material, are known as the lap plates, and have thicknesses  $t_0$ . It is not necessary for  $t_0$  to equal  $1/2 t_1$ .

Because all load must be transferred out of the main plate and into the lap plates before reaching the gap XX, the connection is really that portion shown to the left of XX. A similar connection to the right must transfer the load from the lap plates back into the main plate.

A longitudinal line of holes parallel to the axial load is called a line. A transverse series of holes is called a row. The transverse space between any two lines

is the gage,  $g$ . The gage distances need not be equal but they must be symmetrical about the longitudinal centerline in order to avoid eccentricity of the axial load. The longitudinal space between any two rows is the pitch,  $p$ . In practice these will usually be made equal but they need not be insofar as this analysis is concerned. Rows are numbered 1 to  $n$  beginning at the free end of the lap plate and a pitch between any two rows is indicated by subscripts of those row numbers.

It is assumed that the hole pattern is complete, i.e., a hole is located at each intersection of a line and a row. The holes are perfectly aligned through the plies of plate and the hole diameter,  $d_H$ , exceeds the bolt diameter,  $d_B$ , by an amount  $c$ , the hole clearance. The hole clearance is  $1/16$ " in the usual structural connection.

For purposes of analysis it is assumed that the joint may be divided longitudinally into gage strips (Fig. 2.2) and that the sum of the gage strip loads,  $P_G$ , equals the total joint load,  $P_J$ . Therefore, the development which follows will be concerned with the carrying

capacity of a gage strip.

b. Condition of Assembly

The ultimate load of the bearing type connection is to be predicted, and attention will be centered on the region above the slip load where complete bearing exists. It will be assumed that joint behavior in this range is independent of the time when slip occurs. Such a stipulation permits the inclusion of joints erected in bearing, that is, preslipped. The latter joint offers advantages to a theoretical analysis since it has a continuity of behavior not possessed by the joint which slips. From the beginning of loading it transmits load by shear and by friction. The joint with aligned holes first transmits load by friction alone and only after it slips into complete bearing does it transfer load by shear and friction. The nature of this assumption can be shown schematically with a load vs. overall elongation curve (Fig. 2.3). The following work will be developed for the joint erected in bearing and assumed to be correct for the slip joint in the region indicated by the bold line.

c. Manner of Load Transfer

In normal circumstances most of the load carried by friction is transferred in discrete zones surrounding the bolts. The area of these zones depends upon how the clamping force of the bolt is transmitted through the outer plates. Figure 2.4 shows several assumptions that can be made.

In Fig. 2.4a a cylinder of clamping pressure is shown extending through the plies of plate. The friction at the contact surfaces is distributed over the area of a ring whose outside diameter is the distance across the flats of the bolt head (1.3 inches for a 7/8" bolt) and whose inside diameter is equal to the hole size. Such an assumption indicates a minimum zone of friction and is probably most valid when the lap plates are thin.

In Fig. 2.4b a truncated cone of clamping pressure is indicated. The diameter of the truncated top is equal to the distance across the flats of the bolt head and then the cone flairs out until the diameter at the contact surface has increased by  $2 \tan \alpha (t_w + t_o)$ , where  $\alpha$  is the

pressure angle,  $t_w$  is the thickness of washer, and  $t_o$  is the thickness of the lap plate. For a 7/8" bolt,  $\alpha = 60^\circ$ ,  $t_w = 1/8"$  and  $t_o = 1"$ , the outside diameter of the friction zone at the contact surface is 2.60 inches and the inside diameter is 0.94".

If the friction forces are uniformly distributed over the friction zone the resultant friction force acts at the center of the bolt. As the bolt bends it is possible that the resultant pressure force may be shifted from the center of the bolt thus shifting the zone of friction and the location of the resultant friction force. However, as the bolt deforms it loses clamping force so the shift of the zone of friction is considered of little importance in the ultimate load range. It will be assumed that the resultant friction force acts at the center of each bolt for all values of applied load.

The transfer of load by the bolts themselves is of a different nature. A bolt picks up load through bearing on the plate. It transfers that load across the plane of contact by virtue of the shearing resistance of the bolt

shank. Then it unloads onto the other plate by bearing.

Figure 2.5 shows various bearing stress conditions that exist and the usual design assumption regarding the distribution of bearing pressure. In the plan view it will be assumed that the resultant force against the side of the hole acts at the point of contact of an undeformed bolt and hole. Under no circumstance can load transfer by bearing be considered to act at the center of the bolt.

d. Load Distribution

On the basis of the manner of load transfer discussed in the previous paragraph, it is possible to construct a load transfer diagram in a general way. Such a diagram for a joint with the lap plate thickness equal to one-half of the main plate thickness is shown in Fig. 2.6. Such a connection is symmetrical about the middle row of bolts.

The notation for forces in a gage strip is as follows:

$R_j$  = the force transmitted by Bolt  $j$

$P_{jk}$  = the force in the main plate between rows  $j$  and  $k$



$Q_{kj}$  = the force in two lap plates between rows j and k.

The subscript notation for the pitches between bolt rows is always written in ascending order for the main plate and descending order for the lap plates.

In the load transfer diagram, any horizontal position is a projection from a location in the joint above. The ordinate is in force units and the total height of the diagram equals the load applied to the gage strip,  $P_G$ . The steps descending toward the right represent the force in the main plate whereas the partial steps descending to the left represent the force in the lap plates. The latter is not drawn completely because it is opposite hand to the diagram for the main plate.

The total step at any bolt is equal to the force transferred out of the main plate by that bolt. The sloping portion indicates the force transferred by friction and the vertical drop indicates the force transferred by bearing and shear.

The height of any step above the datum level

represents the force in the main plate in that pitch, for example,  $P_{23}$ .

The diagram of Fig. 2.6 may be idealized as shown in Fig. 2.7a if it is assumed that the total friction transfer of a bolt is also concentrated at the bearing point. At the higher loads under investigation this is a valid simplification because the frictional transfer becomes a small part of the total when the bolt tension relaxes due to shear deformation.

Below the idealized force transfer diagram, in Fig. 2.7b, the main and lap plates are shown with zones marked in which the various forces act.

e. Equilibrium Conditions

Considering either the main plate or the lap plates as a free body (Fig. 2.8) the equilibrium equation, for forces in the horizontal direction, can be written as follows:

$$\sum F_H = P_G - R_1 - R_2 \dots - R_n = 0 \quad (2.1)$$

In this equation  $R_1$  to  $R_n$  inclusive are unknown forces.

To solve for these forces,  $n - 1$  additional independent equations are needed. These will come from deformation conditions.

By cutting free bodies through the main plate at any section the force in the main plate can be written in terms of the applied load and the unknown bolt forces.

$$\left. \begin{aligned}
 P_{12} &= P_G - (R_1) \\
 P_{23} &= P_G - (R_1 + R_2) \\
 &\vdots \\
 &\vdots \\
 P_{mn} &= P_G - (R_1 + R_2 \dots + R_m)
 \end{aligned} \right\} (2.2)$$

By cutting free bodies through the lap plate the forces in the lap plates can be written:

$$\left. \begin{aligned}
 Q_{21} &= P_G - P_{12} = R_1 \\
 Q_{32} &= P_G - P_{23} = R_1 + R_2 \\
 &\vdots \\
 &\vdots \\
 Q_{nm} &= P_G - P_{mn} = R_1 + R_2 \dots + R_m
 \end{aligned} \right\} (2.3)$$

## 2.2 Development of Compatibility Equations

### a. Plate Reference Points

In order to help develop the n-1 deformation equations that are needed to produce a solution for the unknown bolt forces, certain reference points will be set up. The plate reference points are shown in Fig. 2.9a as solid dots. These points are on the edges of a gage strip on the centerline of each aligned hole. In the experimental work to be described later these points were marked by small centerdrill holes. The main plate of the test joints consisted of two plates hence the use of two reference points as shown here. Of course, in a multiple gage joint it is possible to centerdrill on the edges of the joint only.

When the inner and outer plates move with respect to one another the hole reference points are offset by an amount called the hole offset,  $\Delta$ . If a connection is assembled in bearing and is under no applied load the hole offset at each row is the same and equals  $c$ , the hole clearance (Fig. 2.9b). As the plates strain under applied

load the various pitches elongate different amounts and then the hole offsets are no longer equal (Fig. 2.9c).

b. Bolt Reference Points

The hole offsets,  $\Delta$ , do not indicate properly the deformation of the bolts. It is obvious from the cut away portion of Fig. 2.9b that  $\Delta = c$  whereas the bolt deformation is zero. This disparity is even more marked when the joint is under load because of the hole deformations which take place. It is excessive bolt deformation which causes a bolt to fail but it is the hole offset which is visible and can be observed during a test.

Reference points on the bolt will be chosen in a manner similar to that for the plates. Thus, four points are chosen on the centerline of the bolt and at mid thickness of each of the plies of gripped material (Fig. 2.10a). These points are imaginary, that is, they are not actually marked on the bolt during a test. A small cross will be used to designate bolt reference points in order to distinguish them from plate reference points represented by a dot.

As the bolt deforms under load it takes on a shape

due to shearing and bending (Fig. 2.10b). The bent shape is permitted by the non-uniform bearing deformation of the hole (Fig. 2.5). Measurements of bolts after test indicate that the bearing deformations of the A325 bolts themselves are negligible in A7 steel joints.

Figure 2.10b shows that the offset of the bolt reference points,  $\delta_B$ , is slightly less than the maximum deflection of the bolt. The difference consists of the deflection of the outer reference point with respect to the vertical line through X, plus the deflection of the inner reference points with respect to the vertical line through Y.

The bolt deformation may be idealized. This is done in Fig. 2.10c where a bolt subject to shear detrusion only is shown with a bolt offset,  $\delta_B$ , equal to the maximum deflection of the actual bolt. The bearing deformation of the hole would be uniform.

c. Relation of Plate and Bolt Offsets

The plate and bolt offsets may be related to one another as described below. Figure 2.11 shows the first

bolt in a joint, but the relationship to be determined is general and applies to any row.

Consider the hole in the inner plate and the idealized portion of bolt within it. The distance between the plate reference points and the bolt reference points will be evaluated. If the bolt is centered in the hole initially it must slip to the right a distance  $\frac{c}{2}$  before it comes to bear against the side of the hole. When the bolt bears against the side of the hole it compresses the steel there an amount  $\rho_{il}$ . Assuming that the bearing deformation of the bolt itself is negligible the bolt reference points move  $\rho_{il}$  to the right also. Meanwhile, the inner plate under tensile loading is stretching, and the circular hole changes to an oval one with its major axis in the direction of the load. Thus the bolt is able to move to the right an amount  $\lambda_{il}$ , the elongation of the radius of the hole. Adding together these three items the distance between the plate and bolt reference points is obtained as  $\frac{1}{2} c + \rho_{il} + \lambda_{il}$ .

Following the same reasoning a similar expression is obtained for the lap plates. It should be noted that the

hole elongation in the lap plate,  $\lambda_{o1}$ , is not equal to that in the main plate,  $\lambda_{i1}$ , because these are functions of different tensile forces acting in each of the plates. The bearing deformation in the outer plate,  $\rho_{o1}$ , is assumed to equal that in the inner plate,  $\rho_{i1}$ , if the combined lap plate thickness equals the main plate thickness. Another tacit assumption is that the bearing deformation is independent of the magnitude of tensile stress in the plate.

The relationship between the hole offset  $\Delta_1$  and the bolt offset  $\delta_{B1}$  can now be read from Fig. 2.10 as follows:

$$\Delta_1 = \delta_{B1} + \left(\frac{c}{2} + \rho_{i1} + \lambda_{i1}\right) + \left(\frac{c}{2} + \rho_{o1} + \lambda_{o1}\right)$$

$$\Delta_1 = c + (\delta_{B1} + \rho_{i1} + \rho_{o1}) + \lambda_{i1} + \lambda_{o1} \quad (2.4)$$

It will be shown later (Para. 2.3a) that the quantity in parenthesis in Eq. 2.4 is the same as the quantity measured in the shear calibration procedure for single bolts. This will be called the "calibration bolt offset" and designated



simply as  $\delta$ . Thus,

$$\left. \begin{aligned} \Delta_1 &= c + \delta_1 + \lambda_{i1} + \lambda_{o1} \\ \Delta_2 &= c + \delta_2 + \lambda_{i2} + \lambda_{o2} \\ &\vdots \\ \Delta_n &= c + \delta_n + \lambda_{in} + \lambda_{on} \end{aligned} \right\} (2.5)$$

d. Compatibility Equations

The deformations of the bolts and the elongation of the plates in the various pitches must be compatible with one another. The compatibility equations are developed with the help of Fig. 2.12 that shows the edge view of a joint and the plate reference points.

The original location of the aligned holes is indicated by the row numbers at the top of the sketch. The location of these same holes when the joint is loaded is indicated by the hole reference points (solid dots). The elongation of the pitch between any two rows of holes is denoted by the letter  $e$  with subscripts corresponding to the row numbers. The subscripts are in ascending order

for main plate elongations and in descending order for lap plate elongations.

An equation can be determined for each of the  $n - 1$  pitches by equating dimensions along the upper and lower dimension lines. Thus,

$$\Delta_1 + p_{12} + e_{21} = p_{12} + e_{12} + \Delta_2$$

The pitch dimensions may be cancelled and there results the following set of equations:

$$\left. \begin{aligned} \Delta_1 + e_{21} &= e_{12} + \Delta_2 \\ \Delta_2 + e_{32} &= e_{23} + \Delta_3 \\ \vdots & \\ \Delta_m + e_{nm} &= e_{mn} + \Delta_n \end{aligned} \right\} (2.6)$$

Substitution of Eq. 2.5 in Eq. 2.6 gives for the first of the series of equations,

$$c + \delta_1 + \lambda_{i1} + \lambda_{o1} + e_{21} = e_{12} + c + \delta_2 + \lambda_{i2} + \lambda_{o2}$$

Grouping lap and main plate deformations,

$$\delta_1 + \lambda_{o1} + e_{21} - \lambda_{o2} = \delta_2 + \lambda_{i2} + e_{12} - \lambda_{i1} \quad (2.7)$$

This expression can be simplified by observing on Fig. 2.13 that the plate elongation  $e_{12}$  is a function of two loads. The elongation in region a is a function of  $P_G$  whereas the elongation in region b is a function of  $P_{12}$  (Fig. 2.7b). The elongation of region a has been defined previously (Para. 2.2c) as  $\lambda_{i1}$ . Thus, this elongation cancels the term  $(-\lambda_{i1})$  in Eq. 2.7.

The term  $\lambda_{i2}$  of Eq. 2.7 is the elongation in region c, and it is a function of  $P_{12}$ . Because it is a function of the same load it can be added to the elongation of region b. The resulting term will be called  $e'_{12}$ , the elongation in the inner plate from the bearing side of hole 1 to the bearing side of hole 2.

In a similar fashion it can be shown that the last three terms on the left side of Eq. 2.7 equal the elongation of the outer plate from the bearing side of hole 2 to the bearing side of hole 1. This elongation,  $e'_{21}$ , is a

function of the force  $Q_{21}$ .

Thus Eqs. (2.6) become

$$\left. \begin{aligned} \delta_1 + e'_{21} &= e'_{12} + \delta_2 \\ \delta_2 + e'_{32} &= e'_{23} + \delta_3 \\ &\vdots \\ \delta_m + e'_{nm} &= e'_{mn} + \delta_n \end{aligned} \right\} (2.8)$$

Equations 2.8 are the  $n - 1$  compatibility equations that are needed. They are preferred to Eqs. 2.6 because they are in terms of the bolt offset that is directly related to bolt failure, and because the elongations  $e'$  are functions of constant forces.

To obtain a solution for the unknown bolt forces,  $R$ , these equations must be solved in conjunction with the equilibrium condition, Eq. 2.1. The latter is already in terms of the unknown  $R$ 's but the deformations in the compatibility equations must be expressed in terms of  $R$  before the solution can be obtained.

The scope of this dissertation extends the analysis

into the inelastic range of the bolts and plates. The force-deformation relationship will not be linear so deformation will be expressed as a function of force using the following notation:

$$\begin{aligned} f[ ] &= \text{bolt deformation} \\ \varphi[ ] &= \text{main plate elongation} \\ \psi[ ] &= \text{lap plate elongation} \end{aligned}$$

The compatibility equations (Eqs. 2.8) may now be written.

$$\left. \begin{aligned} f[R_1] + \psi[Q_{21}] &= \varphi[P_{12}] + f[R_2] \\ f[R_3] + \psi[Q_{32}] &= \varphi[P_{23}] + f[R_3] \\ \vdots & \\ f[R_m] + \psi[Q_{nm}] &= \varphi[P_{mn}] + f[R_n] \end{aligned} \right\} (2.9)$$

Substituting Eqs. 2.2 and 2.3 these are finally expressed as functions of the unknown bolt forces.

$$\left. \begin{aligned} f[R_1] + \psi[R_1] &= \varphi[P_G^-(R_1)] + f[R_2] \\ f[R_2] + \psi[R_1 + R_2] &= \varphi[P_G^-(R_1 + R_2)] + f[R_3] \\ \vdots & \\ f[R_m] + \psi[R_1 + R_2 + \dots + R_m] &= \varphi[P_G^-(R_1 + R_2 + \dots + R_m)] + f[R_n] \end{aligned} \right\} (2.10)$$

### 2.3 Calibration Procedures

In the foregoing section the deformation compatibility equations were written in terms of the bolt forces. This was done in a general way, that is, bolt and plate deformations were written as functions of force. However, to actually solve these equations the true nature of these relationships must be known. In general the proportionality of deformation to force is not constant and must be found by experiment through calibration tests.

Two calibration tests are needed to obtain data for solving Eqs. 2.1 and 2.10 for the unknown bolt forces, namely,

- (1) bolt shear calibration:  $\delta = f[R]$
- (2) plate calibration:  $e' = \phi[R]$  or  $\psi[R]$

A third calibration test to determine how a hole elongates ( $\lambda$ ) is needed to calculate hole offsets  $\Delta$  according to Eq. 2.5.

a. Bolt Shear Calibration

The purpose of bolt shear calibration is to relate the deformations of a single bolt to known values of applied load. As shown in Eq. 2.4 it is convenient to lump together the bolt offset and the bearing deformations of the inner and outer plates into a quantity called the "calibration bolt offset",  $\delta$ . In practice these three quantities always occur together and there is no reason to separate them for purposes of this analysis. Thus, the problem is to determine how  $\delta$  varies with applied shearing load.

In order that this relationship be indicative of bolt behavior in the large bolted joint, a number of controls are necessary. For example, the bolt to be calibrated must not only be one of the same dimensions as those used in the prototype joint but it should be of the same lot, that is, same basic properties and heat treatment. A fairly large variation in strength is permitted under A325 specifications and use of a bolt of a different lot can lead to erroneous predictions of the ultimate strength of the joint.

The single hole connection used to shear the bolt is called a shear jig. It must be made of a material comparable to that employed in the prototype joint in order that the bearing deformations will be similar. Also, the contact surfaces must be similar in roughness in order to duplicate friction performance.

Two types of shear jigs could be used. One causes double shear of the bolt by applying a tensile load, the other by applying a compressive load. It would seem at first that the tension type should be used because the shearing of the bolt in the prototype joint is caused by a tensile load. However, in the tensile shear jig the hole in the plate elongates and methods of measuring the calibration bolt offset always include the quantities  $\lambda$ . Looking at Eq. 2.5 one might say this is desirable because  $\lambda$ 's appear there. Unfortunately, in the expression for  $\Delta_1$ ,  $\delta_1$  and  $\lambda_{o1}$  are functions of the force  $R_1$  but  $\lambda_{i1}$  is a function of  $P_G$  (Fig. 2.7b). In the tensile shear jig  $\delta$  and both  $\lambda$ 's are functions of the same load.

The compression type shear jig doesn't present the



problem of hole elongation. In addition it is easier to fabricate and to instrument. The type jig used for this study is illustrated in Fig. 2.14. The test details are given in Ref. 27.

The plates were cut from scrap pieces of A7 steel left over from the fabrication of the prototype test joints described in Chapter 3. A D-Lot bolt was inserted in the hole, the jig plates pushed into bearing and the bolt tightened to a tension comparable to that used in the test joints. The jig was loaded slowly in a testing machine and the load, consisting of friction and shear resistance, was measured by the weighing system of the testing machine. The relative movement of the fixed and moving heads of the testing machine was measured by a dial gage. It remains to show that this measurement is the "calibration bolt offset".

To show this, recourse is made to Fig. 2.15. In Fig. 2.15a the plates of the shear jig are assumed infinitely rigid. Under load the bolt undergoes an idealized shear detrusion as in Fig. 2.10 where  $\delta_B$  equals the

maximum deflection of the bolt. This movement is recorded by the dial gage when the testing machine heads move together that amount.

In Fig. 2.15b, under the same load, it is assumed that the plate loses its rigidity in a zone around the hole. The outer plates move up an amount equal to the bearing deformation of the outer plate,  $\rho_o$ , and the inner plate moves down,  $\rho_i$ . The dial gage between the testing machine heads records both of these movements.

Finally, it is assumed that the remaining portions of the plates become elastic and compression takes place in the outer plates below the bolt and in the inner plate above it (Fig. 2.15c). The dial gage records this. However, it can be shown by calculation that the sum of these two compressions is only 1 to 2 percent of the total deformation indicated by the dial gage reading. This can be neglected and the dial gage measuring the relative movement of the cross heads gives,

$$\delta = \delta_B + \rho_o + \rho_i$$

previously defined as the "calibration bolt offset".

The average of results of bolt shear calibration for D-Lot bolts<sup>(27)</sup> is plotted in Fig. 2.16. This curve provides the relationship between the bolt offset and load.

In this study the calibration curve for all bolts in a connection is assumed to be the same. Within the variations of any particular lot of bolts this is true except for the bolts at the free end of the lap plates. These bolts are permitted to bend a little more than others because the lap plates, which provide end fixation for the bolts, are freer to rotate at this region (Fig. 2.10b).

b. Plate Calibration

The purpose of plate calibration is to relate the elongation of certain portions of a gage strip to a known tensile load. This requires isolation of a portion of the gage strip so that its elongation can be measured while it is being loaded by a testing machine whose weighing system records the load.

Equation 2.8 shows that the elongation needed is

that denoted by  $e'$ , the elongation of a pitch from the edge of one hole to the corresponding edge of the next hole. Because the same force acts at every cross section of the calibration plate the elongation from center to center of hole also equals  $e'$ .

The plate calibration specimen should be cut from the same type and quality of material as that used in the prototype connection. It must be of the same thickness and have holes of the same size as the prototype. If the assumption is made that the behavior of one gage strip is not affected by the existence and behavior of adjacent strips the plate calibration specimen may be as shown in Fig. 2.17a.

Use of such a calibration specimen to represent an interior gage strip in a joint may be in error because the interior strip is restrained from necking by the adjacent material whereas the calibration plate has free edges. The same reasoning may apply to the edge gage strip of a multiple gage joint. For this reason a calibration specimen as shown in Fig. 2.17b was investigated.

The total width of this plate presents a difficulty in testing because it will fit in only the larger size testing machines. Also, it must be assumed that the portion of the total load carried by each strip is in proportion to the gage strip width.

A brief study of this problem was undertaken and the results (Fig. 2.17c) show that there is no systematic difference among three types of calibration plates.

In a connection the plate is clamped by bolts. The clamping action by itself probably increases the longitudinal strains in the vicinity of the holes at least in the early stages of loading. This can be visualized with the aid of Fig. 2.18a. As load is increased  $\sigma_y$  decreases because the plate strain in the y direction permits the bolt to relax and because inelastic shearing of the bolt also causes relaxation of the clamping force.

Because of friction acting on the contact surfaces between the washers and lap plates, the washers act as integral parts of the outer plates. The washer reinforces the plate in the area around the hole and serves as a

stress by-pass permitting stress to flow out of and then back into the plate beyond the hole (Fig. 2.18b). Therefore, the net section area of the lap plate carries less stress and longitudinal deformations in the vicinity of the hole are reduced.<sup>(28)</sup> However, as the bolt clamping force decreases this stress by-pass becomes ineffective and all the load must be carried by the plate.

The inner plate presents a different situation. Although clamped by the bolt tension transmitted through the outer plates, the inner plate is not flanked by inert washers, but rather by stressed outer plates. No reinforcement of the inner plate can occur so it acts more like a plain perforated plate.

In order to investigate the effect of clamping, several exploratory tests were conducted on calibration plates with bolts in the holes. The bolts were tightened to simulate initial conditions in the prototype joint but since these bolts were not subject to shearing no loss of clamping could occur because of shear detrusion.

These test specimens are shown in Fig. 2.19a and

the results are plotted in Fig. 2.19b. The curve for PC 1-c shows the bolted plate to be stiffer than the plain plate PC 1-a. However, the specimen PC 1-c is not representative of conditions in a joint. The plates used to provide the proper grip for the bolts furnish an effective stress by-pass at all times. Being large and rigid they span the region where necking of the calibration plate occurs and thus prevent relaxation of the bolt. Examination of the other test results shows that there is a small difference between a plain calibration plate and one which is bolted.

Exploratory tests have indicated that the single gage and multiple gage calibration specimens yield approximately the same results and that bolt clamping has only a small effect. Furthermore, it is known that the strength of steel plate will vary across the rolled width. These calibration plates were cut from various locations in a 24 inch wide plate and so were subject to that variation in strength. In view of these facts it was decided to use the plain plate calibration specimen for this work.

The dimensions of the plate calibration specimens are tabulated in Fig. 2.20. Because the main plate of the prototype test joints was composed of two one-inch plates it was possible to calibrate a one inch plate and then double the load to give  $P_G$ , the load on a two inch thick gage strip. If the main plate had been one two-inch piece this would not have been permissible. A separate test would have been required for the main plate and the lap plate. The results are plotted in Fig. 2.21. The heavy dash lines at the .4 abscissa indicate the ultimate strength of the plate calibration specimen obtained by multiplying the coupon stress by the net area of the plate. For future reference the bolt shear calibration curve is plotted to the same scale.

c. Hole Calibration

During the plate calibration tests the elongation of the holes was measured using inside calipers and a .001" micrometer. If it is assumed that the holes elongate in a symmetrical fashion the elongation  $\lambda$  can be found as one half of the difference between the original hole diameter and the long axis of the elongated hole. Results are plotted in Fig. 2.22.



## 2.4 Solution of Equations

### a. Description of Procedure

Having obtained the bolt shear and plate calibration curves, the solution of the equilibrium and compatibility equations can be made. Inspection of the first of Eqs. 2.10 shows that three of the four terms are functions of the unknown  $R_1$  alone. If  $R_1$  becomes known, or is assumed, that equation can be solved for  $R_2$ . Once  $R_2$  is known the second equation becomes solvable for  $R_3$ . In a similar way the remaining equations may be solved for the other unknown bolt forces. All these values are predicated on the originally assumed value of  $R_1$ . To check these values  $R_1$  to  $R_n$  inclusive must be substituted in the equilibrium equation to see if they sum to  $P_G$ , the load on the joint. If they do not, a new value of  $R_1$  must be assumed and the procedure repeated.

According to this procedure one chooses  $R_1$ , enters the bolt shear calibration curve ( $\delta = f[R]$ ) with that value, and reads off  $\delta_1$  (Fig. 2.23). The lap plate calibration curve ( $e' = \psi[R]$ ) gives the value of  $e'_{21}$

corresponding to  $R_1$ . If the main plate calibration is entered with  $P_G - R_1$  as an argument the value of  $e'_{12}$  may be read. Knowing these three terms in the equations, the fourth term may be computed. This fourth term is  $\delta_2$  and the value of  $R_2$  corresponding to it can be read from the bolt shear calibration curve. This procedure must be carried out for each equation and then the equilibrium check made. Obviously such a procedure, though workable, would be very time consuming.

A graphical procedure, due to Brock<sup>(21)</sup> does essentially the same thing but makes it possible to see how convergence to the correct answer is taking place. With a little experience an acceptable answer can be reached in several trials. Solutions for two cases will illustrate the method.

b. Illustration of Graphical Procedure

When the combined thickness of the lap plates is not equal to the thickness of the main plate the load carried by each bolt is different. No advantage of symmetry can be taken. To illustrate the graphical solution

a five-bolt connection with  $t_o < \frac{1}{2} t_i$  will be considered. The plate and bolt shear calibration curves for the material of this connection are shown in Fig. 2.23. These are fictitious curves chosen so that the graphical solution is possible within the scale set by page size. The problem is to find  $R_1$  to  $R_5$  inclusive when the load on the gage strip is  $P_G$ . The steps in the solution are as follows: (Refer to Fig. 2.24)

- (1) Plot lap plate calibration curve, L, and bolt shear calibration curve, B, to the same scales on the same sheet of graph paper.
- (2) Plot the main plate calibration curve, M, to the same scales then trace it on a piece of transparent paper.
- (3) Turn the transparent paper over, thus inverting the main plate calibration curve. Set the origin of this curve, M, at the ordinate  $P_G$  on the other curves L and B.
- (4) Assume a value of  $R_1$ . Draw a horizontal

line at that ordinate and from its intersection with B project downward to  $\delta_1$ .

- (5) On the horizontal line at ordinate  $R_1$  lay off  $\delta_1$  to the right of  $e'_{21}$ , where  $e'_{21}$  is the lap plate elongation due to  $R_1$ .
- (6) The ordinate  $R_1$  is also the inverted ordinate  $(P_G - R_1)$  for M and so  $e'_{12}$  is known. From Eq. 2.8 the remaining portion of the horizontal line at ordinate  $R_1$  is the bolt offset  $\delta_2$ . Thus, the dimensions above and below the horizontal line at  $R_1$  clearly represent the compatibility condition (Eq. 2.8).
- (7) Lay off  $\delta_2$  on x-axis and read  $R_2$  from B.
- (8) Add  $R_1$  and  $R_2$  and draw a horizontal line at that ordinate.
- (9) At the ordinate  $R_1 + R_2$  read  $e'_{32}$  from L, lay off  $\delta_2$ , read  $e'_{23}$  from M and then determine  $\delta_3$ .

- (10) Repeat the last three steps until  $R_5$  is known.
- (11) Lay off the ordinate  $R_1 + R_2 + R_3 + R_4 + R_5$ . The difference between it and the ordinate  $P_G$  is the error in the equilibrium check (Eq. 2.1).
- (12) Assume a new value for  $R_1$  and repeat the procedure until the error is zero or is considered negligible.
- (13) To find the bolt forces due to another load  $P_G$  slide the tracing paper so the origin of the inverted curve,  $M$ , coincides with the new  $P_G$ .

If the thickness of one lap plate equals one-half the thickness of the main plate ( $t_o = \frac{1}{2} t_i$ ) the solution is expedited by the use of symmetry. For example, in the five-bolt connection shown in Fig. 2.25, Bolt 3 is the axis of symmetry. The bolt offsets and bolt forces are symmetrical about that line.

In Fig. 2.25 the solution is shown for a connection whose lap and main plates follow the plate calibration curve

marke "Main Plate" in Fig. 2.23. The solution proceeds as in the preceding paragraph except that the equilibrium check may be made at  $\frac{1}{2}P_G$  where the curves L and M intersect.

c. Solution for Test Joints

To solve for the theoretical bolt forces in the test joints described in the next chapter the plate and bolt calibration curves of Fig. 2.21 were drawn to a greatly enlarged scale. Enlargement was required to make it possible to read accurately in the elastic range of the plate calibration curves.

The solution proceeded as in Fig. 2.25 for the symmetrical type of joint. Trial solutions were made until the error was 1% or less. This was necessary to arrive at consistent values for the inner bolts. It should be noted that the intersection of the horizontal line at  $R_1$  and the bolt curve, B, is very acute and that very small changes in  $R_1$  make much larger changes in  $\delta_1$ . This requires very accurate work because  $\delta_1$  exercises a great influence on the remainder of the solution.

The results of these solutions will be discussed in Chapter 4.

### 3. EXPERIMENTAL WORK

#### 3.1 Purpose of Tests

The experimental work to be described and correlated with the theoretical analysis consists of the static tension tests of eight bolted joints designated D-Series - Part a. These tests form part of an investigation known as the Large Bolted Joints Project that has been in progress at the Fritz Engineering Laboratory, Lehigh University, since 1956.

The primary purpose of this project has been to determine the tension-shear ratio that will produce a balanced design at ultimate load. Stated in other words, the purpose has been to determine the proportions of a joint so that the bolts will shear and the net section of the plate will tear simultaneously. The first test series of short, compact joints<sup>(2)</sup> established this ratio at 1/1.10. However, it was realized from the literature on the subject of load distribution that if this same ratio were used to design long joints, a bolt failure could be

expected at a lower average shear stress. In order to determine the seriousness of the effect of joint length the D-Series - Part a was designed and tested.

### 3.2 Description of Joints

In the eight double shear splices of the D-Series - Part a, the main variable was the number of bolts in line with the load. This varied from 10 for the joint marked D101 to 3 for joint D31 (Fig. 3.1). The bolts were 7/8" diameter A325 bolts arranged in two lines and with a pitch of 3 1/2". All bolts were of the same lot, designated as D-Lot. These bolts satisfied the proof load requirements of the A325 Specification<sup>(4)</sup> and showed an average ultimate tensile strength of 56.7 kips, about 106 percent of the minimum strength. A typical load-elongation curve is shown in Fig. 3.2.

Since the tension-shear ratio was to be kept constant at 1/1.10, it was necessary to change the net section area as the number of bolts was varied. In this case the



thickness of the plates was kept constant and the width was varied. The combined thickness of the lap plates was made equal to the thickness of the main plate. In order not to introduce variable plate strengths the main plate was built up of two plates of the same 1" thickness as the lap plates.

The plate was ASTM-A7 structural steel<sup>(29)</sup>. Each required width was burned from a 24" wide universal mill plate and machined to its final dimension. All 24" plates were from the same heat and rolling and coupons for all joints showed very little variation in strength. The average properties are tabulated below:

Static Yield Level	28.4 ksi
Ultimate Tensile Strength	60.0 ksi
% Elongation in 8 inches	33.2%

These values place this material at the lower limit of the ASTM Specification<sup>(29)</sup>. The average stress-strain diagram is shown in Fig. 3.3.

All holes were 15/16 inch diameter and were drilled

through the four one inch plies simultaneously thereby assuring perfect hole alignment. Bolts were installed by a turn-of-nut method<sup>(30)</sup> resulting in initial tensions in the plastic range of the bolt at about 140% of the proof load.

For greater detail on the description of the joints, properties of the materials, method of fabrication and the bolting procedure the reader is referred to Ref. 7.

### 3.3 Instrumentation

While strength properties were of primary concern, certain inexpensive instrumentation was prepared to facilitate a verification of the theory developed in the preceding chapter. This instrumentation was identical for every joint except D101. D101 was the first joint tested and a few modifications were suggested by the experience of this test. Since deformations had to be measured in the region of the ultimate load where many portions of the plate would be straining inelastically, the measuring devices had to be capable of measuring elongations of up to .25 inches within a gage length of 3.5 inches. Yet, at the same time, elongations of a few ten-thousandths of an inch might be encountered in the relatively inactive zones of the connection.

Electric resistance strain gages of the SR-4 type were too sensitive for this requirement and would become inoperative at the high strains.

The idea of making strain gages using linear motion transducers was explored. These were abandoned

because of the great number required and the unit cost of each transducer.

Mechanical dial gages offered the cheapest and simplest means of making the necessary measurements, and these were used. A certain amount of danger was involved in taking these dial gage readings at loads close to ultimate.

The general layout of instrumentation is shown schematically in Fig. 3.4.

The overall elongation of the bolted joint was measured over a gage length extending from one pitch distance above the first row of bolts to one pitch below the last row. Readings were taken by means of .001 inch dial gages mounted on the centerline of each face (Fig. 3.5). Test showed very good agreement of the two gages.

Two .0001 inch dial gages, called slip gages, were mounted on the edges of the joint (Fig. 3.5). These gages measured the relative movement of Row n in the main plate and Row x in the lap plates (Fig. 3.4). The name

"slip gages" is somewhat of a misnomer since these gages record slip at the last row plus the elongation in the lap plates in the pitch  $nx$ .

On Joint D101 the slip gages measured the movement between Row 0 in the main plate and Row 1 of the lap plates. This arrangement was abandoned in favor of the one described in the previous paragraph because the reading was affected slightly by curling of the free end of the lap plate.

The determination of pitch elongations involves many readings, especially in the longer joints. It was not possible to use a fixed position dial gage for each of these. Instead, a hand-held extensometer was used (Fig. 3.6). This instrument, made at the Fritz Laboratory, has been called a "slidebar extensometer". Two points fit into small drilled holes and a .0001 inch dial gage records the relative movement of the two points. The total travel of the dial gage is 0.5" but only about 0.4" is generally available for measurement in one direction.

The successful operation of this instrument depends

on having carefully drilled holes in the test specimen and on the skill of the user in holding it in a uniform manner and with uniform pressure. With care duplication of readings within two ten-thousandths of an inch is possible. The centerdrill holes were located on the centerline of both edges of each plate and on the centerline of the exposed faces of each of the lap plates (Fig. 3.4).

### 3.4 Calculation of Hole Offsets

During a test the most noticeable sign of distress in the joint is the hole offset. The offset is very apparent in Fig. 3.5 which shows Joint D91 just after the first bolt failed.

The amount of hole offset occurring at various holes was measured from time to time with a steel scale giving readings to .01 of an inch. Usually, the hole offset was computed from the slidebar extensometer and slip gage readings in the following manner. Refer to Fig. 3.7 which uses a joint with 5 bolts in line to illustrate the

method. Proceeding from the Row  $x$  and equating dimensions up to Row 5, it follows that

$$\Delta_5 + p + e_{x5} = p + \text{slip gage reading}$$

$$\Delta_5 = \text{slip gage reading} - e_{x5}$$

Again, equating dimensions from Row 5 to Row 4

$$\Delta_4 + p + e_{54} = \Delta_5 + p + e_{45}$$

$$\Delta_4 = \Delta_5 + (e_{45} - e_{54})$$

This process can be repeated between any two rows.

In general terms, for a joint with  $n$  bolts in line, the expressions for the hole offsets are:

$$\Delta_n = \text{slip gage reading} - e_{xn} \quad (3.1)$$

$$\Delta_j = \Delta_k + e_{jk} - e_{kj} \quad (3.2)$$

$$j = m \text{ to } 1$$

In these expressions the notation is the same as that used in Chapter 2. The values of  $e$  are those measured experimentally by the slidebar extensometer.

### 3.5 Check on Measurements

If we assume that a line circumscribing the joint through Rows 0 and x (Fig. 3.4) remains a straight line at all times, it is possible to relate three types of measurements made during the test. This is readily seen from Fig. 3.7 where

$$\begin{aligned} \sum \text{main plate pitch elongations} + \text{slip gage reading} \\ = \text{overall elongation dial gage reading.} \end{aligned} \quad (3.3)$$

This equation serves as a check of the accuracy of the deformation readings taken.

In addition, the direct measurements of hole offsets, made by use of a steel scale and recorded in the log of test, serve as an appropriate check on the calculated values of hole offset.



### 3.6 Results of Tests

The results of these tests are documented in detail in Ref. 7 but a tabulation is repeated here for ready reference (Table 3.1). The most important part of the table, insofar as this paper is concerned, is the type of failure and the load at which failure occurred.

Joints D101 to D71 inclusive failed by shearing of a bolt or bolts. The load recorded is the value,  $P_J$ , that appeared on the load dial of the testing machine at the instant the first bolt sheared. This load has been designated as the failure load even though complete rupture did not occur. In several instances higher loads were recorded later when load was reapplied.

The manner in which unequal distribution of bolt forces affects joint behavior is illustrated by Fig. 3.8 which shows how progressive failures work inward from the most heavily loaded end bolts. The first number opposite a bolt indicates its order of failure and the second number indicates the load at which it occurred. This sequential type of failure has been dubbed "unbuttoning".

Joints D61 to D31 failed by the plate reaching a maximum load. In the cases of D61 and D51 the plate actually tore at the net section of the main plate at Row 1, while for D41 and D31 the test was stopped after reaching the maximum load but before tearing took place. The shear stress shown is the nominal or average stress on the bolts at the maximum load.

### 3.7 Deformation of Joints

The various deformations of a joint were measured as described previously, recorded on data sheets, and finally plotted as a function of the gage load. The complete work on each joint is collected in the project files at the Fritz Laboratory. The curves for Joint D91 are presented here as typical ones.

Figure 3.9 shows the overall elongation of the joint in the 35" gage distance. This curve clearly shows the loading history of the joint through the following sequence:

Phases 1 and 2	0 to 200 <sup>k</sup>	- no slip and partial slip
Phase 3	200 <sup>k</sup> to 350 <sup>k</sup>	200 <sup>k</sup> - inception of major slip
		342 <sup>k</sup> - yielding of the net section
		350 <sup>k</sup> - the apparent completion of slip, partial bearing
Phases 4 and 5	350 <sup>k</sup> to 679 <sup>k</sup>	396 <sup>k</sup> - yielding of gross section
		bolts in bearing and deforming under load. The beginning of complete bearing is difficult to determine
Phase 6		679 <sup>k</sup> - first bolt failed
		674 <sup>k</sup> - after partial unloading of testing machine second bolt failed on reapplication of load
		686 <sup>k</sup> - after partial unloading of testing machine four more bolts failed on reapplication of load
		0 <sup>k</sup> - load removed and test discontinued leaving 12 bolts intact

Numerical values for overall elongation during Phases 4 and 5 are tabulated in Table 3.3

The average of the two slip gage readings is plotted on Fig. 3.9 for the region of Phases 4 and 5. The numerical values are tabulated in Table 3.2.

Figures 3.10 and 3.11 show the pitch elongations of the main and lap plates drawn to an enlarged scale so that the elongations of the relatively inactive parts of the plates are observable. Figures 3.12 and 3.13 show the same pitch elongations to a scale that permits reading to the ultimate load. The points plotted are the average of readings taken on both edges. Comparison of the curves for the lap plates with those for the main plate shows that the joint was symmetrical in its behavior.

Numerical values of  $e$ , as read from these curves, are tabulated in Table 3.2. They will be used to calculate the hole offsets. Again, the symmetry of joint behavior can be observed by comparing the numbers above and below the centerline between  $e_{45}$  and  $e_{65}$ . Generally it has been observed that the pitch elongations of the main plate were greater than those of the lap plate.

In Table 3.3 the observed readings of overall

elongation, slip gage and pitch elongations are checked by Eq. 3.3. On the second line are values obtained by adding the slip gage reading and the summation of the pitch elongations in the main plate as recorded in Table 3.2. These values should equal the overall elongation readings on the third line but a difference occurs. The difference is expressed in absolute terms and as a percent of the overall elongation. It is reasonable to expect that exact agreement of the two sides of the equation will not occur because of the following sources of error:

1. The overall elongation measured at the middle of the joint is probably greater than that which would be measured near the edges of the joints. This may occur because of non-uniform stress distribution caused by a concentration of the gripping action of the testing machine. In other words, the circumscribing line mentioned in Para. 3.5 does not remain straight. SR-4 gages placed on some 18" wide joints showed the transverse strain

distribution to be uniform as long as the gages remained operative. This error probably is not very great but if it does occur the reading of the overall elongation will be on the high side.

2. The slip gage is mounted on the lower, inactive end of the main plate and therefore translates only. However, the T-bracket against which the dial gage plunger bears, is subject to rotation. Three and one-half inches above the position of the bracket the lap plates are subject to their greatest necking. The edges of the lap plate slope inward toward that point and the outer ends of the T-brackets move upward. This upward movement compresses the dial gage plunger and subtracts from its normal downward movement under tensile loading. Thus the slip gage readings are probably on the low side.

3. The readings of the hand extensometer are subject to errors of plus or minus several thousandths, but these are compensating, and

therefore do not affect this check appreciably.

For the reasons stated it is possible for the overall elongation readings to be on the high side and the slip readings on the low side of the true reading. In most cases it was found that slip plus summation of pitch elongations was less than the overall elongation. Nevertheless, agreement was reasonably good with the maximum difference being about 8% and the average for all joints 3.3%.

The check is shown graphically on Fig. 3.9 where the dashed line represents the slip gage measurements plus the summation of pitch elongations in the main plate, and the solid line represents the overall elongation. The horizontal distance between the two is the difference.

The hole offsets calculated according to Eqs. 3.1 and 3.2 are tabulated in Table 3.3. Again, the symmetry of joint behavior can be observed by noting the symmetry of these numbers about the line  $\triangle_5$ .

## 4. COMPARISON OF THEORY WITH EXPERIMENTAL WORK

### 4.1 Theoretical Bolt Forces

The results of the theoretical solution for the unknown bolt forces of Joints D101 to D31 are shown in graph form in Fig. 4.1 to 4.4 inclusive. The abscissa is the bolt force,  $R$ , and the ordinate is the load on the gage strip,  $P_G$ . The black bar marked on the vertical axis indicates approximately the region of slip during the test (Phase 3 as described previously in Para. 1.3c). The load calculated to cause yielding of the net section is indicated as  $P_{yn}$ . The line at an abscissa of 55 kips indicates the proportional limit of the bolt as shown by the calibration curve in Fig. 2.16. However, it is not until a force of about 70 kips that this same curve becomes markedly flat.

Joint D91 in Fig. 4.1 will be the basis for discussion. This connection is symmetrical about Row 5. Beginning at the lower end of the curves the entire connection is still elastic and the end bolt,  $R_1$ , is carrying



an increasing proportion of load as indicated by the divergence of the line  $R_1$  from the group of four lines.

The first of Eqs. 2.8 may be rewritten in the form

$$\delta_1 = \delta_2 + (e'_{12} - e'_{21})$$

This shows that  $\delta_1$  is dependent upon the differential elongation of the main and lap plates. The elongation in the lap plate,  $e'_{21}$ , is small so  $\delta_1$  is affected principally by the main plate elongation,  $e'_{12}$ . Thus, when the main plate in pitch 12 passes its proportional limit,  $\delta_1$  increases more rapidly. If the bolt is still elastic,  $R_1$  increases in proportion to  $\delta_1$ . The circle on the line  $R_1$  indicates the proportional limit of  $e'_{12}$ , and it is seen that the rate of increase of  $R_1$  is greater to the right of that circle.

When Bolt 1 passes its proportional limit,  $R_1$  increases at a slower rate than does  $\delta_1$ . This is indicated by the change in sign of the curvature of the line  $R_1$  in the vicinity of  $R$  equal to 58 kips. Redistribution begins to take place and Bolt  $R_2$  is called upon to carry

more load.

Shifting attention to  $R_2$  it is seen that as the load  $P_G$  is increased the force in the main plate between the second and third bolts finally forces  $e'_{23}$  beyond the proportional limit (circle on curve  $R_2$ ). According to the second of Eqs. 2.8  $\delta_2$  must increase.  $R_2$  increases proportionately because it is still elastic. The increase in  $R_2$  is accentuated because  $R_1$  already has begun the redistribution of load to other portions of the joint. This effect is great enough to overshadow the slower rate of increase of bolt force caused by Bolt 2 passing its proportional limit. It is not until  $R_2$  equals about 70 kips that its slope begins to increase indicating that  $R_2$  is beginning to redistribute load.

At  $P_G$  equal to 500 kips both  $R_1$  and  $R_2$  are well past the bolt proportional limit, and  $e'_{34}$  reaches the proportional limit of the plate. Therefore,  $R_3$  begins to pick up load. In this case, this occurs at about twice the normal working load.

The redistribution of load to interior bolts is

felt by  $R_1$  at  $P_G$  equal to about 590 kips, and the force carried by that bolt increases rapidly. The analysis shows that the large increases in  $R_3$  and  $R_4$  permit Bolt 5 to relax slightly. This is possible because the bolt and the portions of plate adjacent to it are still elastic. Eventually, at the very top of the curve,  $R_5$  appears to be picking up load again but the joint fails before any significant increase takes place.

This illustration indicates clearly the unequal distribution of load among the bolts of a long connection. Inspection of the graphs for the other joints shows that as the length of the joint decreases the partition of load among the bolts is more uniform. Joint D31 in Fig. 4.4 shows that with three bolts in line each bolt carries nearly an equal share of the load.

This analysis does not indicate as large a disparity of bolt forces under elastic conditions as one would expect from previous research. However, it must be remembered that the distribution of load among the fasteners depends upon the relative stiffnesses of the fasteners and

the connected member. Comparisons cannot be made unless these relative stiffnesses are taken into account. The next chapter will show the influence of the tension-shear ratio as an example of one of the factors affecting load partition.

#### 4.2 Predicted Ultimate Strength of Joint

For the purpose of this analysis the ultimate strength of a connection will be defined as that value of  $P_G$  corresponding to a force on the extreme bolt equal to the ultimate strength of a single bolt. The D-Lot bolts used in this study had an ultimate double shear strength of 100 kips (Fig. 2.16). Inspection of Fig. 2.16 also shows that having reached its ultimate strength the bolt begins to unload rather rapidly and with only .04 inch more deformation it ruptures. Thus, the ultimate strength of the connection as defined above is almost synonymous with the load which causes the first bolt to rupture.

It should be recognized that the ultimate strength

of the joint also may be controlled by tension on the net section. No study is being made of that problem since it has been covered by others. (31, 32) However, the method developed by Schutz for predicting net section failures will be used later for joints D61 to D31 that failed in that manner.

The predicted ultimate strength for the bolt failure of a joint may be found as the ordinate  $P_G$  corresponding to the intersection of the  $R_1$  line with the abscissa 100 kips as shown in Figs. 4.1 to 4.4. A comparison of the predicted ultimate strength and the test failure load is tabulated below for the four joints which had bolt failures.

<u>Joint</u>	<u><math>P_G</math> Test Strength kips</u>	<u>Predicted Ult. Strength kips</u>	<u>Percent Diff.</u>
D101	753	750	-0.40
D91	679	680	+0.15
D81	612	612	-4.52
D71	563	555	-1.42

Unfortunately, for demonstrating the success of the theory in predicting bolt failures, the shorter joints D61 to D31 had tensile plate failures. Predicted and test strengths are compared in the tabulation below.

<u>Joint</u>	<u>P<sub>G</sub> Test Strength kips</u>	<u>Predicted Ult. Strength (Plate Failure) kips</u>	<u>Per- cent Diff.</u>	<u>Predicted Ult. Strength (Bolt Failure) kips</u>	<u>Per- cent Diff.</u>
D61	497	491	-1.21	508	+2.21
D51	425	423	-0.05	443	+4.24
D41	345	349	+1.16	380	+10.14
D31	257	263	+2.33	293	+14.01

The comparison of the test strength and the predicted ultimate strength for a plate failure is the proper one to make. It shows that Schutz's method<sup>(32)</sup> for computing the effective net section of riveted and bolted joints gives close agreement with these tests.

Though bolt failures did not take place in these tests some qualitative measure of the worth of the predicted bolt failure load may be had by viewing the last

two columns of the table in conjunction with Figs. 4.5 and 4.6. After test these connections were sawed lengthwise through a line of bolts revealing the permanent bolt deformations. Looking at these photographs in descending order, it is evident that the end bolts in D61 have an extreme deformation whereas the end bolts in the other joints show a lesser and lesser amount. The shorter the joint the more bolt deformation capacity it has available before a bolt failure takes place. This agrees with the relationship of predicted bolt failure and actual test strength shown in the table.

Another way to evaluate the condition of the bolts in the last four joints is to measure the deformed contour of each bolt and compare it to the deformed shape of a control bolt under a known load. This has been done<sup>(33)</sup> and it was found that the end bolts were carrying the following loads:

D61	100 kips
D51	98 kips
D41	94 kips
D31	90 kips

These values indicate that D61 was on the verge of failure whereas the end bolts in D31 could carry about 10 kips more load. These observations are consistent with the theoretical predictions.

#### 4.3 Unbuttoning Factor

The theoretical results may be compared with the results of tests other than D101 to D31 by use of a non-dimensional quantity known as the "unbuttoning factor",  $U$ .  $U$  is defined as the average shear stress at the time the first bolt fails divided by the shear strength of a single bolt.

In Fig. 4.7 the unbuttoning factor is plotted against the length of the joint expressed in terms of the number of pitches. The theoretical values of  $U$  are shown along with test results of D101 to D31, compact joints,<sup>(2)</sup> and variable grip long joints.<sup>(8)</sup> The correlation with all these test results is good. It is to be expected that  $U$  for the wide compact joints would fall below the theoretical values because the latter do not take into account the lateral force on corner bolts caused by plate necking.



#### 4.4 Hole Offsets

When the values of  $R$  have been determined by the theoretical solution, the forces acting in the various portions of the plates can be computed by Eqs. 2.2 and 2.3. These in turn determine values of  $\lambda$  according to Fig. 2.21. Thus, it is possible to calculate the theoretical hole offsets,  $\Delta$ , by means of Eq. 2.5.

In a test the hole offsets are calculated from observed readings by use of Eqs. 3.1 and 3.2. Tabulated values for D91 appear in Table 3.3.

A comparison of the calculated and observed hole offsets serves as another measure of the validity of the theoretical solution. This comparison is made graphically in Figs. 4.8 to 4.15 inclusive. The dashed line gives the theoretical prediction and the solid line through the points represents the values of hole offset calculated from test data.

Again focusing attention on Joint D91 that has been the basis of previous discussion (Fig. 4.9) it is

seen that the agreement of the two curves is very good. Other joints do not show the same degree of agreement but in general both theoretical and experimental values follow the same trends. The agreement for the end bolts is good but some discrepancies occur for the inner bolts. This may be due to instrument errors which for the inner bolts constitute a larger part of the total deformation.

#### 4.5 Distribution of Bolt Forces

In Figs. 4.1 to 4.4 the theoretical bolt forces are portrayed graphically, and it is obvious that each bolt does not carry an equal share of the applied load. The non-uniformity of the partition of load at different values of load can be seen more clearly in Figs. 4.16 to 4.19. In these graphs the abscissa represents the bolt force as a percentage of the equally distributed bolt force. If all the bolts carried the same load all of the curves would be vertical lines at the abscissa 100. The ordinate is also non-dimensional and represents the

applied load,  $P_G$ , as a percentage of the maximum gage load.

Joint D91 (Fig. 4.16) will be used as a basis for the discussion of these curves. Between the ordinates of 50 to 68% Bolt 1 is carrying an increasing proportion of the applied load as  $e'_{12}$  passes its proportional limit (indicated by circle on line  $R_1$ ). At 60% of the maximum load Bolt 1 passes its proportional limit and at approximately 65% it reaches  $R_1 = 70$  kips. (It was pointed out in Para. 4.1 that at about 70 kips the bolt shear calibration curve (Fig. 2.16) becomes markedly flat.) The first bolt is now beginning the redistribution process as evidenced by the bending of the  $R_1$  curve back toward the uniform distribution abscissa of 100% and the bending of the  $R_2$  curve to the right.

When bolt 2 passes its proportional limit in the neighborhood of 68% of the maximum load it too begins to redistribute load to the inner bolts.  $R_3$  picks up load and the curve bends to the right. Later,  $R_4$  carries an increasing percentage of load.

At the maximum load all the curves, except  $R_5$ , are headed in a direction toward the equal distribution line at 100%.  $R_5$  is just beginning to show a tendency to turn when the maximum load is reached, Bolt 1 having exhausted its deformation capacity. By this time the percentage of load carried by  $R_1$  has dropped from a maximum value of 144% to 132%.

Inspection of the remaining graphs (Figs. 4.16 to 4.19) shows a trend that is expected. The shorter the joint the more uniform is the partition of load among the bolts. This is shown by the concentration of the curves in the vicinity of the 100% abscissa.

The intact bolts removed from joints D61 to D31 after test can serve as a check on the theoretical prediction of bolt force. The method of evaluating the force on these bolts at the time of failure was explained in Para. 4.2. The results are represented in Figs. 4.18 and 4.19 as solid squares at the ordinate corresponding to the plate failure. These show good agreement with the theoretical curves.

## 5. EFFECT OF VARIATION IN TENSION-SHEAR RATIO

The tension-shear ratio is a convenient way to speak of the proportions of a joint. It is the ratio of the average tensile stress on the net section of the plate to the average shear stress on the bolts and is customarily written as T/S. The tension-shear ratio can also be written in terms of the proportions of the joint: the ratio of the shearing area of the bolts to the area of the net section of the plate,  $A_s/A_n$ . The desirable ratio is that which causes the ultimate load of the bolts in shear to equal the ultimate load of the plate in tension. Such a condition is known as "balanced design at ultimate load".

It was pointed out in Chapter 3 that tests of short, compact joints<sup>(2)</sup> established the balanced design T/S ratio at 1/1.10. The joints D101 to D31 that have been analyzed in the previous chapter were designed with that T/S ratio. Since bolted joints have been designed for T/S ratios other than 1/1.10 the question arises as

to how the T/S ratio affects the load partition in bolted joints.

In order to show the effect of variation in T/S ratio several fictitious joints have been set up by combining various plate widths with a given number of bolts. By combining existing plate calibration specimens with various numbers of bolts different T/S ratios can be obtained but no new plate calibration tests have to be made. For example, by combining the plate calibration specimen PC101 with 8 bolts in line ( $n = 8$ ) a connection with a T/S ratio of  $1/1.38$  is obtained. Each fictitious joint has been assigned a mark corresponding to the denominator of the T/S ratio. Thus, S1.38 indicates a joint with a T/S ratio of  $1/1.38$ .

In addition to the joint described above three other fictitious connections were analyzed, namely: S1.54 ( $n = 5$ , PC71), S0.82 ( $n = 8$ , PC61) and S0.77 ( $n = 10$ , PC71). The results of the analysis of these joints can be used in conjunction with joints D51, D81, and D101 which had the same number of bolts.

In Fig. 5.1 theoretical bolt force curves are plotted for S1.38 and S0.82. Since they represent 8 bolts in line they should be compared with the corresponding curve for D81 ( $T/S = 1/1.10$ ) in Fig. 4.2. These three sets of curves have the same general characteristics but for S1.38 the curves are bunched indicating more nearly uniform distribution whereas at the other extreme (S0.82) they are dispersed. For S0.82 the first bolt is carrying about five times the load of the fourth bolt at the time plate failure is predicted at 497 kips.

The predicted bolt failure loads are 712 kips for S1.38, 612 kips for D81, and 510 kips for S0.82. Recalling that  $T/S$  equals  $A_s/A_n$ , the numbers 1.38, 1.10, and 0.82 represent the relative net areas of the three joints. Thus, it can be seen that the ultimate load-carrying capacity of 8 bolts in line increases with an increase in the area of the connected member. With more plate area the pitch elongations are less because the plate remains elastic longer. It is seen from Eq. 2.8 that with low plate strains the differential strain,  $e'_{21} - e'_{12}$ , remains small and therefore the difference between  $\delta_1$  and  $\delta_2$  is small.

It follows that  $R_1$  and  $R_2$  are more nearly equal. Similar analysis serves for the remainder of the joint. At any specific load, plate area in excess of that for balanced design restricts the magnitude of the differential plate strains thus reducing the amount of bolt deformation capacity utilized. As a result a higher ultimate load can be reached before the end bolts reach their limiting deformation.

The effect of the T/S ratio on bolt force distribution is more readily apparent in Fig. 5.2 where the results of the same three joints are shown in non-dimensional form. The applied load is given as a percent of the maximum load and the bolt force is given as a percent of the equally distributed bolt force. The abscissa 100% represents the condition in which each bolt is carrying an equal share of the load. The graph for D81 is that of Fig. 4.17 drawn one-half size. The curves for S1.38 are grouped in the neighborhood of the 100% abscissa indicating a fairly uniform distribution of load whereas those for S0.82 are spread widely.



The end bolts are the critical ones and the percentage of load carried by them is important. The effect of T/S ratio on the end bolts is represented in Fig. 5.3. The percentage of equally distributed bolt force carried by the end bolts at failure is plotted against the T/S ratio. Curves are shown for  $n = 10, 8$  and  $5$  where  $n$  is the number of bolts in line. The "balanced design" abscissa is at 1.10. The curves clearly indicate that the load on the end bolts is reduced if there is an excess of plate material. On the other hand the end bolts must carry a larger load when the net section area is less than that required for "balanced design". The latter condition will cause failure of the joint at a lower ultimate load. The short joint such as  $n = 5$  is less sensitive to variations in the T/S ratio than is a long joint.

The effect of variation in T/S ratio on bolt force distribution in the elastic range can be seen with the help of the graphical solutions in Fig. 5.4a and b. In each of the plots the bolt calibration curve, B, is the same. However, in Fig. 5.4a the curves M and L represent equal thickness main and lap plates of a given width whereas in

Figure 5.4b the curves M and L represent plates of the same properties and thickness but of a wider width. Being wider the latter plates undergo less elongation for a given load. Thus, the lines are steeper.

There are several observations that can be made concerning the solutions and the effect that the slopes of lines M and L play in the solutions. If L and B are added together they give the dashed line whose abscissa at the ordinate  $R_1$  is  $\delta_1 + e'_{21}$ . Line M, whose abscissa is  $e'_{12}$ , intersects the dashed line at point x. A necessary condition for the satisfaction of Eq. 2.8 is that the ordinate  $R_1$  be equal to or greater than that at x since  $\delta_2$  cannot be negative. The point x in Fig. 5.4a is higher than point x in Fig. 5.4b indicating that  $R_1$  must be greater for the plates with the flatter calibration curves.

At several places previous to this mention has been made of the differential plate elongations,  $e'_{jk} - e'_{kj}$ , and the control it exercises over the bolt offsets. In the graphical solution the differential plate elongation appears as the horizontal distance between the lines L and M.

It is clear from either of the graphs that this distance is the difference between  $\delta_j$  and  $\delta_k$ . The greater the acute angle between the plate calibration curves the greater will be the disparity between  $\delta_j$  and  $\delta_k$ . This same disparity will exist between the bolt forces because of the linear proportionality of  $R$  to  $\delta$ .

Thus, it is seen in Fig. 5.4b that the steeper lines L and M permit a lower value of  $R_1$  and the smaller horizontal distance between the lines results in more equal values of  $R_j$  and  $R_k$ . The net result is a more uniform distribution of bolt forces for the joint with the larger plate area.

The preceding observations concerning the effect of the T/S ratio on the behavior of bolt connections may be substantiated by the results of tests on bolted lap joints<sup>(34)</sup> restrained from bending. These lap joints were made of the same plate material as that used for joints D101 to D31 (Para. 3.2). However, since the grip differed from the previous series other bolts had to be used. For this reason the comparison of theory with experiment

is made on a non-dimensional plot such as the unbuttoning factor curve (Fig. 4.7). In doing this in Fig. 5.5 only predicted values and test results of the lap joints are shown.

Joint L2, with 2 bolts in line ( $N = 1$ ), is a statically determinate joint, and it is expected that regardless of the T/S ratio each bolt will carry a load equal to the strength of a single bolt. The test confirmed this. The unbuttoning factor was 0.99.

At the other extreme Joint L10 had 10 bolts in line at a T/S = 1/1.10 and the test result confirmed the prediction almost exactly.

Joint L7, with 7 bolts in line ( $N = 6$ ) and a T/S ratio of 1/1.57, failed by shearing all of the bolts simultaneously at an unbuttoning factor of 0.91. As expected from the previous finding, this is greater than the predicted value of 0.79 for "balanced design". The simultaneous failure of all bolts indicates that the partition of load among the bolts was fairly uniform such as was predicted for S1.38 (Fig. 5.3).

Joint L5, with 5 bolts in line ( $N = 4$ ), had a T/S ratio of 1/1.32. The test was stopped after one bolt had sheared at  $U = .89$ . The predicted value for "balanced design" was 0.88 which confirms the prediction in Fig. 5.3 that bolts in compact joints are less sensitive to variations in T/S ratio.

The unbuttoning factor for the last two joints, L7 and L5, is above those values predicted for joints with T/S ratios of 1/1.10 thus substantiating that the carrying capacity of a given number of bolts increases as the denominator of the T/S ratio increases.

## 6. SUMMARY AND CONCLUSIONS

This dissertation has developed a theoretical solution for the unequal distribution of load among the bolts of a double shear splice under axial load. Attention has been focused on the region from slip load to the ultimate load in which the bolts and plates are deforming in a non-linear manner. The theoretical solution has been used to predict the performance of joints with from 3 to 10 bolts in line and of "balanced design" at ultimate load.

The validity of the theoretical solution has been substantiated by a comparison of both ultimate load and joint deformations with the results of tests of eight large bolted joints.

The theoretical solution has been used to demonstrate how various proportions of plate and bolts affect the distribution of load and ultimate strength of connections of unbalanced design.

Specific findings of this study are summarized below.

(1) The study has shown that it is possible to predict the behavior of the bolts in an axially loaded double-shear plate splice in the region from slip load to the ultimate load. Determination of the unknown bolt forces may be accomplished through the solution of an equilibrium equation and a set of deformation compatibility equations. The required relationships of force to deformation may be obtained experimentally by calibration tests of representative portions of plate and single bolts. Because these relationships are non-linear the solution of the equations is made by a graphical procedure, (Figs. 2.24 and 2.25), which offers the advantage of showing visually the effect of certain quantities on the partition of load among the bolts.

(2) The theoretical predicted ultimate strength of four long joints as been compared with the

ultimate strength determined by test (Figs. 4.1 and 4.2). The difference between the two ranged between + 0.15% and - 4.52%. The theoretical ultimate strength has been defined as that load which causes the force on the critical end bolt to reach a specified maximum load.

(3) Further confirmation of the theoretical solution has been obtained by comparison with other test results by use of the non-dimensional "unbuttoning factor" (Fig. 4.7). The "unbuttoning factor" is an efficiency factor defined as the average shear stress at the time the first bolt fails divided by the shear strength of a single bolt. The maximum difference between theoretical and test values for 13 different tests is within 10%.

(4) The relative offset of the hole centerlines when the plates of the joint are in a slipped condition also has been used as validation of the theoretical solution (Figs. 4.8 to 4.15 inclusive).



Agreement of the theoretical and experimental hole offsets is good for the end holes but some discrepancies occur for the inner holes. The difference may be due in part to instrument errors which, for the inner bolts, constitute a larger part of the total deformation. Nevertheless the general trends are sufficiently close to one another for the hole offsets to be considered further validation of the theory.

- (5) The structural designer usually makes the assumption that each bolt carries an equal share of the load. This is not true because it violates compatibility conditions. When the actual bolt forces are represented as a percentage of the equally distributed bolt force (Figs. 4.16 to 4.19) they demonstrate the amount of error in this common assumption. The longer the joint the more unequal will be the distribution. With the bolts and plate used in this study the end bolt in a 10 in line connection is carrying 133% of the equally distributed force at the time it

fails. However, with 3 bolts in line the end bolt carries only 102% failure.

- (6) Measurements of deformed bolts removed from joints that had experienced tensile plate failures served to confirm the bolt force distribution at the time failure occurred. The force on each bolt, as determined by comparison of the deformed shape with that of a control bolt, shows good agreement with the theoretical prediction (Figs. 4.18 and 4.19).
- (7) The theoretical solution has been used to show the effect of a variation in the tension-shear ratio on the bolt force distribution. It has been shown that the load on the end bolts is reduced if there is more plate area than that required for "balanced design" and that the load is increased if the plate area is less. This condition holds in both the elastic and inelastic ranges. Tests of several joints have verified the beneficial effect of a surplus of plate area.

- (8) The results of this dissertation could be used to provide a more rational design procedure in which the factor of safety against rupture of the long joint will be the same as that for the short joint.

## 7. NOMENCLATURE

### Capital Letters

$A_n$	Area of net section
$A_s$	Total shear area of bolts
B	Bolt or bolt calibration curve
F	Force
L	Lap plate calibration curve
M	Main plate calibration curve
N	Number of pitches
$P_G$	Load on gage strip
$P_J$	Load on joint
$P_{jk}$	Force in main plate between Rows j and k
$P_{yg}$	Load that causes yielding of gross section
$P_{yn}$	Load that causes yielding of net section
$Q_{kj}$	Force in lap plates between Rows j and k
$R_j$	Force transmitted by Bolt j
S	Average shear stress (in T/S ratio)
T	Tensile stress on net section (in T/S ratio)
U	Unbuttoning factor

Small Letters

c	Hole clearance
$d_B$	Bolt diameter
$d_H$	Hole diameter
$e_{jk}$	Elongation of one pitch length of plate from the centerline of Hole j to the centerline of Hole k *
$e'_{jk}$	Elongation of one pitch length of plate from the bearing side of Hole j to the bearing side of Hole k *
f	Function of - used for bolt deformations
g	Gage
i	Inner (main) plate
j	Row of bolts or holes, $j = 1, 2, 3, \dots m$ .
k	Row of bolts or holes, $k = j + 1$
m	Next to the last row of bolts or holes
n	Number of bolts in line or last row of bolts or holes
o	Outer (lap) plates
p	Pitch
$r_B$	Radius of bolt
$r_H$	Radius of hole

-----  
 \* Normal order of subscripts indicates main plate elongations; inverted order indicates lap plate elongations.

t	Thickness
w	Washer
x	A line one pitch beyond Row n

Greek Letters

$\alpha$	Pressure angle
$\delta$	Calibration bolt offset
$\delta_B$	Offset of bolt reference points
$\lambda$	Elongation of the radius of a hole due to plate tension
$\rho$	Bearing deformation
$\sigma$	Normal stress
$\phi$	Function of - used for main plate elongations
$\psi$	Function of - used for lap plate elongations
$\Delta$	Hole offset
$\Sigma$	Summation

8. TABLES AND FIGURES

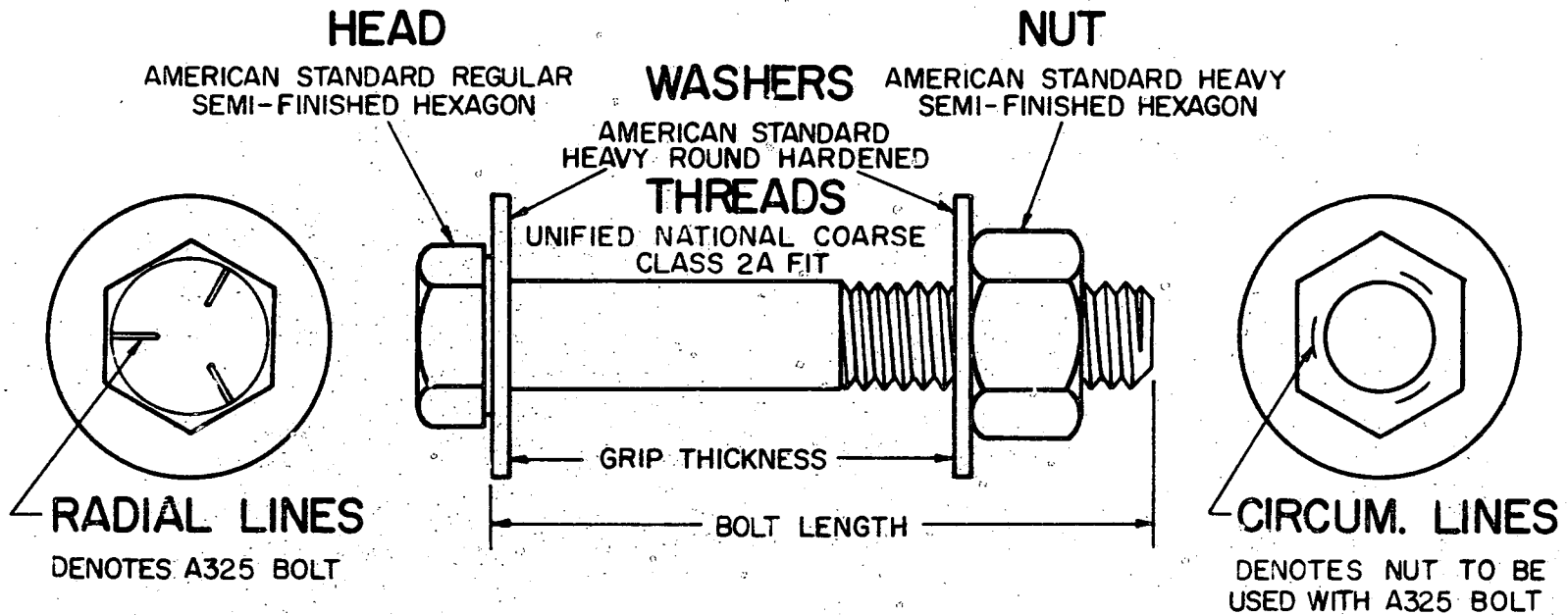


FIG. 1.1 THE A325 HIGH STRENGTH BOLT



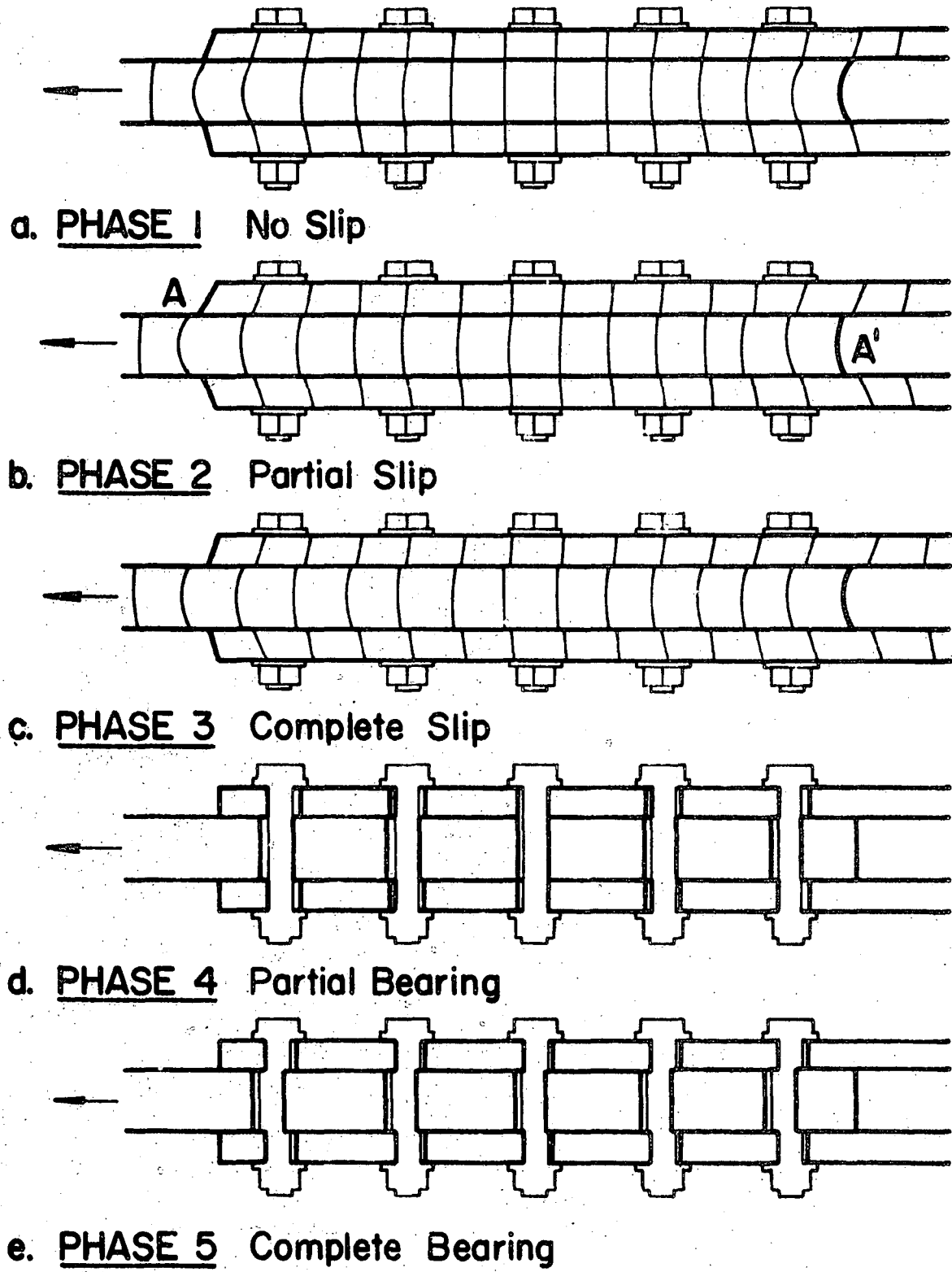


FIG. 1.2 BEHAVIOR OF A BOLTED JOINT

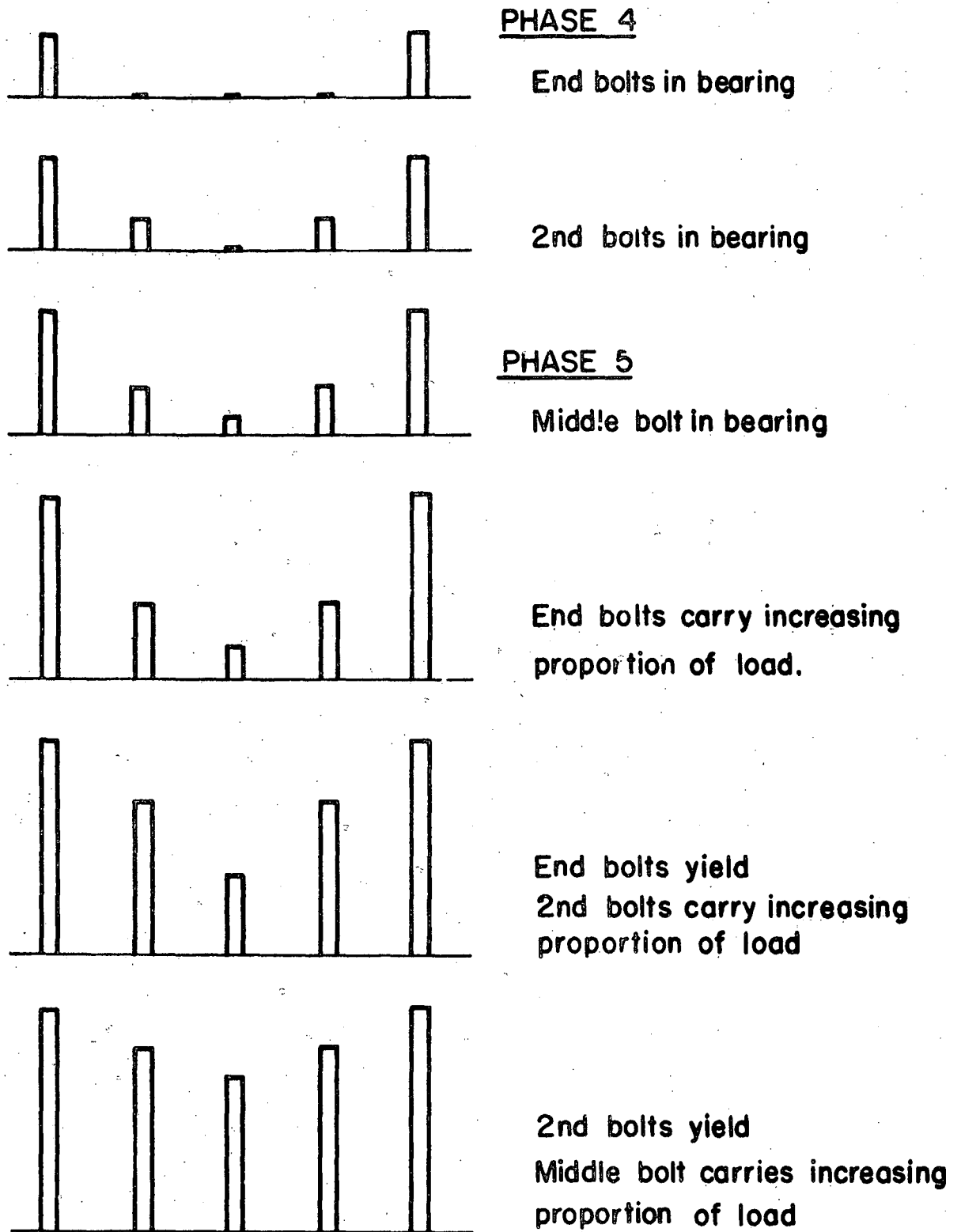


FIG. 1.3 LOAD CARRIED BY BOLTS DURING BEARING PHASES

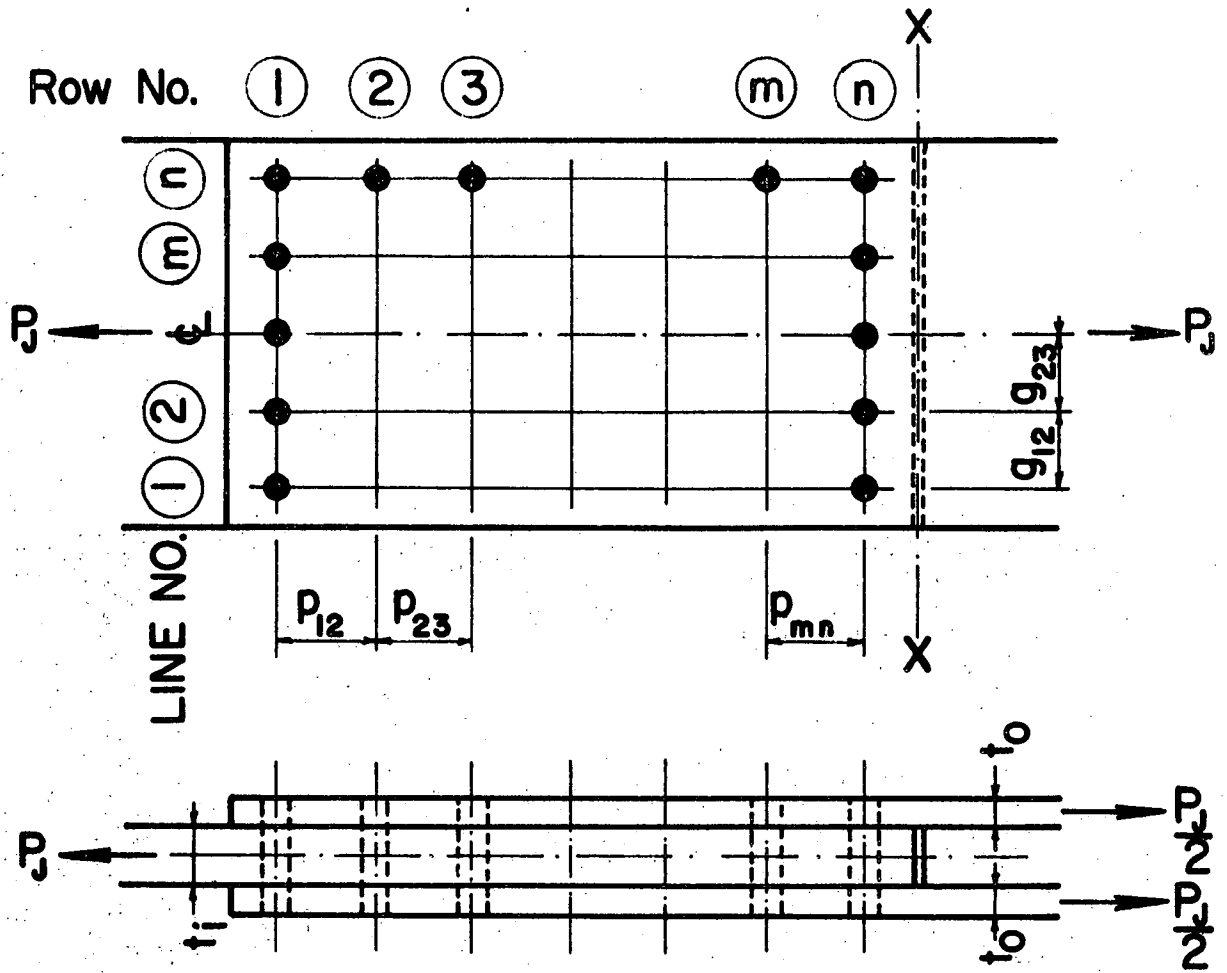


FIG. 2.1 GEOMETRY OF JOINT

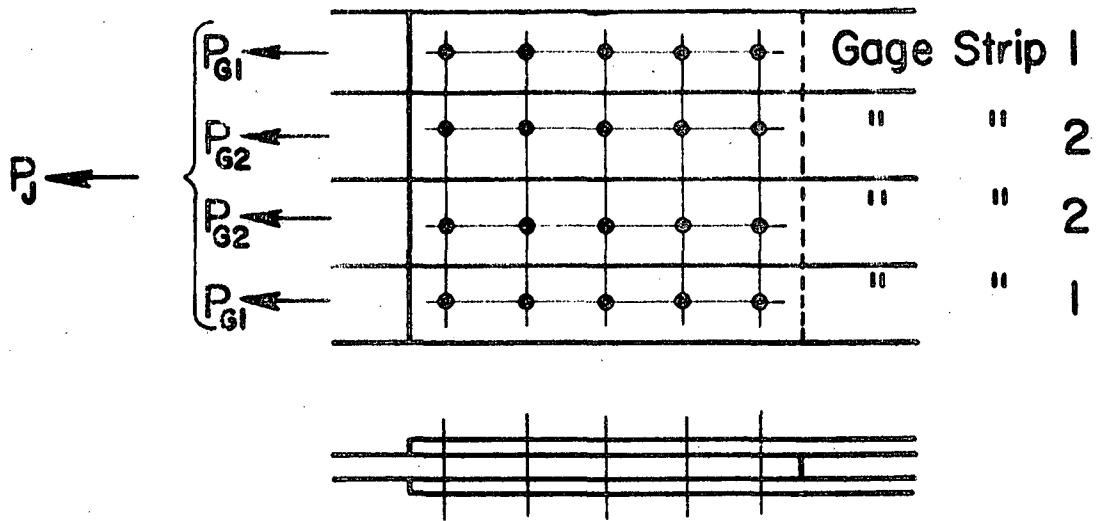


FIG. 2.2 DIVISION OF JOINT INTO GAGE STRIPS

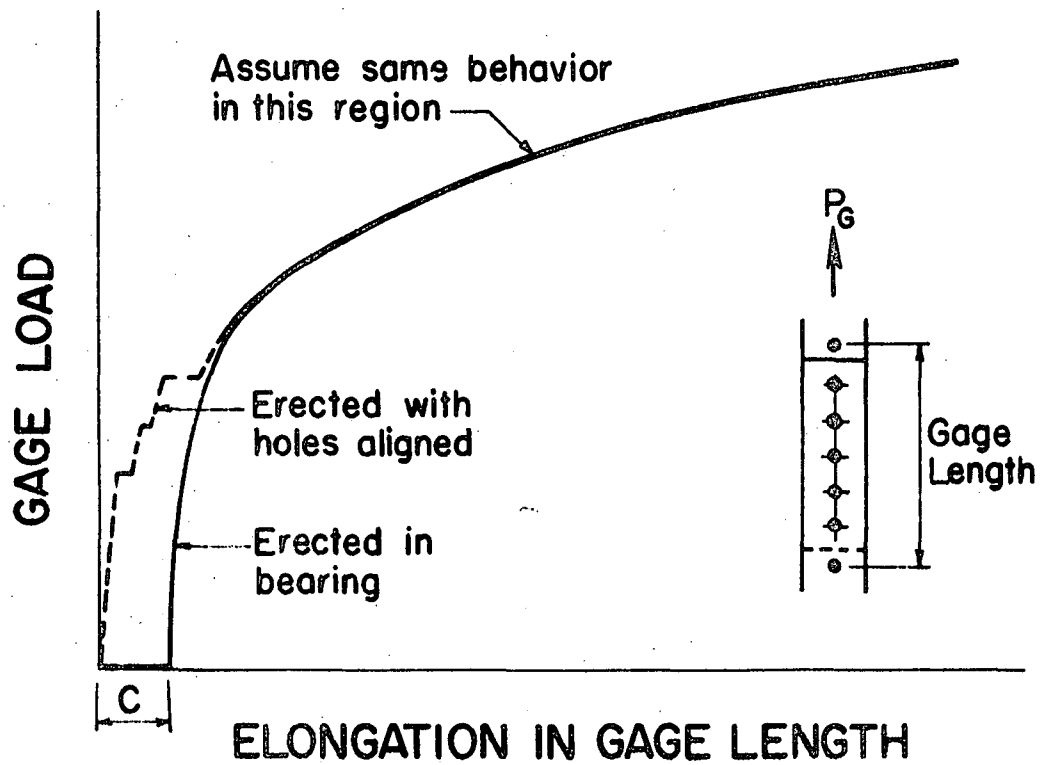
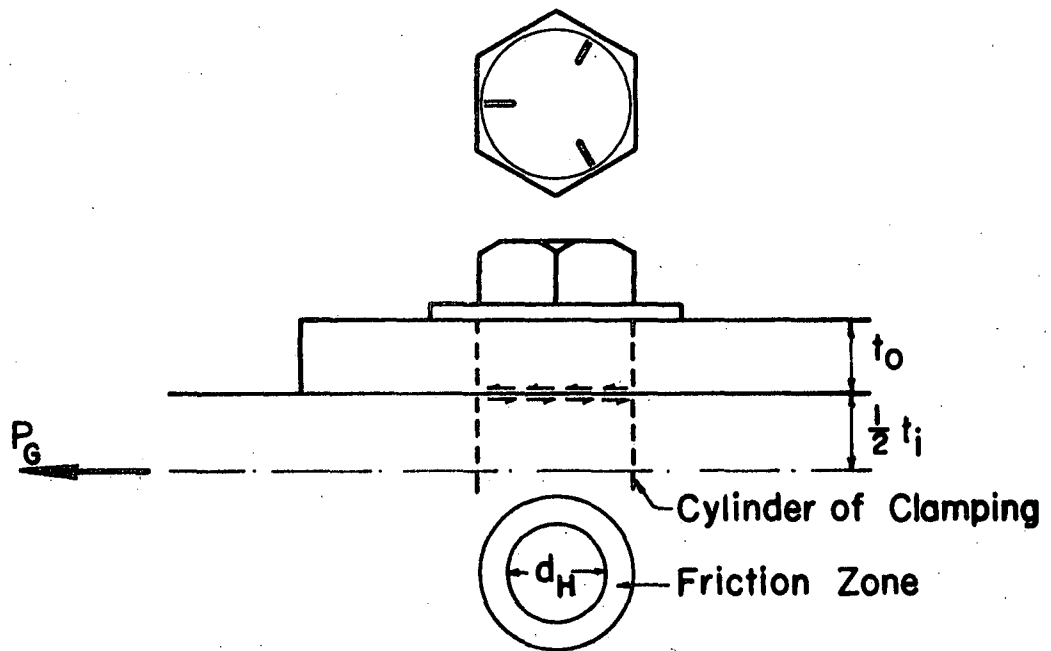
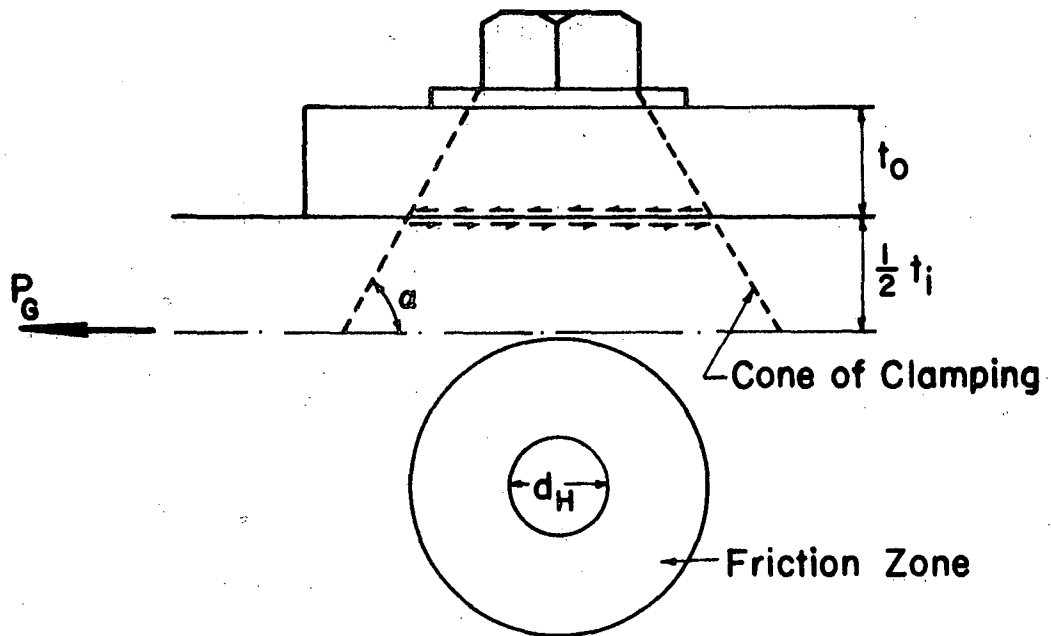


FIG. 2.3 PICTORIAL REPRESENTATION OF ASSUMPTION

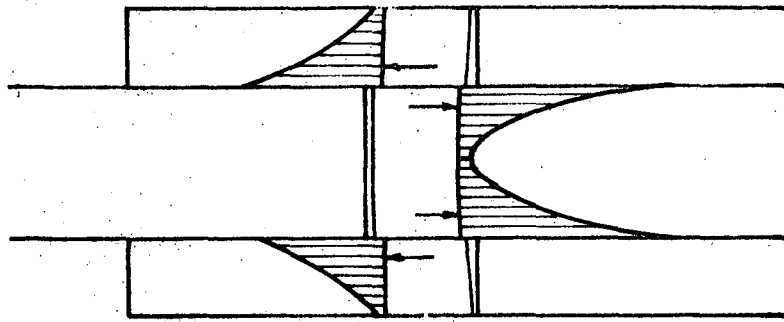


a) Cylinder of Clamping

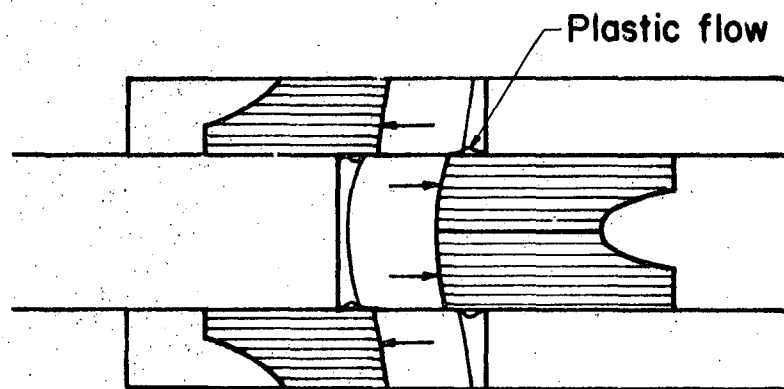


b) Cone of Clamping

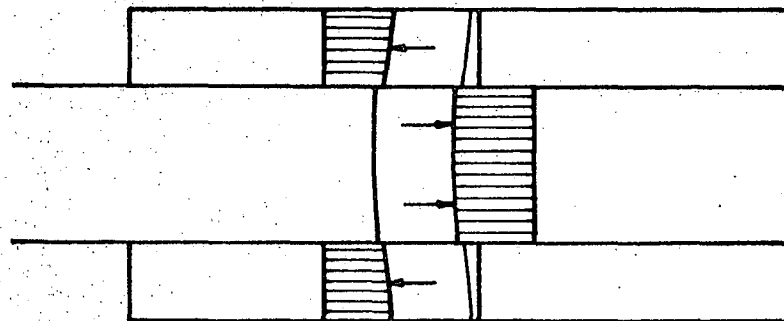
FIG. 2.4 POSSIBLE FRICTION ZONES



a. Elastic Bearing Stresses



b. Elastic-Plastic Bearing Stresses



c. Design Assumption : Uniform Bearing Stresses

FIG. 2.5 BEARING STRESS CONDITIONS

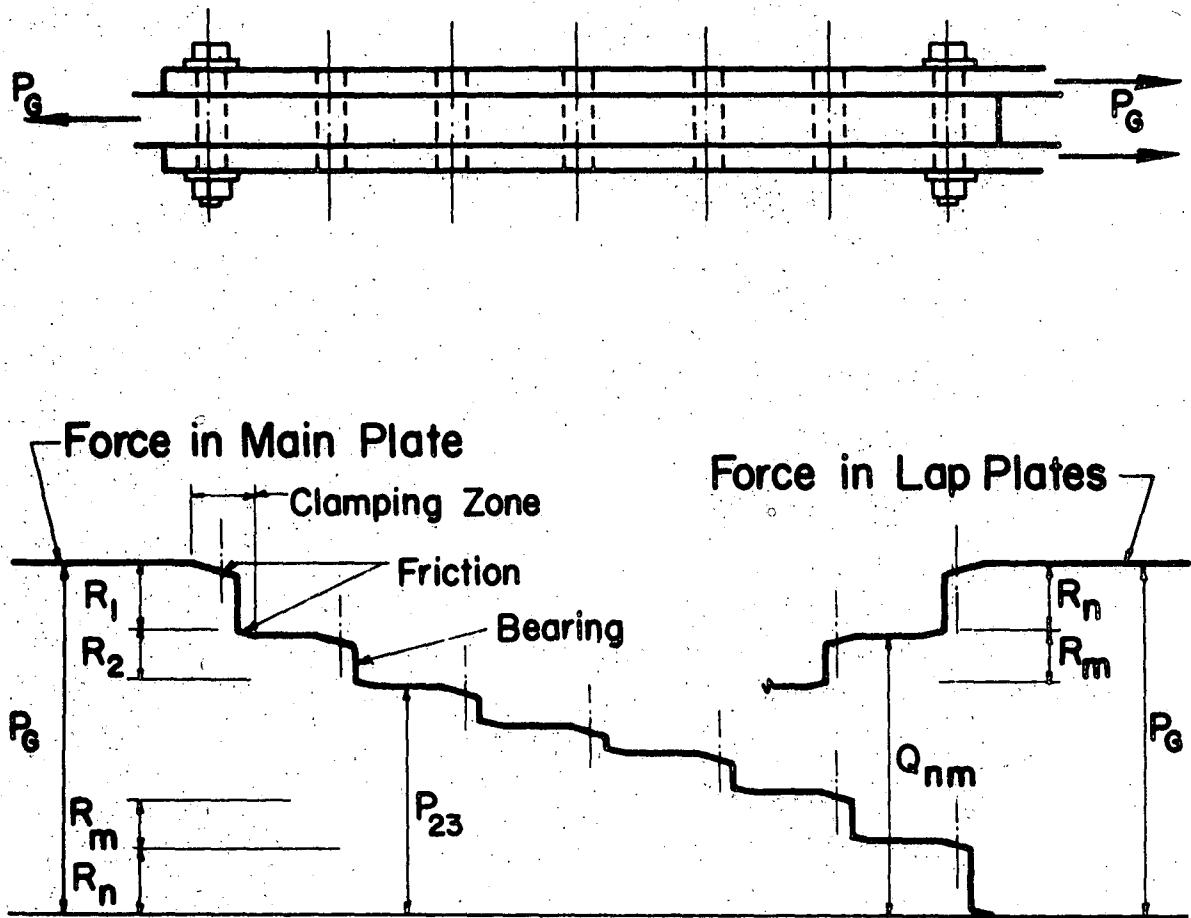
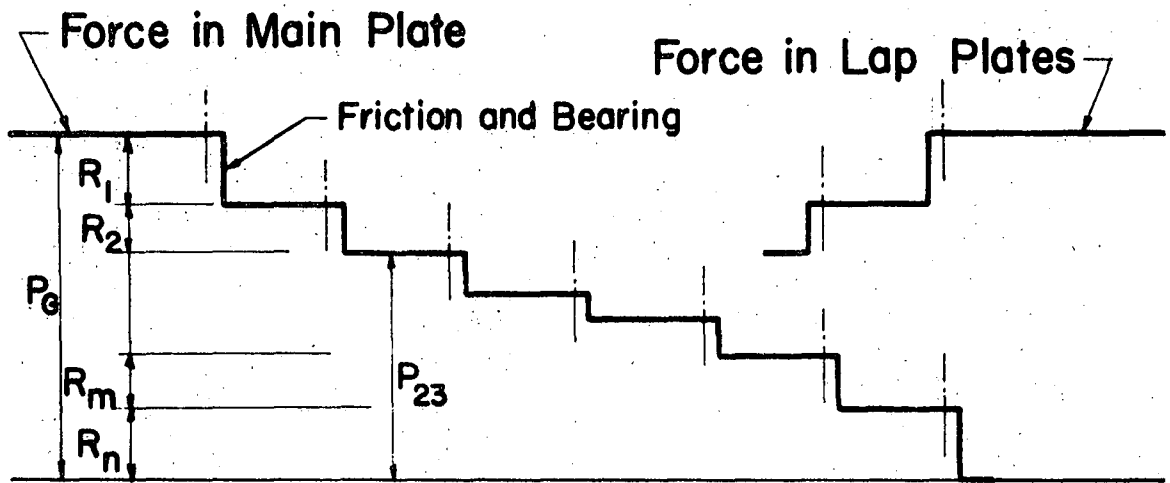
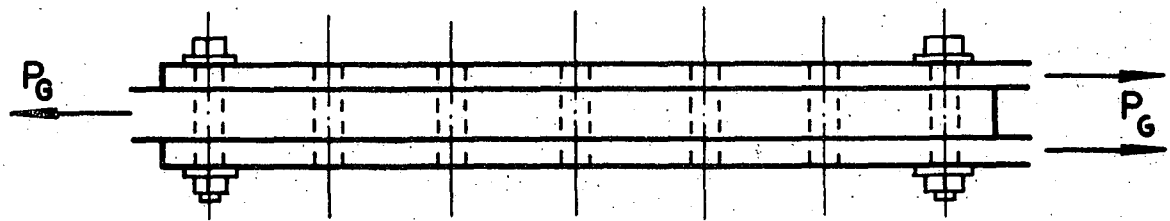
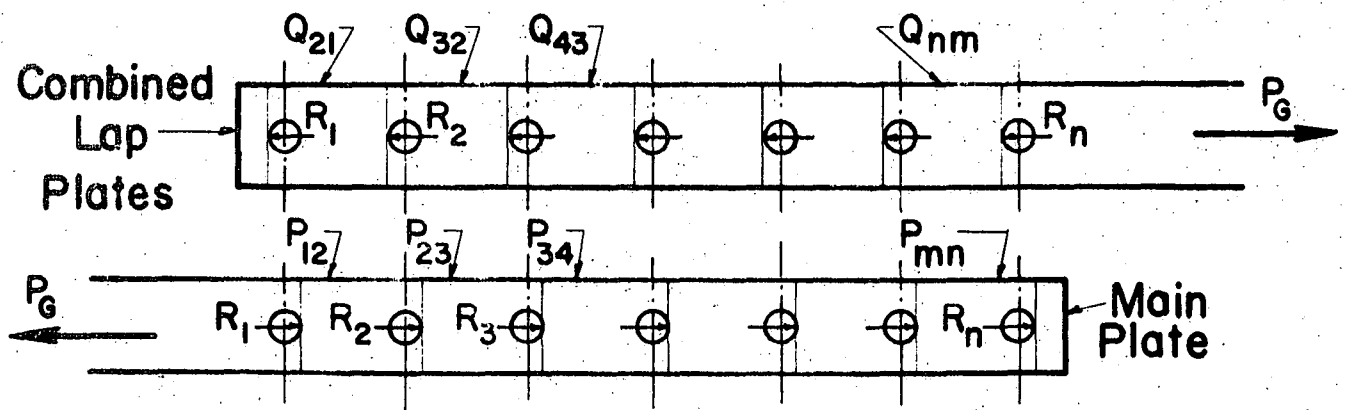


FIG. 2.6 POSSIBLE LOAD TRANSFER DIAGRAM



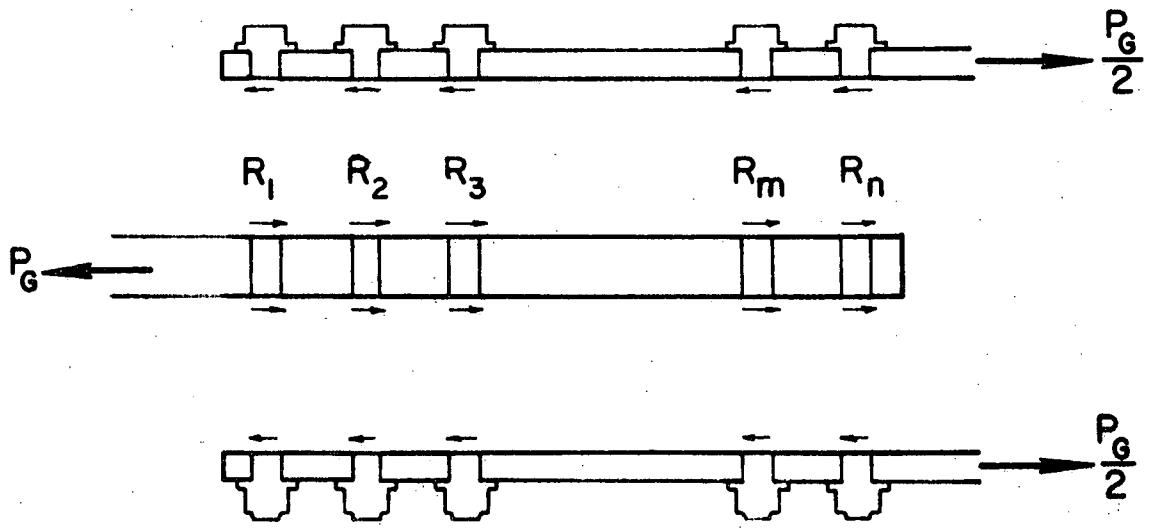
a. Idealized Load Transfer Diagram



b. Force Zones

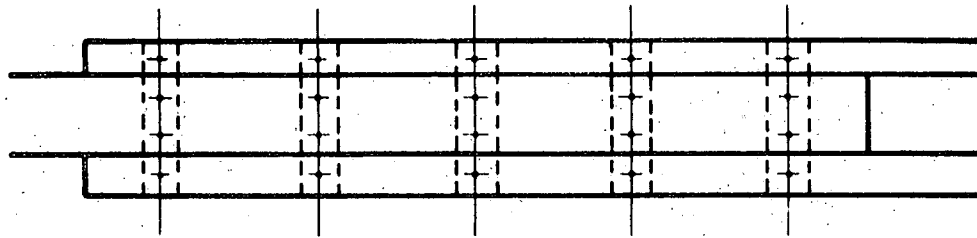
FIG. 2.7 IDEALIZED LOAD TRANSFER DIAGRAM



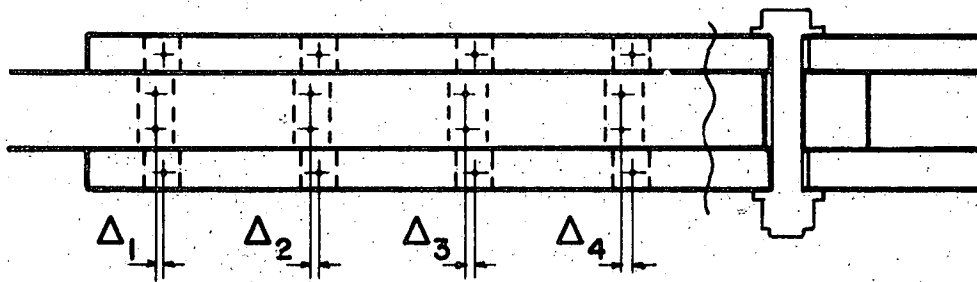


$$\Sigma F_H = 0; \quad P_G - R_1 - R_2 \dots - R_n = 0$$

FIG. 2.8 EQUILIBRIUM CONDITION

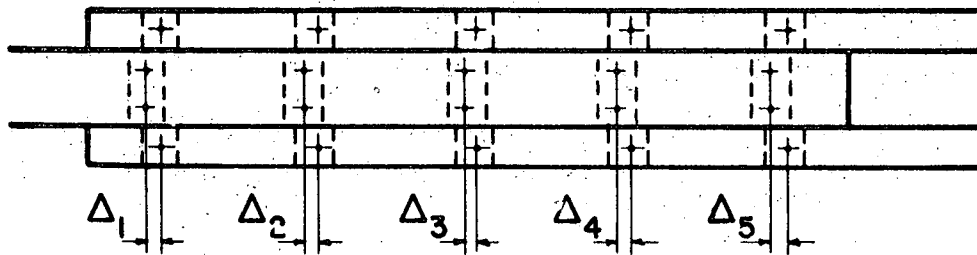


a. No Load Holes Aligned



$$\Delta_1 = \Delta_2 = \dots = \Delta_n = c$$

b. Erected in Complete Bearing (D.L. Negl.)



$$\Delta_1 \neq \Delta_2 \neq \Delta_3$$

c. Under Load

FIG. 2.9 PLATE REFERENCE POINTS

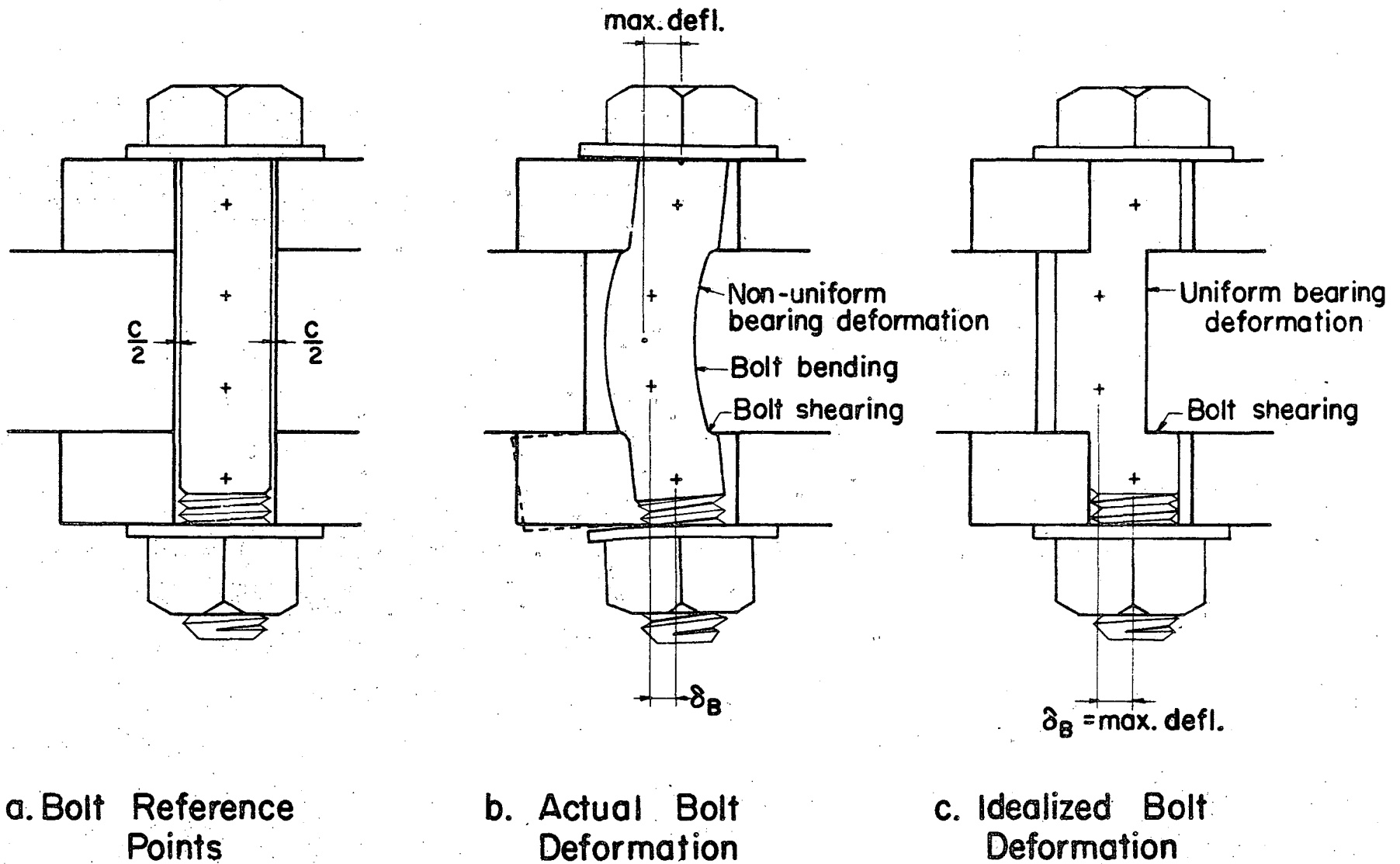


FIG. 2.10 BOLT REFERENCE POINTS

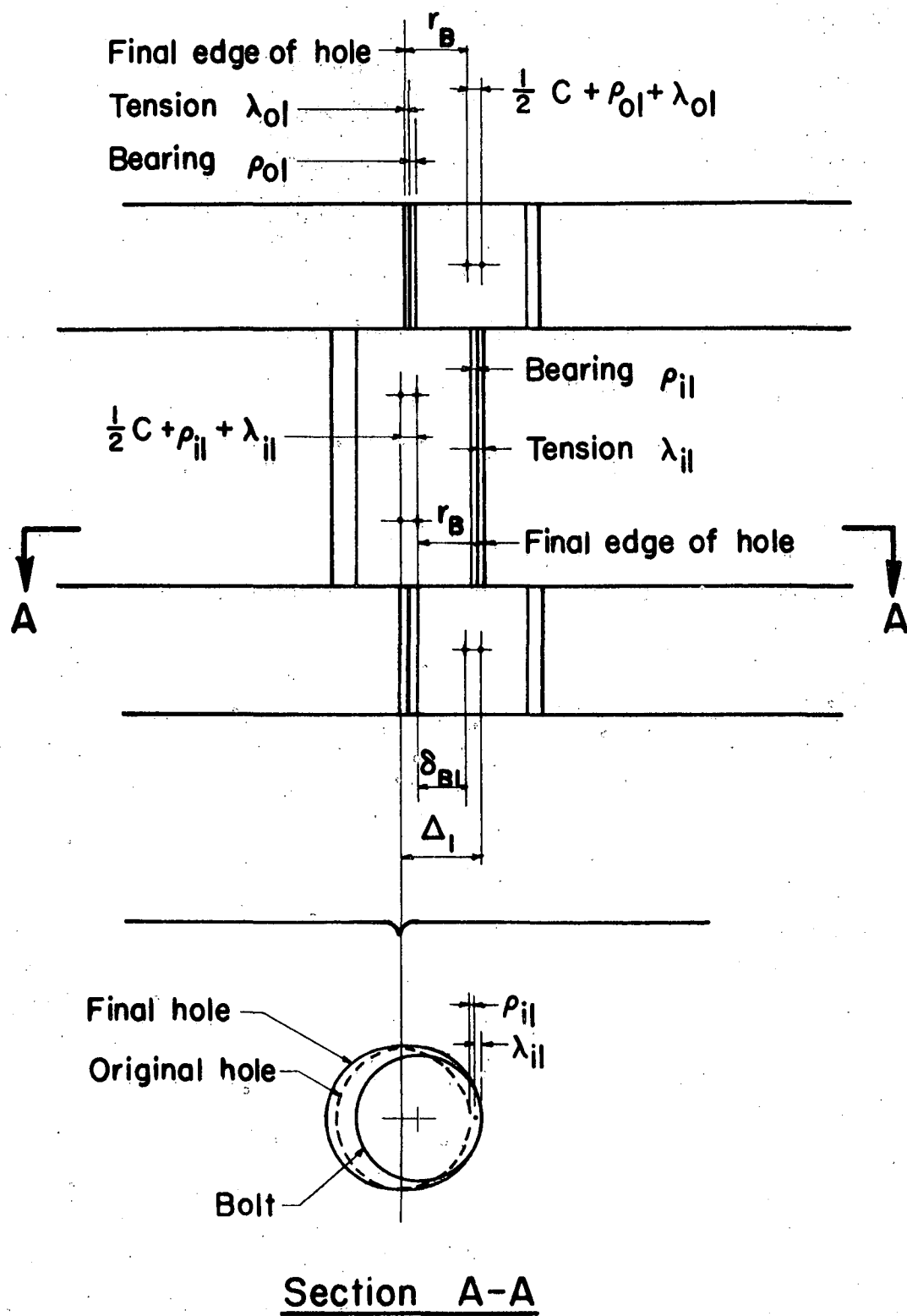


FIG. 2.11 RELATION OF HOLE AND BOLT OFFSETS

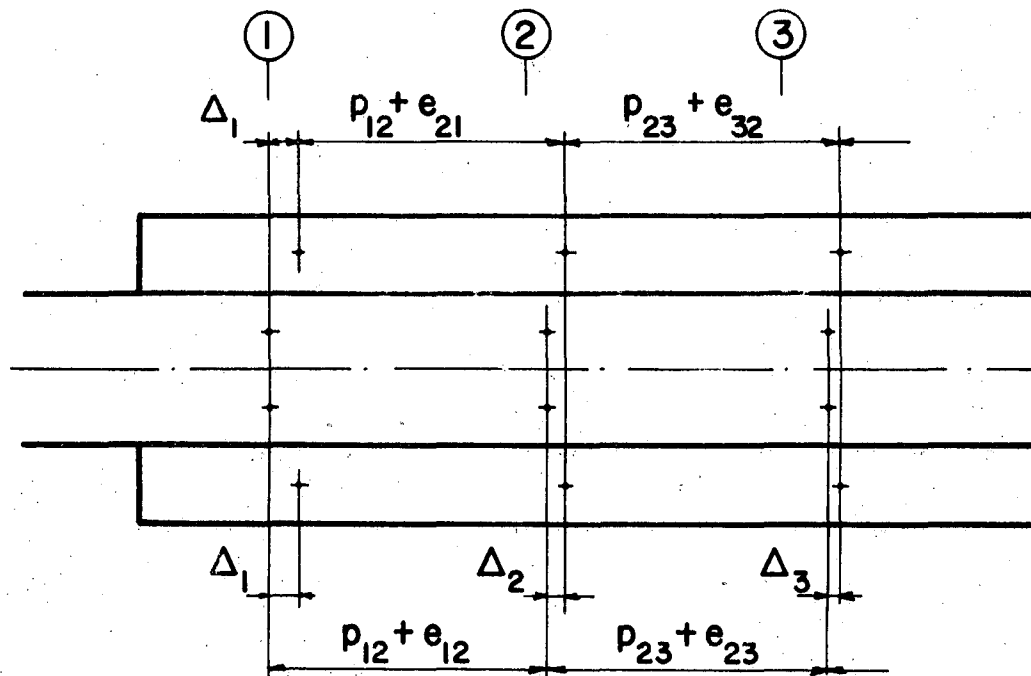


FIG. 2.12 COMPATIBILITY CONDITION

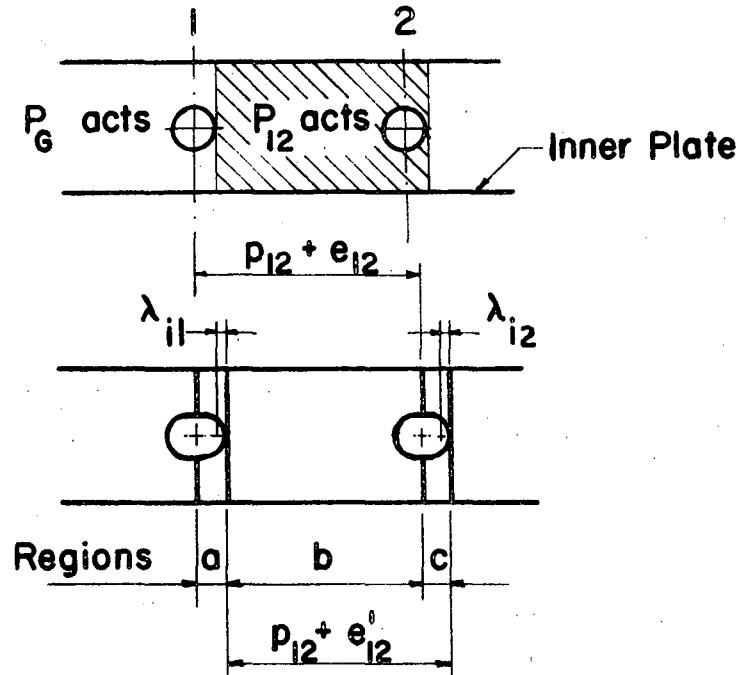


FIG. 2.13 PLATE ELONGATION RELATIONS

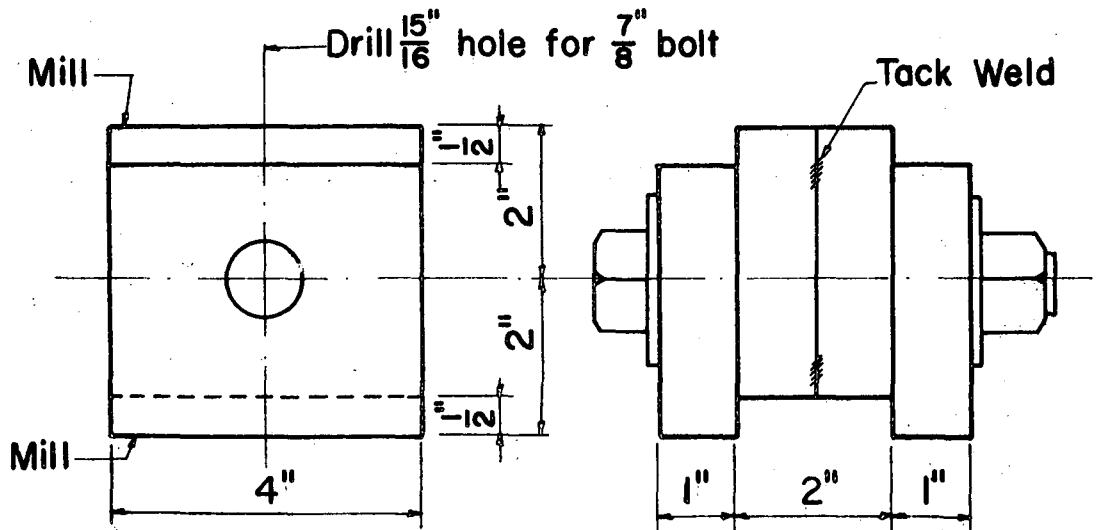
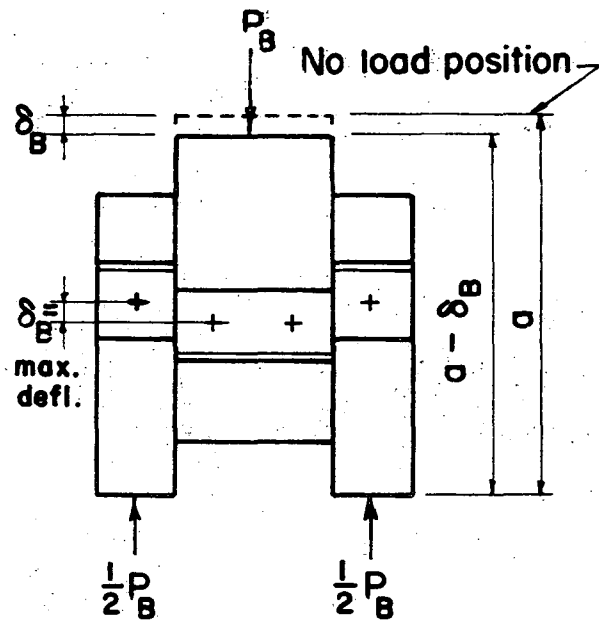
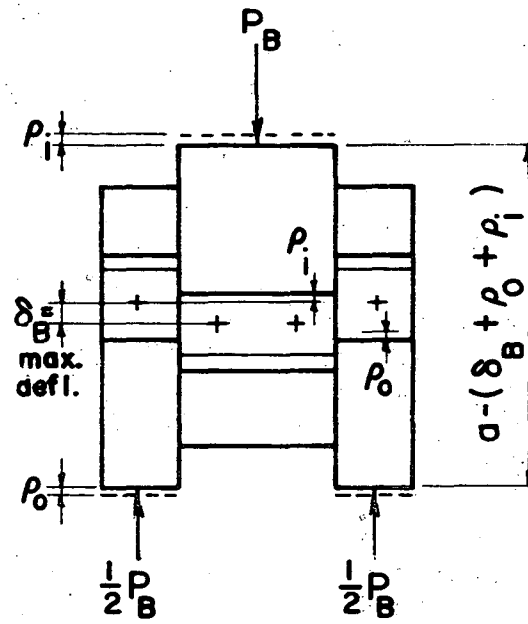


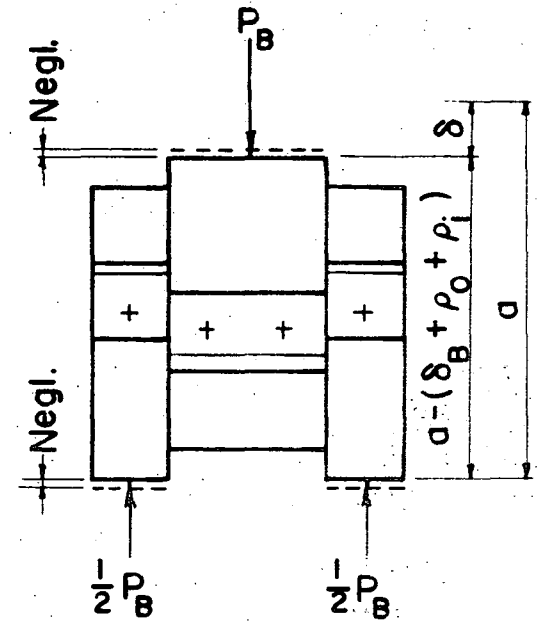
FIG. 2.14 COMPRESSION SHEAR JIG



**a. STEP 1.**  
Shear of Bolt Only



**b. STEP 2**  
Uniform Bearing Deform.



**c. STEP 3**  
Compression of Plates

FIG. 2.15 IDEALIZED BEHAVIOR OF SHEAR JIG

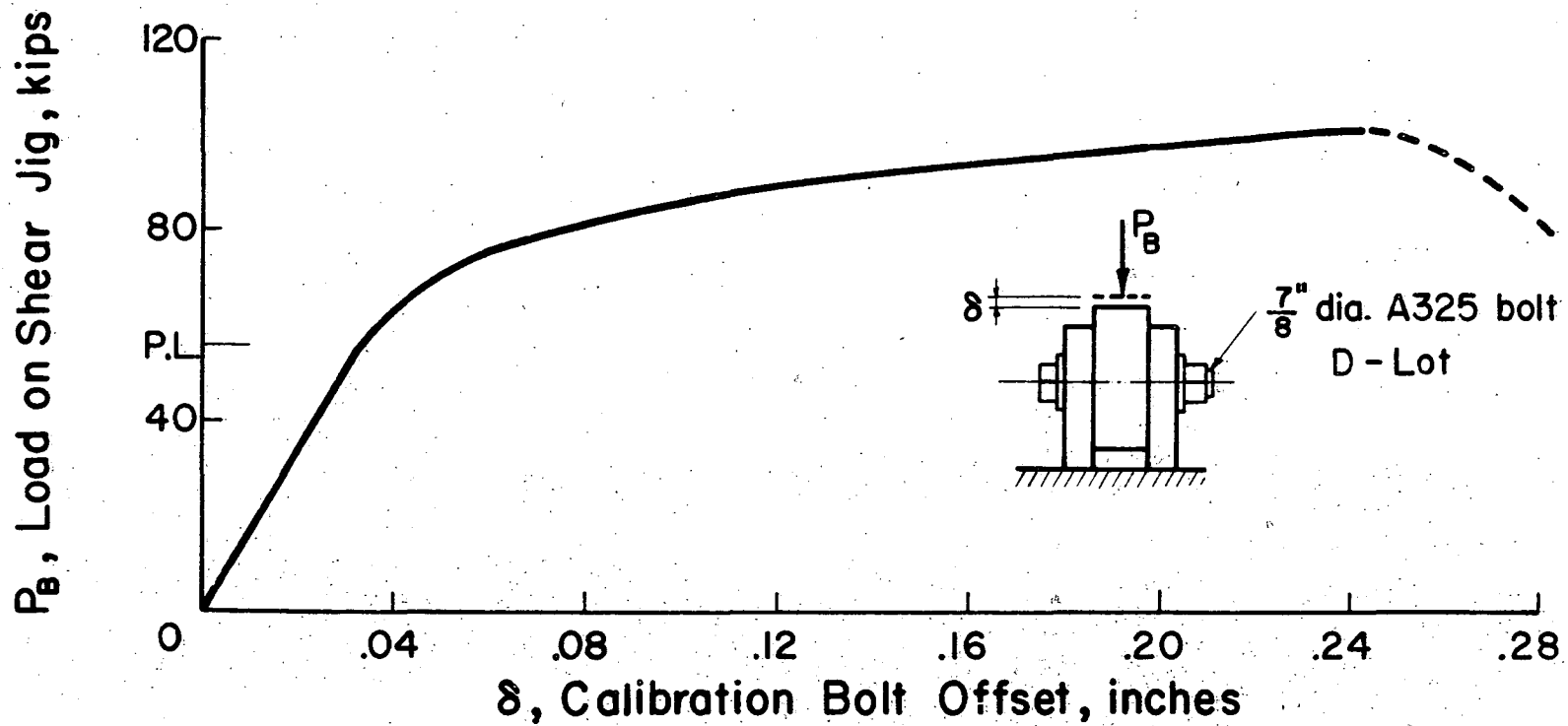
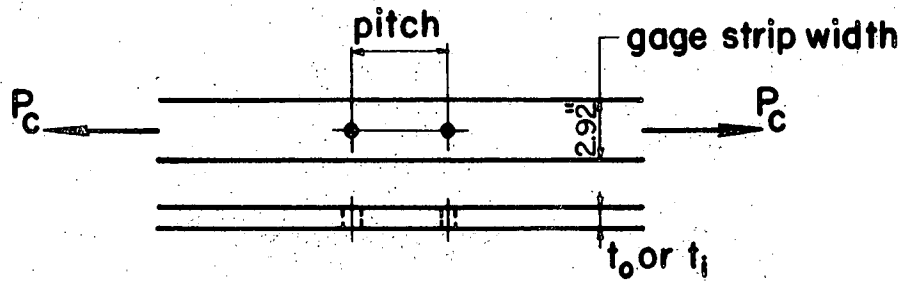
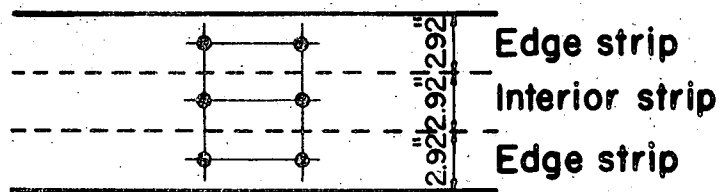


FIG. 2.16 AVERAGE BOLT SHEAR CALIBRATION CURVE

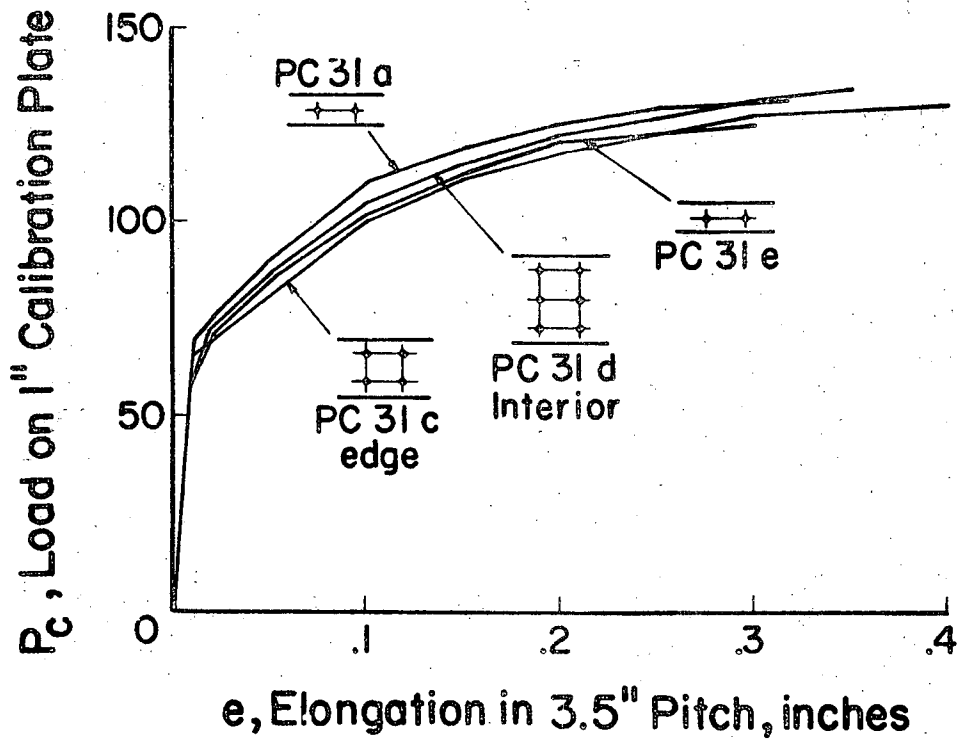




**a. Single Gage Calibration Plate**

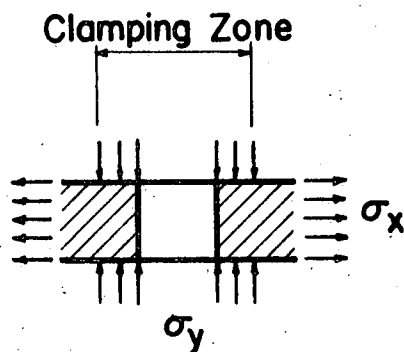


**b. Multiple Gage Calibration Plate**

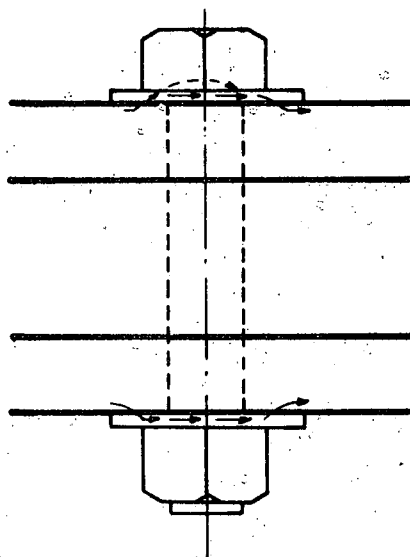


**c. Effect of Type**

FIG. 2.17 TYPES OF PLATE CALIBRATION SPECIMENS

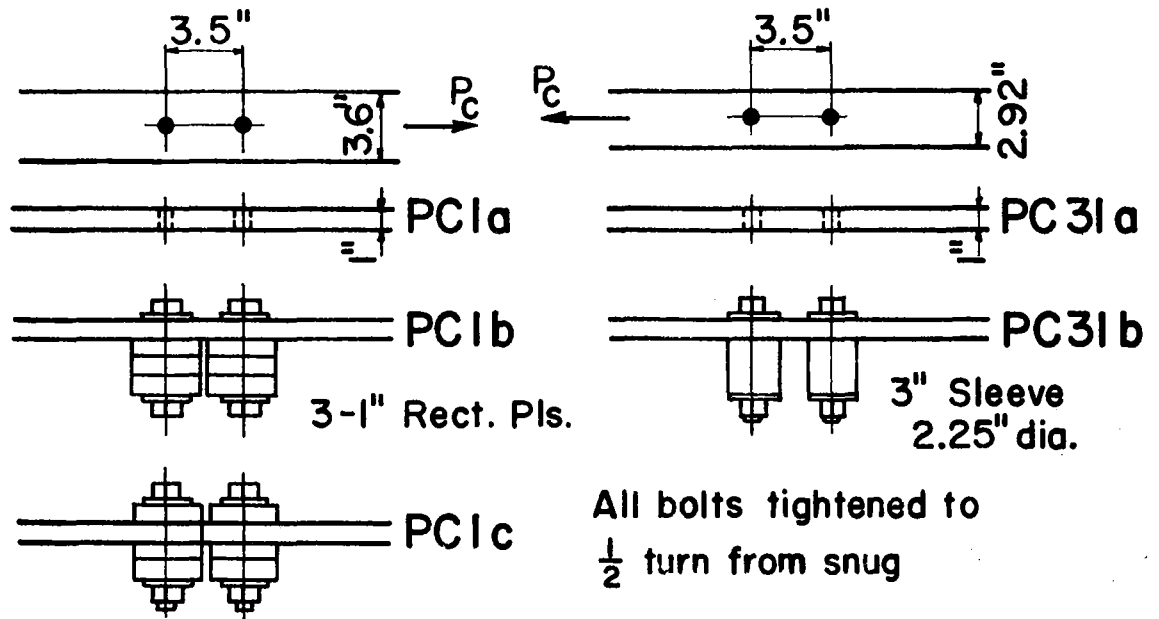


**a. Stress Condition at Holes**

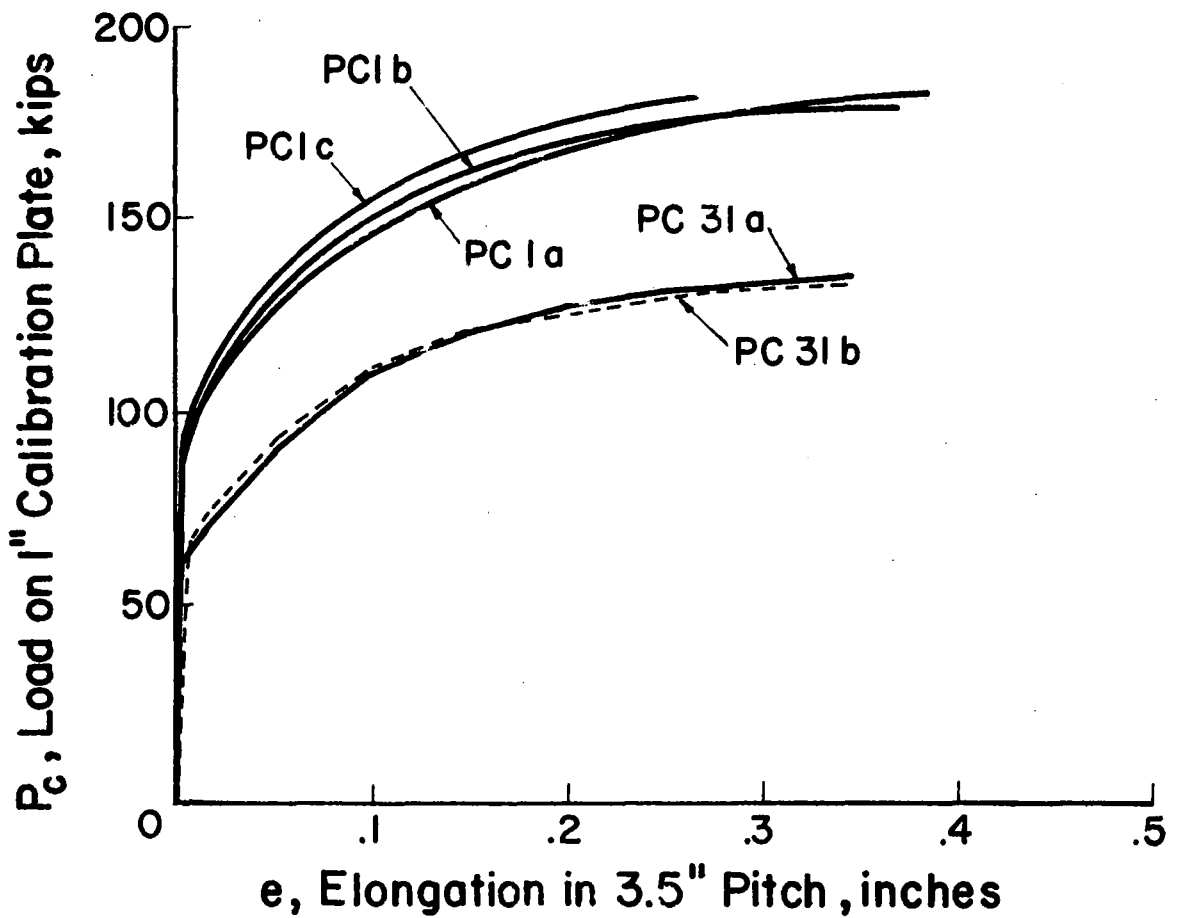


**b. By-pass of Stress through Washers**

FIG. 2.18 CONDITIONS AT HOLES

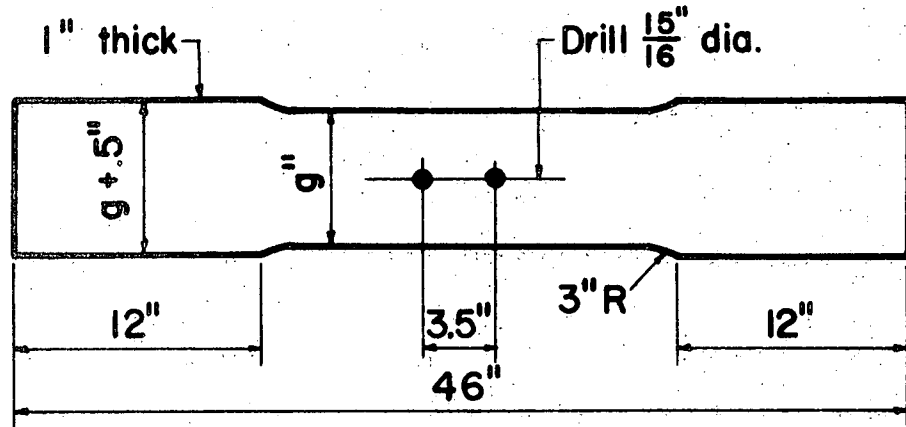


**a. Types of Specimens**



**b. Effect of Type**

FIG. 2.19 BOLTED PLATE CALIBRATION SPECIMENS



Mark	$g$ , in.
PC 3  e	2.92
PC 4  a	3.58
PC 5  a	4.24
PC 6  b	4.90
PC 7  b	5.56
PC 8  b	6.22
PC 9  b	6.88
PC 10  a	7.54

FIG. 2.20 DIMENSIONS OF PLATE CALIBRATION SPECIMENS

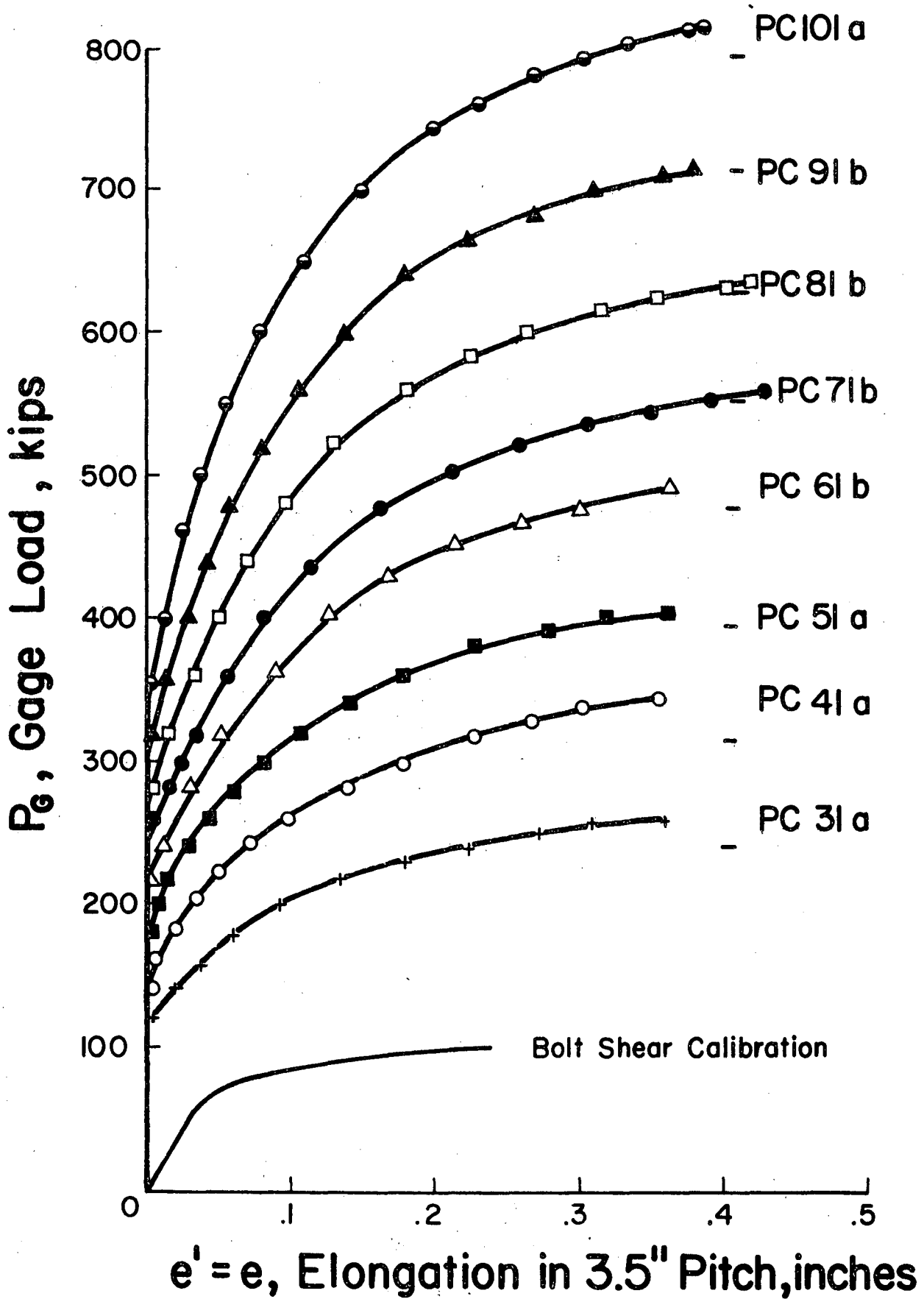


FIG. 2.21 PLATE CALIBRATION CURVES

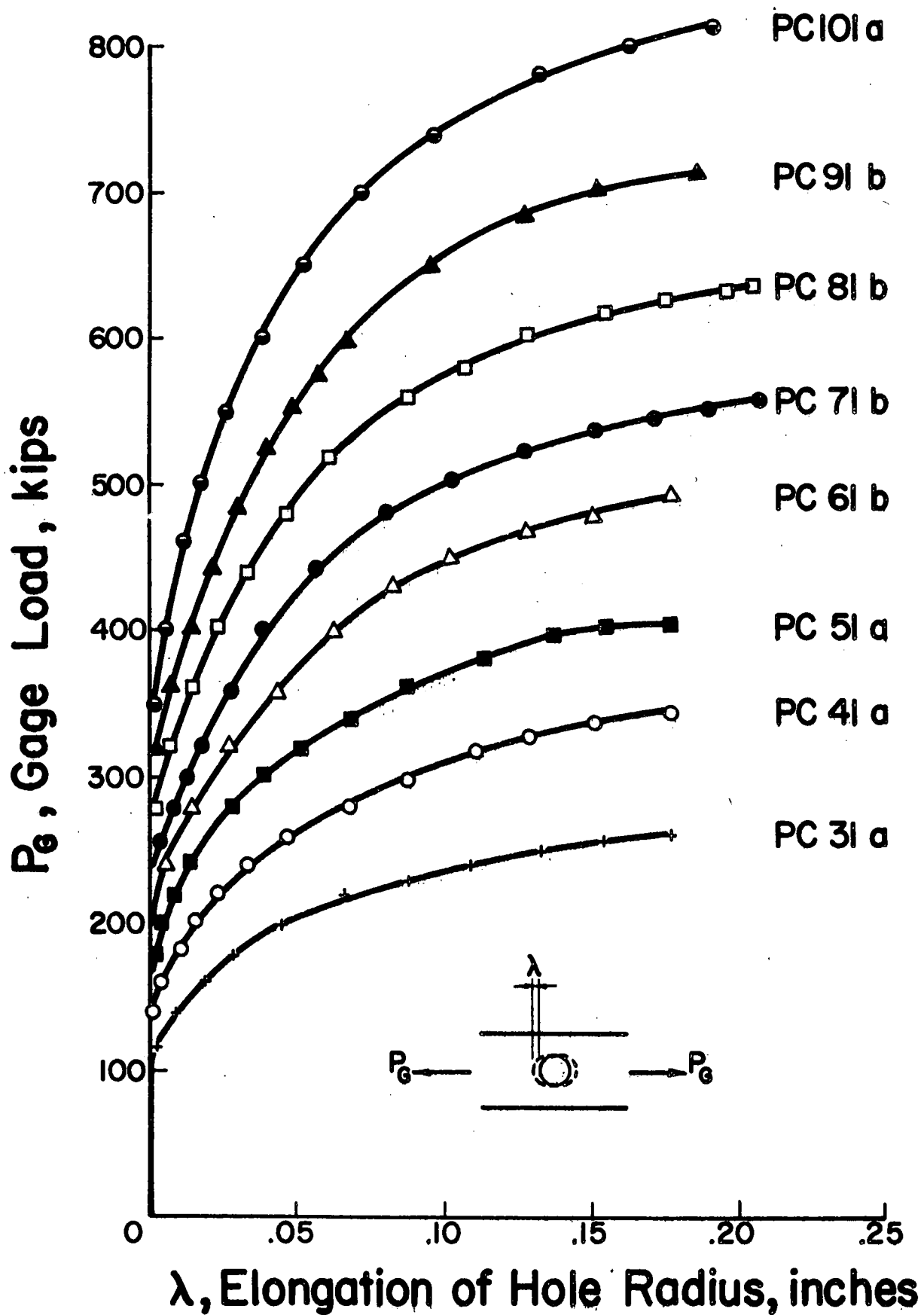


FIG. 2.22 HOLE CALIBRATION CURVES

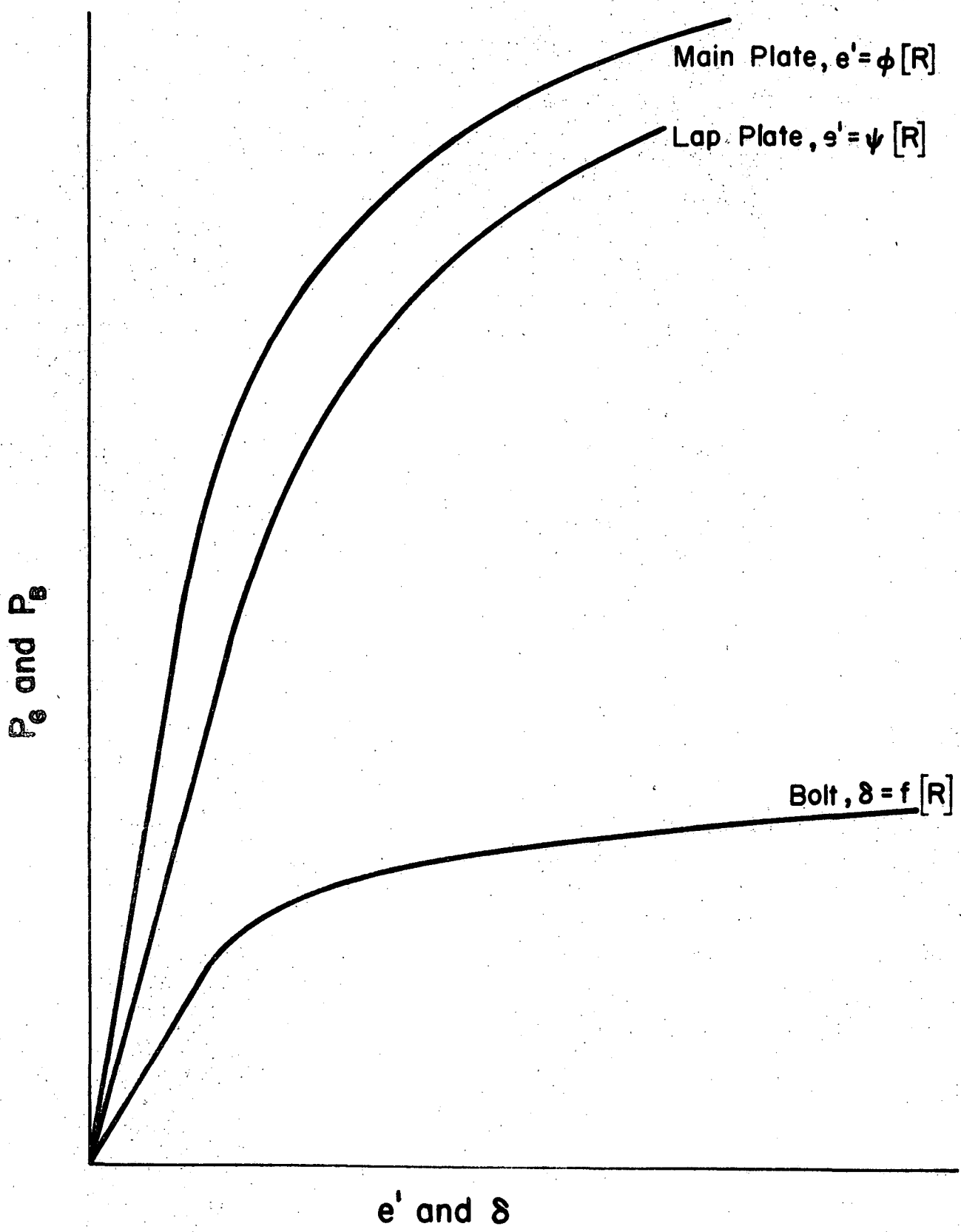


FIG. 2.23 ASSUMED CALIBRATION CURVES

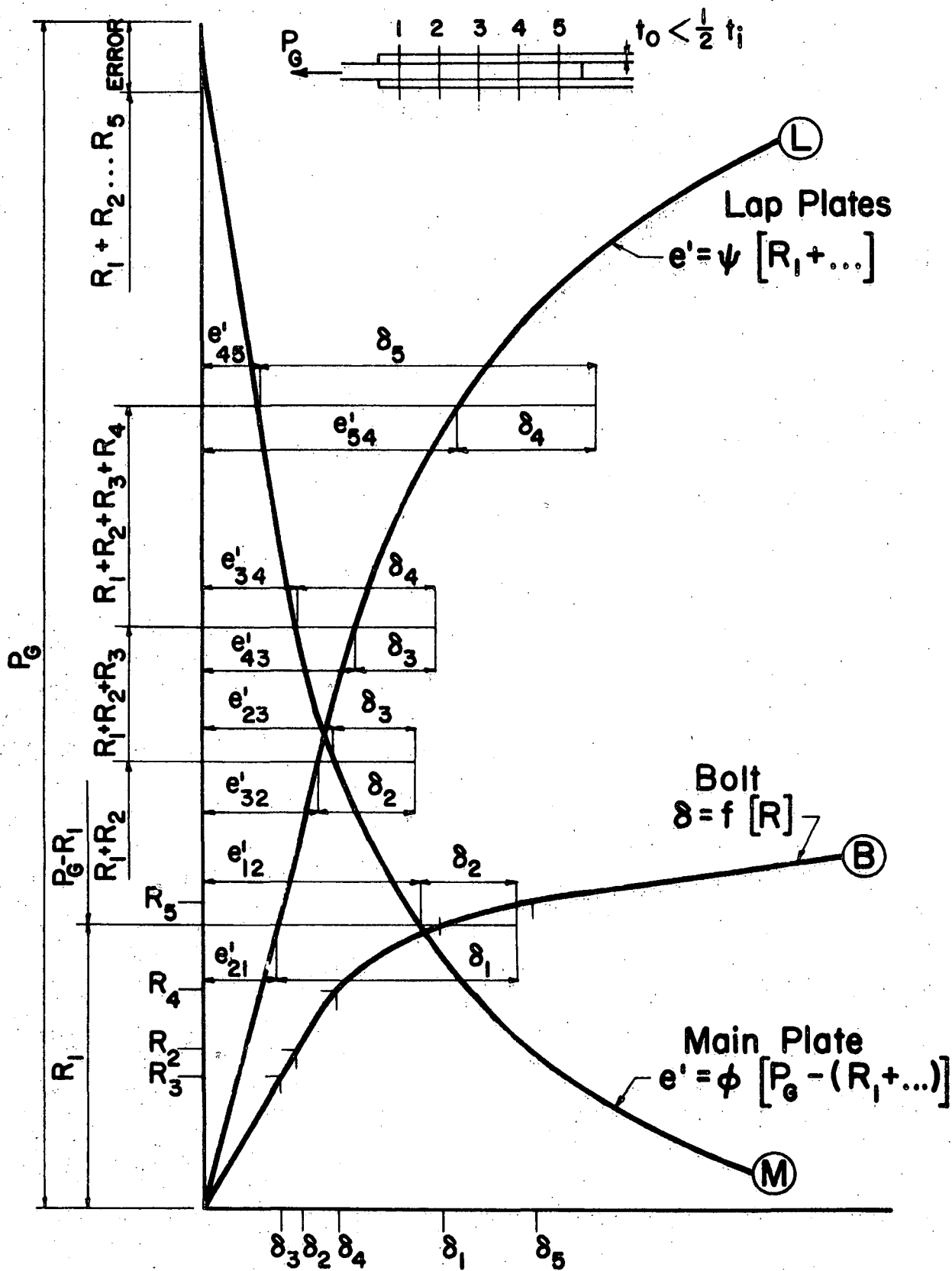


FIG. 2.24 SOLUTION OF EQUATIONS - GENERAL CASE



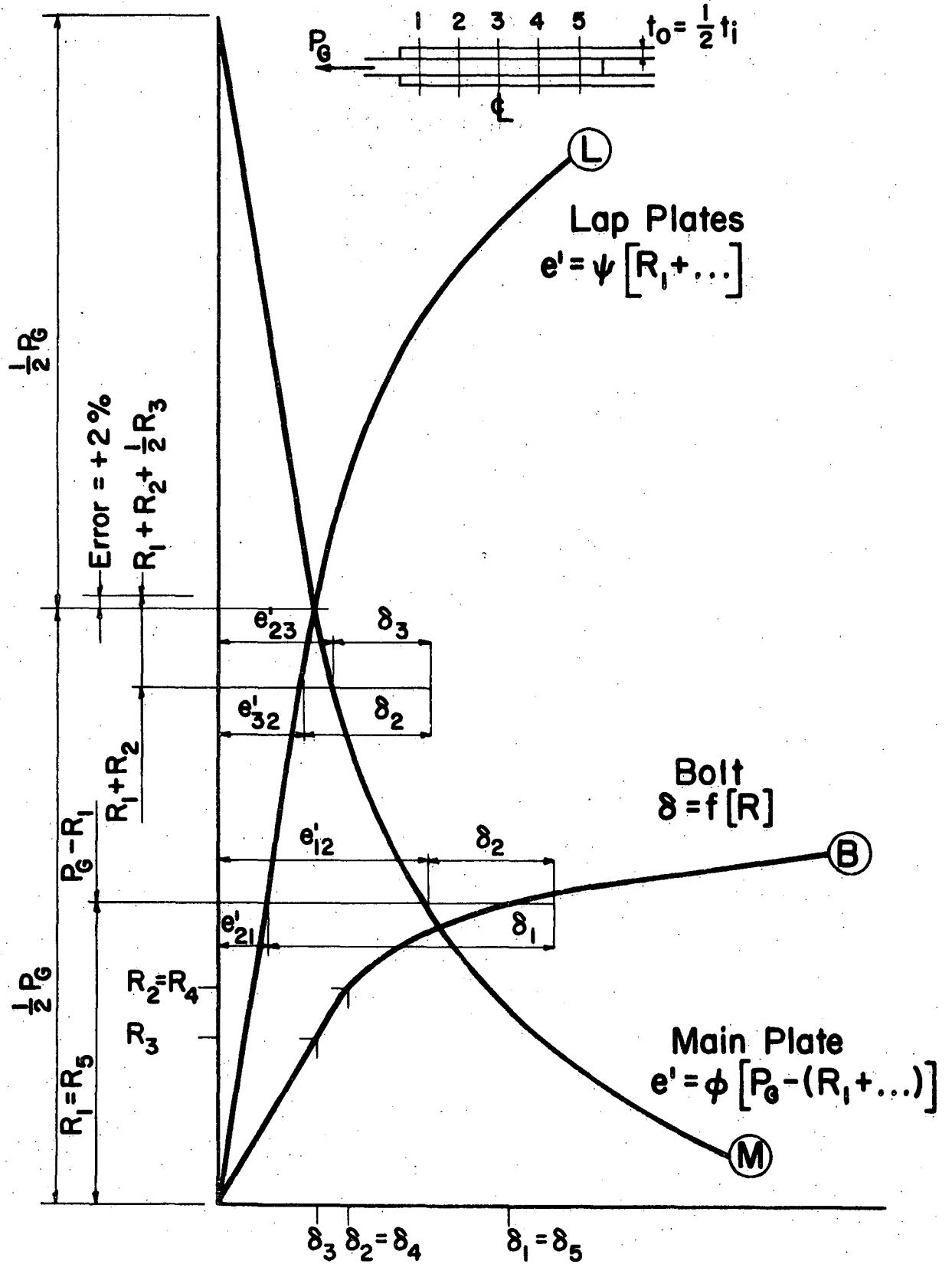
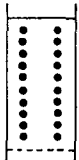
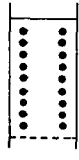
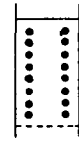

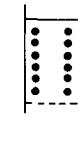
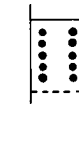




FIG. 2.25 SOLUTION OF EQUATIONS - SYMMETRICAL CASE

TABLE 3.1 Results of Joint Tests, D-Series - Part a

ITEM	UNITS	D101	D91	D81	D71	D61	D51	D41	D31
<b>PATTERN</b>									
All holes drilled $\frac{15}{16}$ "									
All pitches $3\frac{1}{2}$ "									
Gage = $\frac{1}{2}$ " width									
<b>BOLTS</b>									
No. in line		10	9	8	7	6	5	4	3
No. of $\frac{7}{8}$ " A325 bolts		20	18	16	14	12	10	8	6
Nom. shear area (=actual)	sq in	24.04	21.64	19.23	16.83	14.42	12.02	9.62	7.21
<b>PLATES</b>									
Nom. width	in	15.10	13.78	12.46	11.12	9.80	8.48	7.16	5.84
Nom. thickness	in	2 @ 1/2	2	2	2	2	2	2	2
Nom. gross area	sq in	30.20	27.56	24.92	22.24	19.60	16.96	14.32	11.68
Nom. net area	sq in	26.45	23.81	21.17	18.49	15.85	13.21	10.57	7.93
% dev. in net area	%	-1.51	-0.38	-0.80	-1.68	-1.96	-0.38	0	-1.13
<b>T/S RATIO (<math>A_g/A_{net}</math>)</b>									
Nominal		1:1.10	1:1.10	1:1.10	1:1.10	1:1.10	1:1.10	1:1.10	1:1.10
Actual		1:1.08	1:1.10	1:1.09	1:1.08	1:1.08	1:1.09	1:1.10	1:1.09
<b>WORKING LOAD (<math>T=20,000</math> <math>S=22,000</math>)</b>	kips	529	476	423	370	317	264	212	159
<b>SLIP LOAD (First Major)</b>	kips	568	405	560	358	338	348	234	176
Nom. bolt shear	ksi	23.6	18.8	29.1	21.3	23.4	29.0	24.3	24.4
Nom. tens. - net sect.	ksi	21.5	17.0	26.5	19.4	21.3	26.3	22.1	22.1
Avg. elongation of bolts	in	.0381	.0368	.0329	.0310	.0313	.0324	.0267	.0249
Clamping force per bolt*	kips	53.1	53.0	52.3	52.0	52.0	52.1	51.0	50.6
Slip coefficient		.267	.212	.335	.246	.271	.334	.287	.289
<b>TYPE OF FAILURE</b>		bolt	bolt	bolt	bolt	plate	plate	plate	plate
Load at failure	kips	1506	1358	1282	1126	994	850	690	514
Nom. bolt shear	ksi	62.6	62.8	66.7	66.9	68.9	70.7	71.7	71.3
Nom. tens. - net sect.	ksi	57.0	57.1	60.6	60.8	62.6	64.3	65.3	64.6
Act. tens. - net sect.	ksi	57.8	57.3	61.0	61.9	64.0	64.6	65.3	65.5
<b>EFFICIENCY %</b>									
g/d						5.23	4.52	3.82	3.11
Theoretical						80.9	77.9	73.8	67.8
Test						85.6	83.5	79.6	74.0
Net						105.8	107.2	107.8	109.1

\*As measured from the direct tension calibration curve

TABLE 3.2

JOINT D91 - PLATE ELONGATIONS

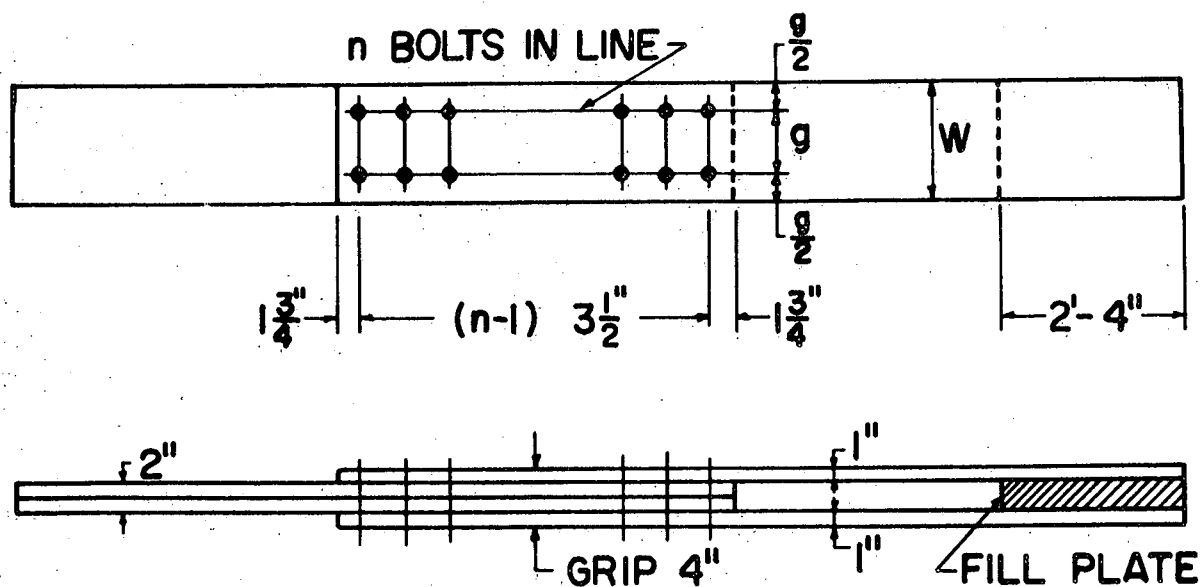
GAGE LOAD, P <sub>G</sub> kips	300	350	400	450	500	550	600	650	679
<u>SLIP GAGE, inches</u>									
	.0866	.0951	.1251	.1631	.2111	.2791	.3621	.4791	.5681
<u>PITCH ELONGATIONS, inches</u>									
e01	.0029	.0053	.0160	.0320	.0500	.0740	.1080	.1425	.1715
e21	.0000	.0000	.0000	.0000	.0000	.0000	.0000	.0000	.0000
e12	.0029	.0053	.0150	.0280	.0450	.0665	.0950	.1355	.1605
e32	.0004	.0005	.0006	.0007	.0008	.0009	.0009	.0010	.0011
e23	.0025	.0039	.0086	.0180	.0280	.0420	.0600	.0855	.1030
e43	.0007	.0009	.0011	.0012	.0015	.0018	.0021	.0025	.0030
e34	.0018	.0026	.0039	.0070	.0140	.0225	.0325	.0460	.0570
e54	.0009	.0011	.0014	.0018	.0024	.0031	.0043	.0085	.0105
e45	.0014	.0018	.0024	.0031	.0048	.0090	.0159	.0225	.0295
e65	.0011	.0015	.0019	.0024	.0042	.0078	.0140	.0225	.0295
e56	.0011	.0013	.0017	.0021	.0027	.0035	.0048	.0080	.0130
e76	.0017	.0024	.0033	.0060	.0129	.0209	.0295	.0430	.0520
e67	.0007	.0008	.0010	.0011	.0012	.0014	.0017	.0023	.0028
e87	.0023	.0035	.0081	.0165	.0252	.0390	.0565	.0780	.0955
e78	.0004	.0004	.0005	.0006	.0006	.0007	.0008	.0008	.0009
e98	.0029	.0046	.0140	.0269	.0440	.0640	.0900	.1245	.1540
e89	.0000	.0000	.0000	.0000	.0000	.0000	.0000	.0000	.0000
e <sub>x9</sub>	.0033	.0051	.0165	.0295	.0475	.0675	.0950	.1280	.1605

TABLE 3.3

JOINT D91 - CHECK OF ELONGATIONS AND CALCULATED HOLE OFFSETS

GAGE LOAD, P <sub>G</sub> kips	300	350	400	450	500	550	600	650	679
$\Sigma$ MAIN PLATE PITCH ELONGATIONS AND SLIP GAGE READING, inches	.1003	.1165	.1742	.2550	.3574	.4987	.6808	.9222	1.1063
OVERALL ELONGATION, inches	.1075	.1265	.1825	.2595	.3655	.5125	.6935	.9555	1.1465
DIFFERENCE, inches	.0072	.0100	.0083	.0045	.0081	.0138	.0127	.0333	.0402
PERCENT DIFFERENCE	6.7	7.9	4.5	1.7	2.2	2.7	1.8	3.5	3.5
HOLE OFFSETS, inches									
$\Delta_9$	.0833	.0900	.1086	.1336	.1636	.2116	.2671	.3511	.4076
$\Delta_8$	.0804	.0854	.0946	.1067	.1196	.1476	.1771	.2266	.2536
$\Delta_7$	.0785	.0823	.0870	.0908	.0950	.1093	.1214	.1494	.1590
$\Delta_6$	.0775	.0807	.0847	.0859	.0833	.0898	.0936	.1087	.1098
$\Delta_5$	.0775	.0805	.0845	.0856	.0818	.0855	.0844	.0942	.0933
$\Delta_4$	.0780	.0812	.0855	.0869	.0842	.0914	.0960	.1082	.1123
$\Delta_3$	.0791	.0829	.0883	.0927	.0967	.1121	.1264	.1517	.1663
$\Delta_2$	.0812	.0863	.0963	.1100	.1239	.1532	.1855	.2362	.2682
$\Delta_1$	.0841	.0916	.1113	.1380	.1689	.2197	.2805	.3717	.4287*

\* Bolt failed at 358<sup>k</sup>



MARK	n	GAGE in.	WIDTH in.	$g/d$	SHEAR AREA sq.in.	NET AREA sq.in.	$T/S$
D10I	10	7.55	15.10	8.06	24.04	26.45	1:1.10
D9I	9	6.89	13.78	7.35	21.64	23.81	1:1.10
D8I	8	6.23	12.46	6.65	19.23	21.17	1:1.10
D7I	7	5.56	11.12	5.94	16.83	18.49	1:1.10
D6I	6	4.90	9.80	5.23	14.42	15.85	1:1.10
D5I	5	4.24	8.48	4.52	12.02	13.21	1:1.10
D4I	4	3.58	7.16	3.82	9.62	10.57	1:1.10
D3I	3	2.92	5.84	3.11	7.21	7.93	1:1.10

FIG. 3.1 DIMENSIONS OF JOINTS, D-SERIES - PART a

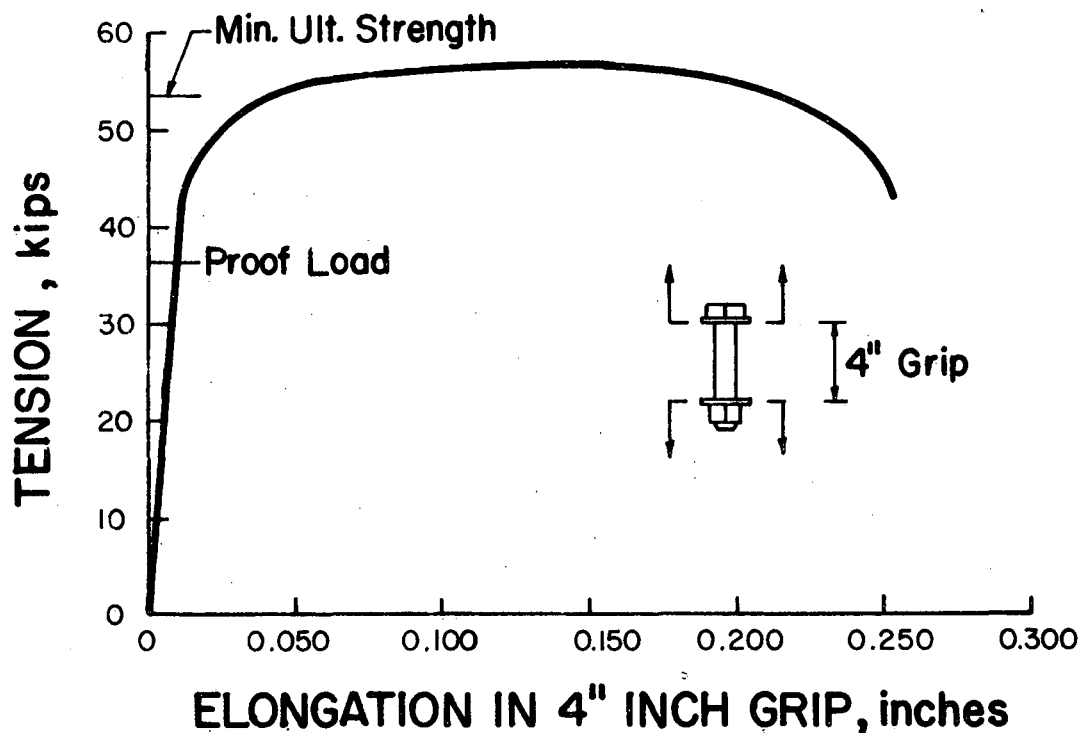


FIG. 3.2 TENSION-ELONGATION CURVE, 7/8" D-LOT BOLT

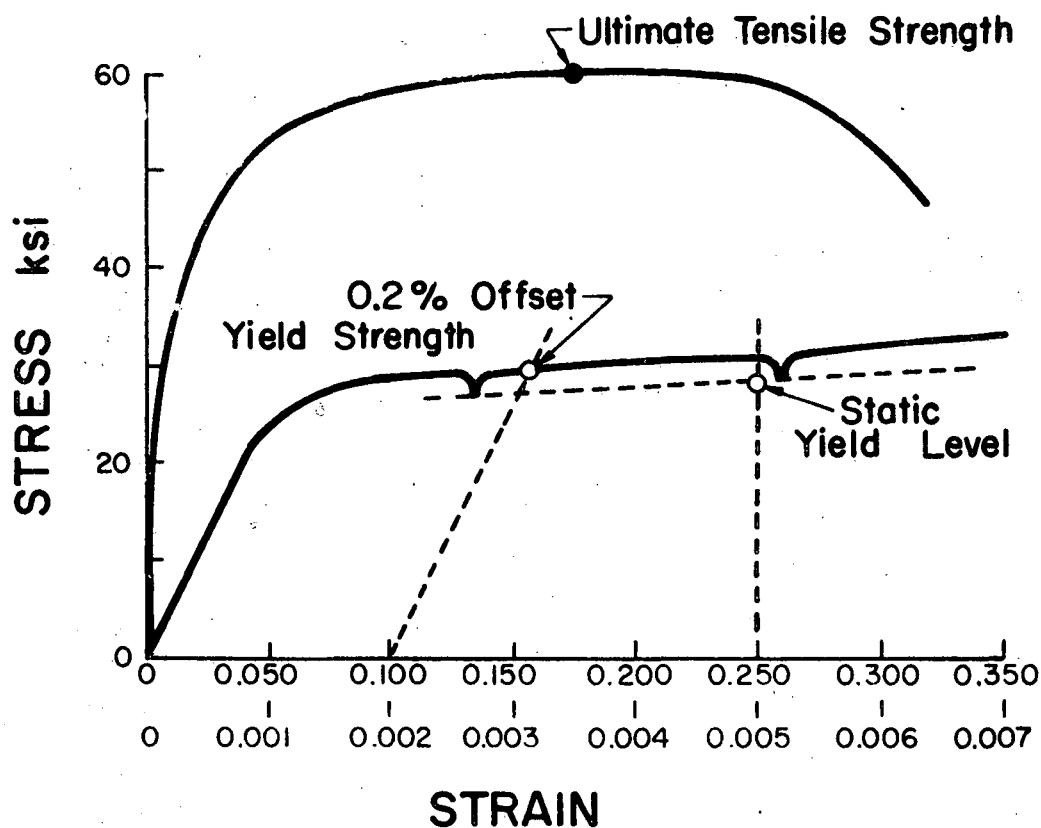


FIG. 3.3 STRESS STRAIN DIAGRAM, A7 PLATE

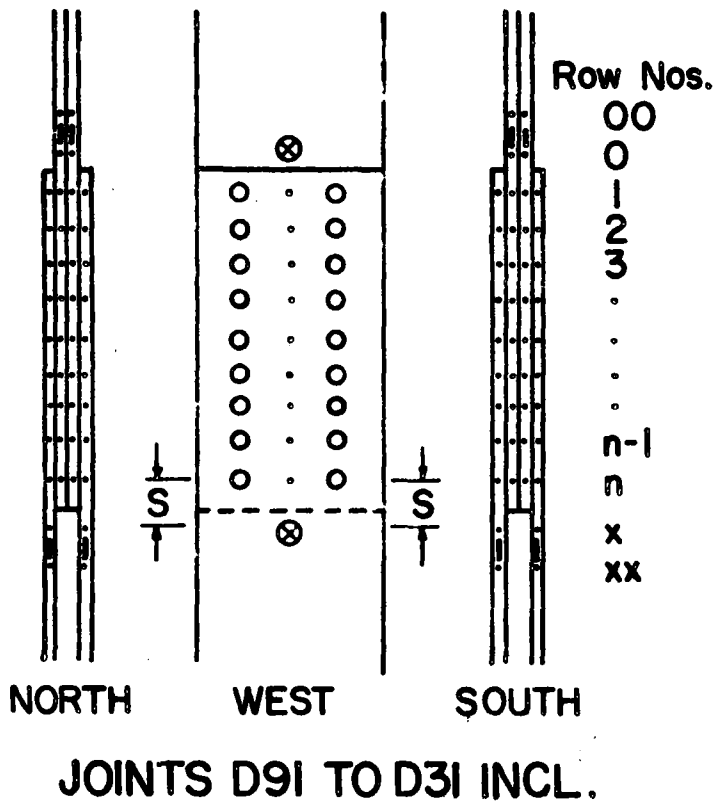
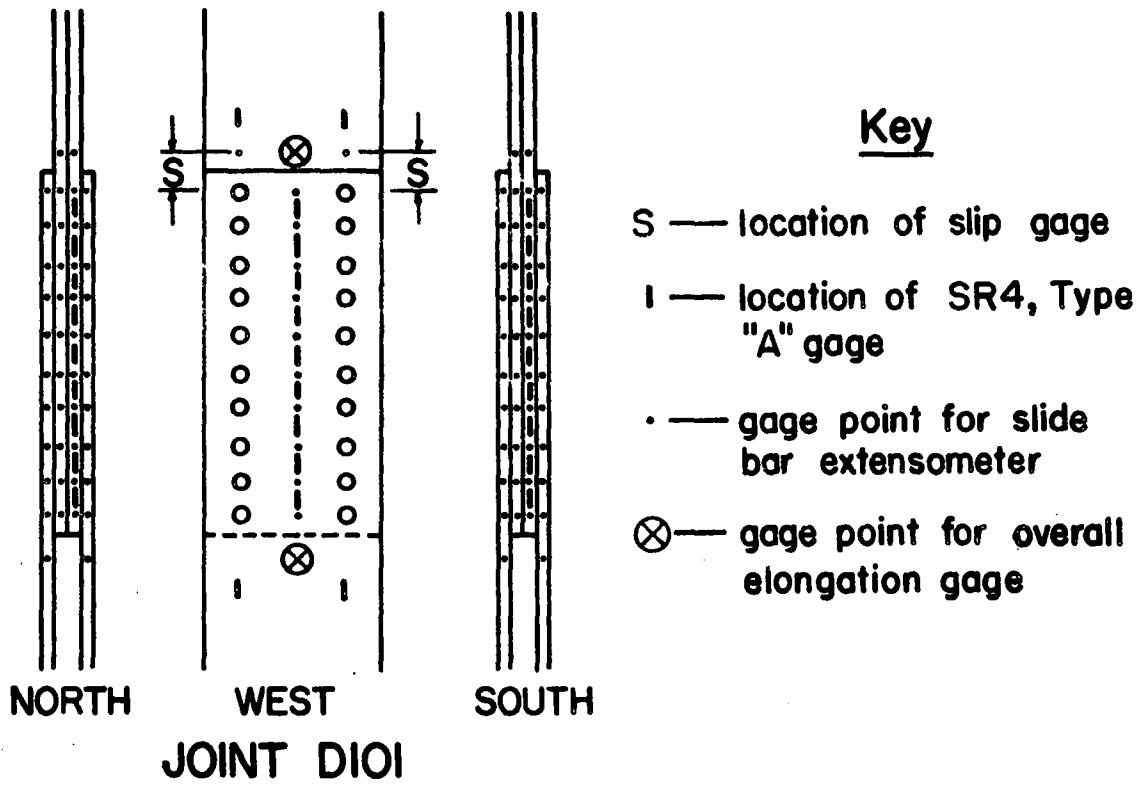


FIG. 3.4 LAYOUT OF INSTRUMENTATION

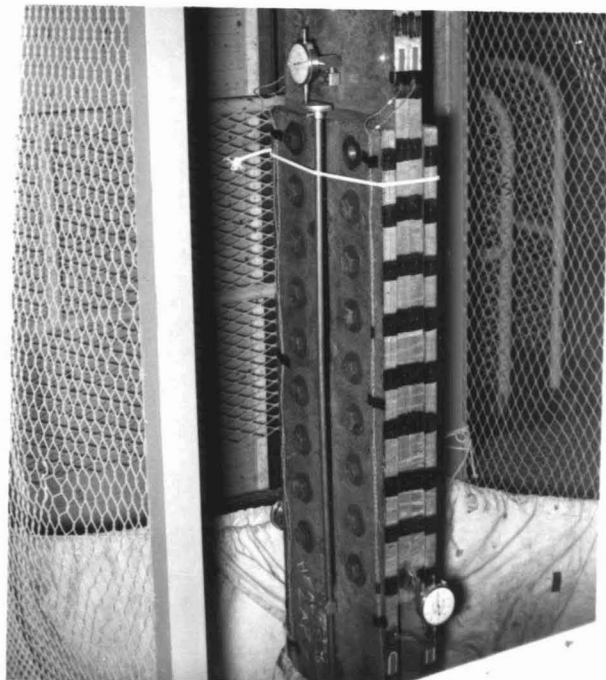


FIG. 3.5 INSTRUMENTATION ON JOINT D91

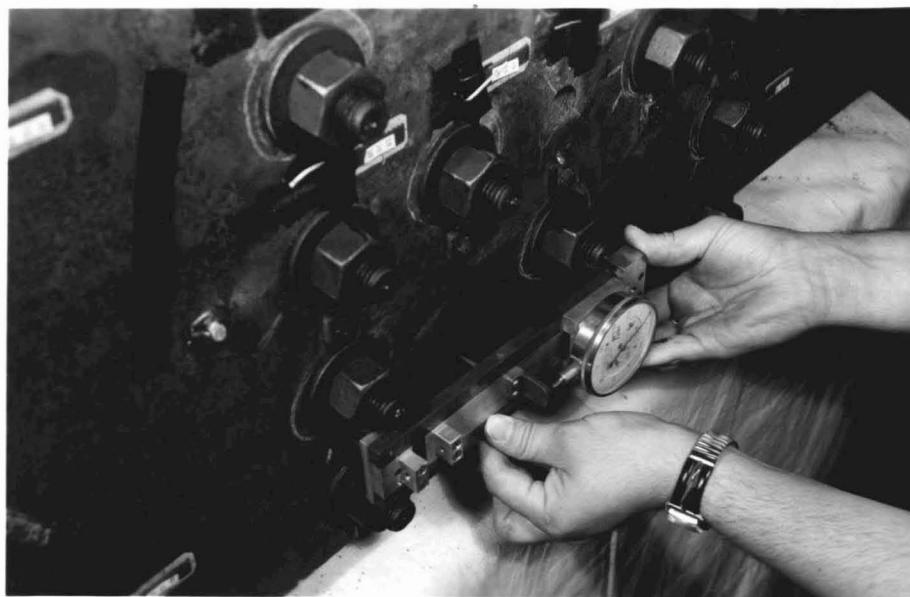
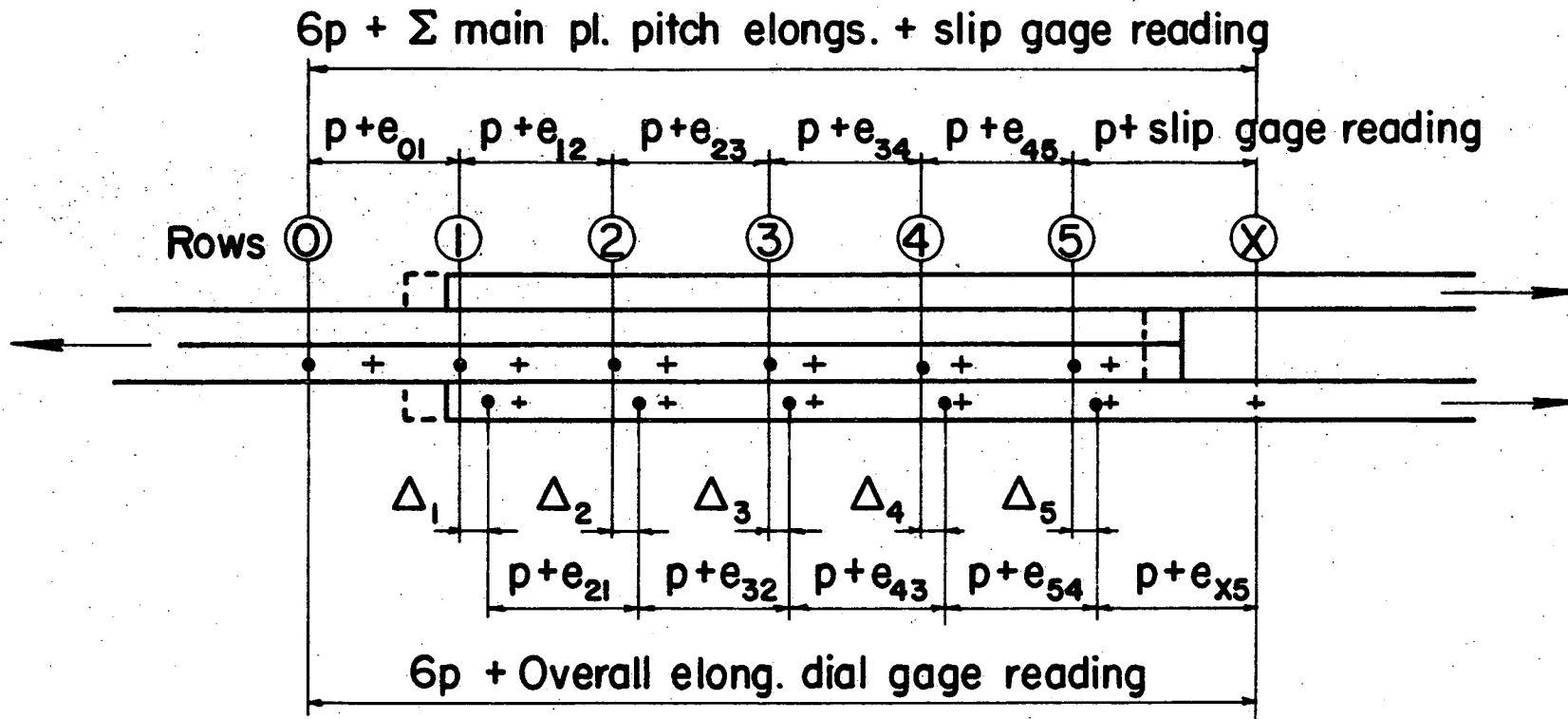


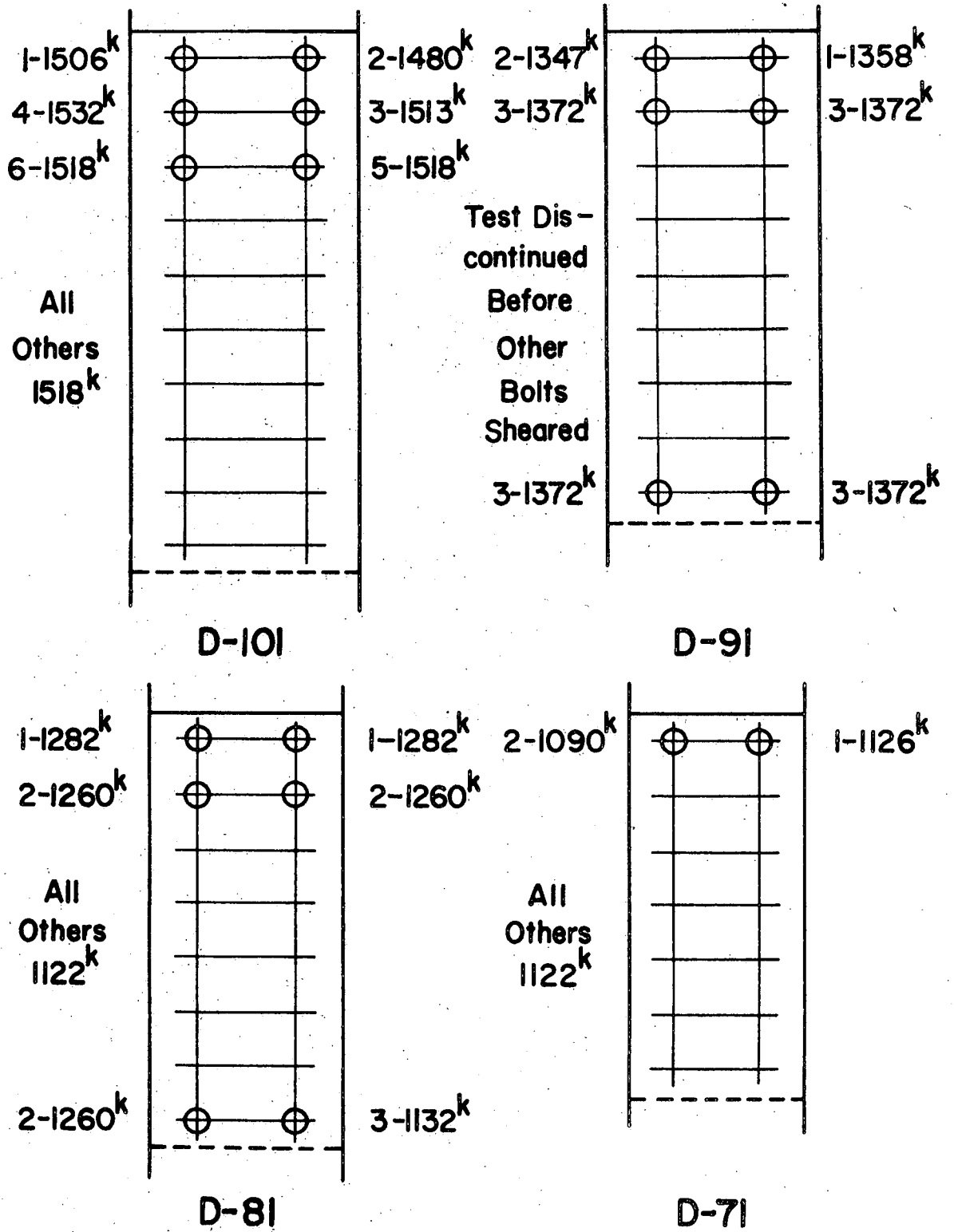
FIG. 3.6 SLIDEBAR EXTENSOMETER





- + Original position of gage point
- Final position of gage point
- p-Original pitch

FIG. 3.7 GEOMETRY OF JOINT IN SLIPPED POSITION



**Note:**  
Bolts Unbuttoned By Shearing At Head End

FIG. 3.8 UNBUTTONING SEQUENCE

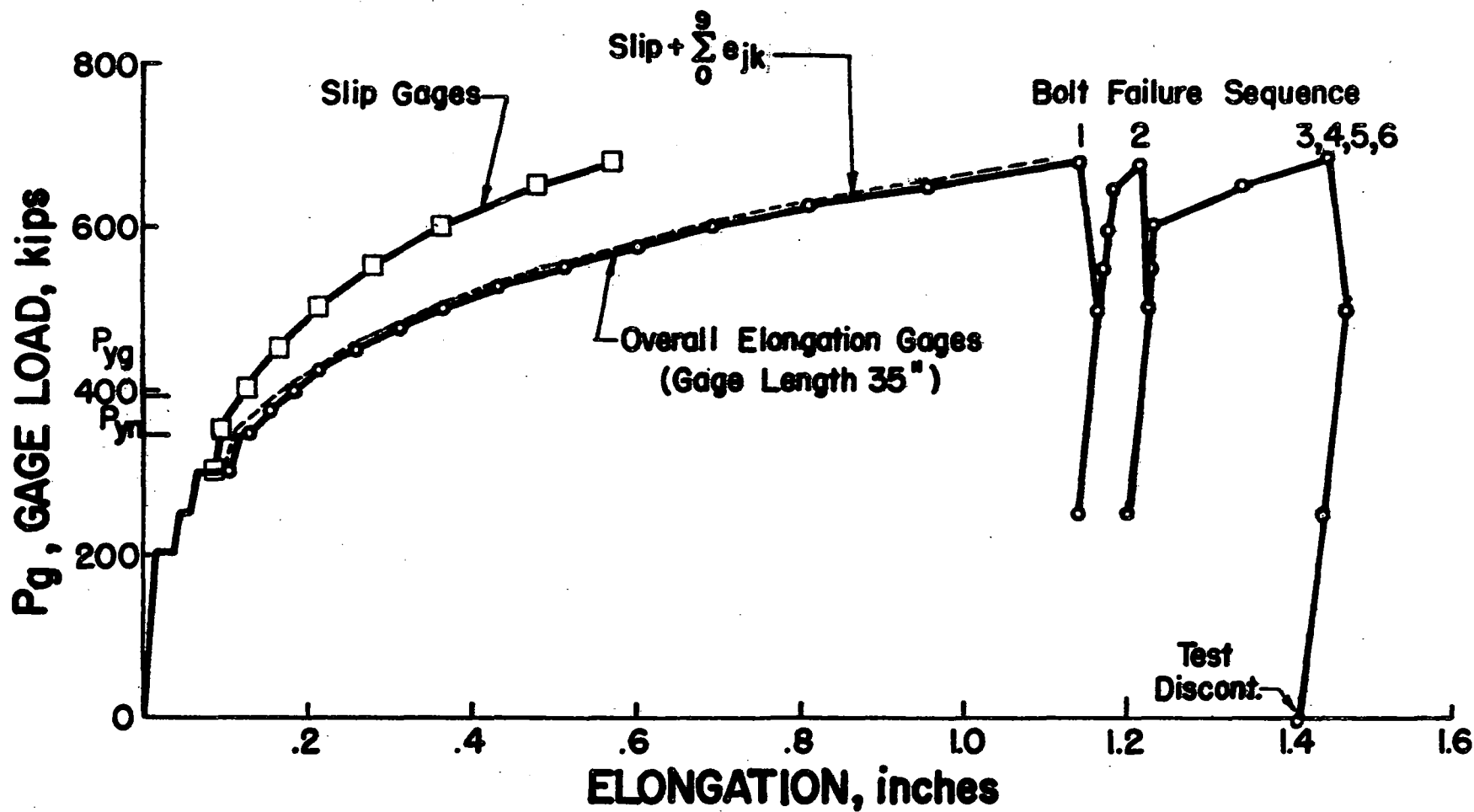


FIG. 3.9 JOINT D91, LOAD-ELONGATION CURVE

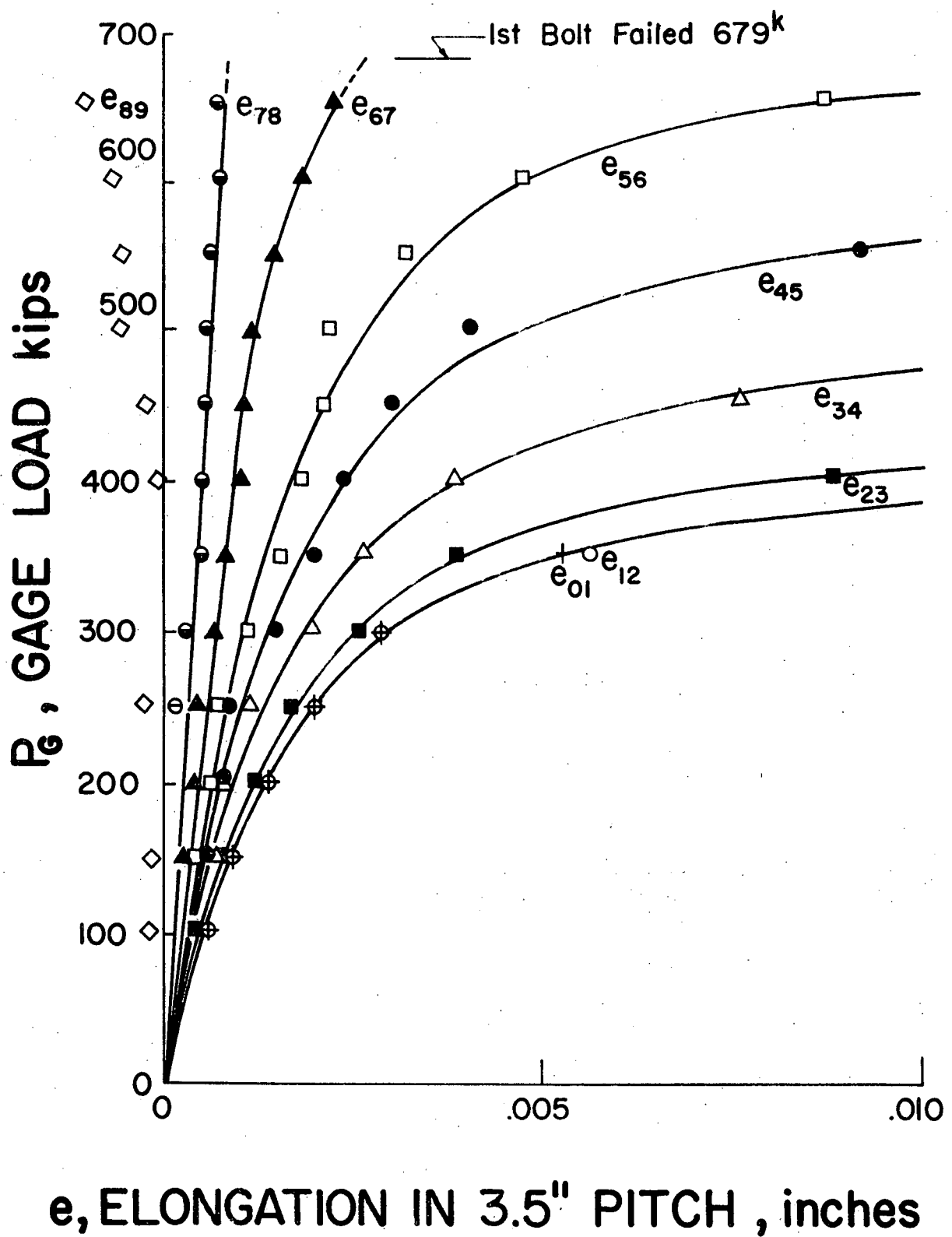


FIG. 3.10 JOINT D91, MAIN PLATE PITCH ELONGATIONS

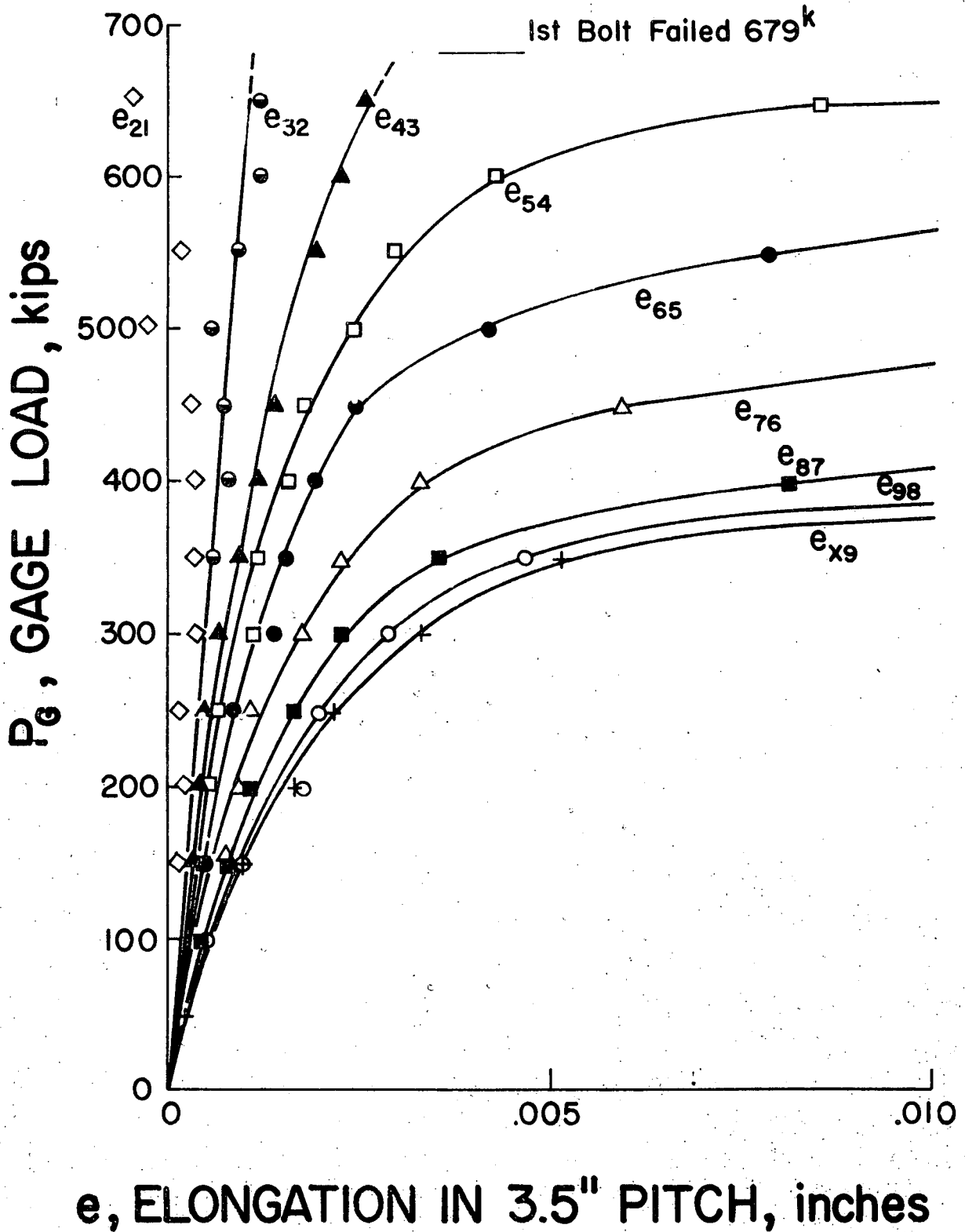


FIG. 3.11 JOINT D91, LAP PLATE PITCH ELONGATIONS

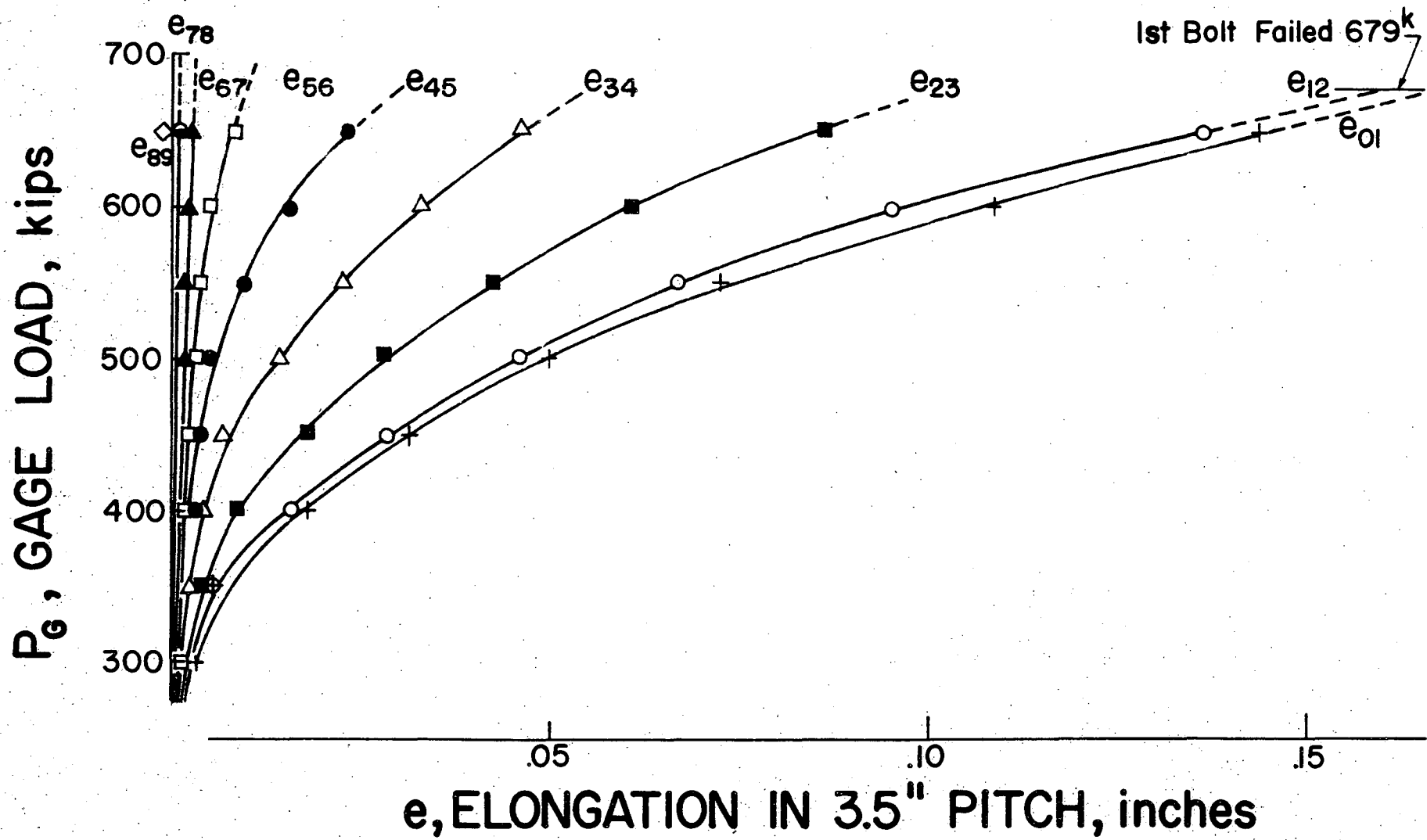


FIG. 3.12 JOINT D91, MAIN PLATE PITCH ELONGATIONS

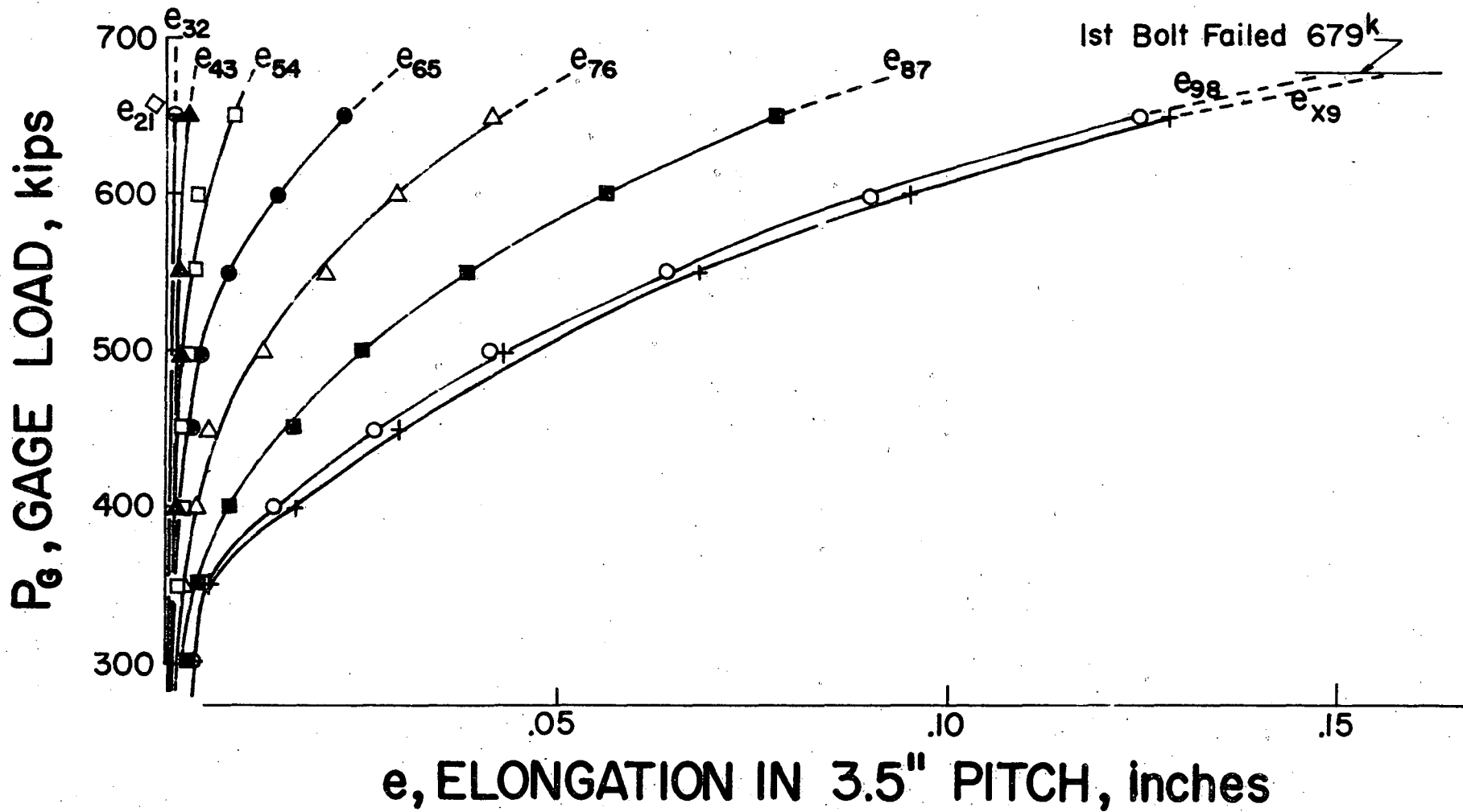


FIG. 3.13 JOINT D91, LAP PLATE PITCH ELONGATIONS

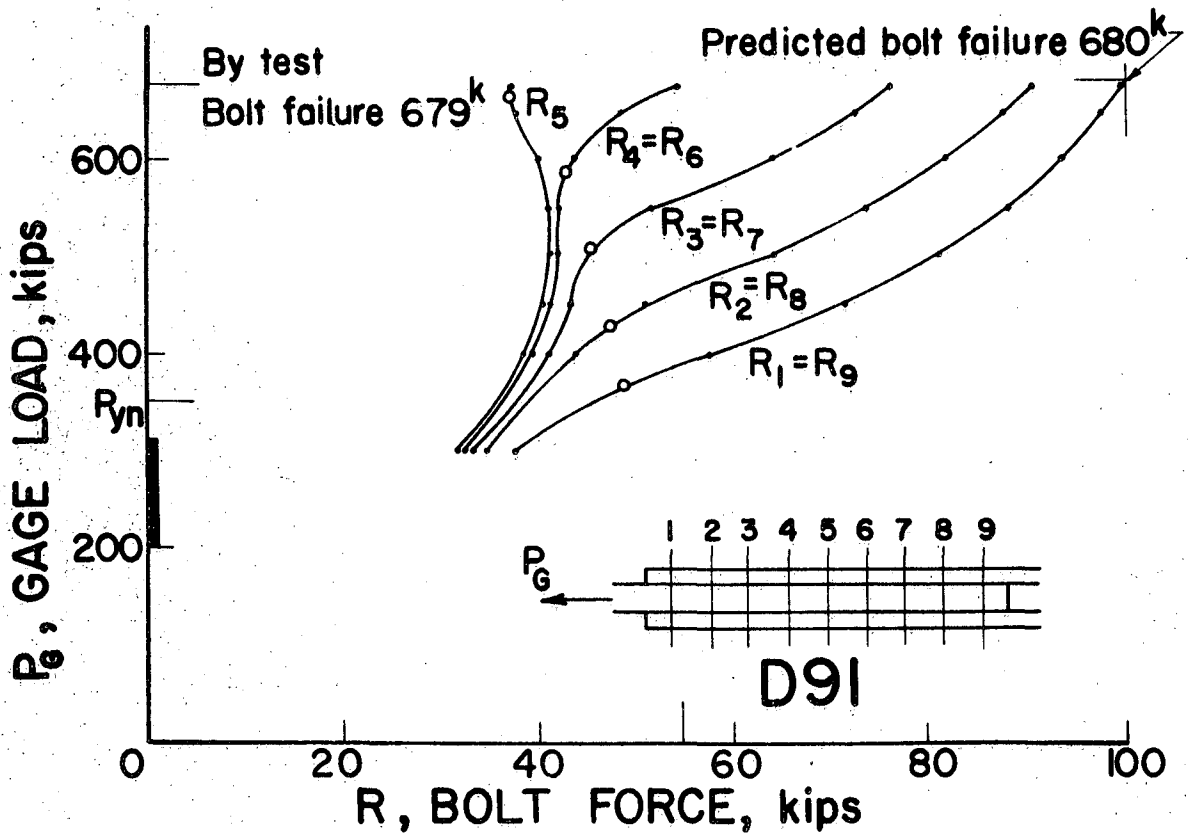
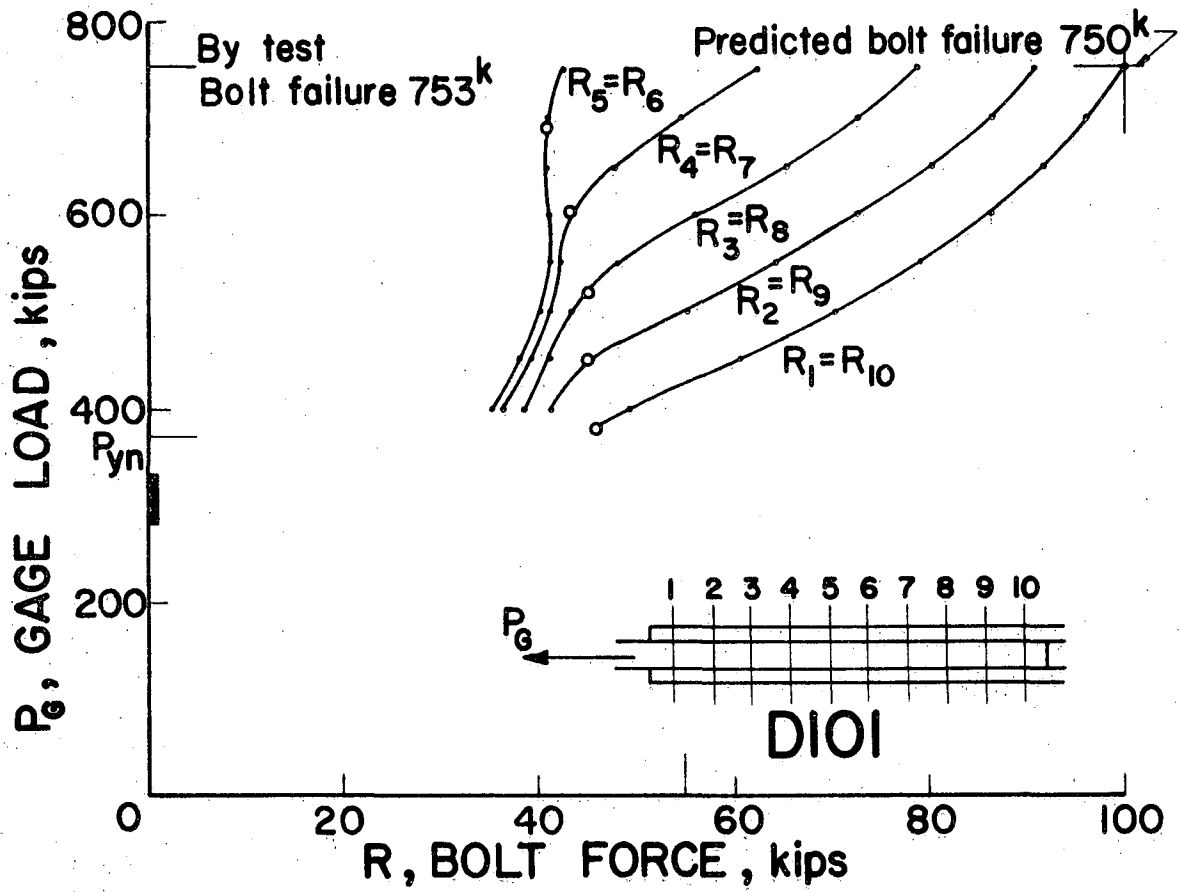


FIG. 4.1 JOINTS D101 AND D91, THEORETICAL BOLT FORCES



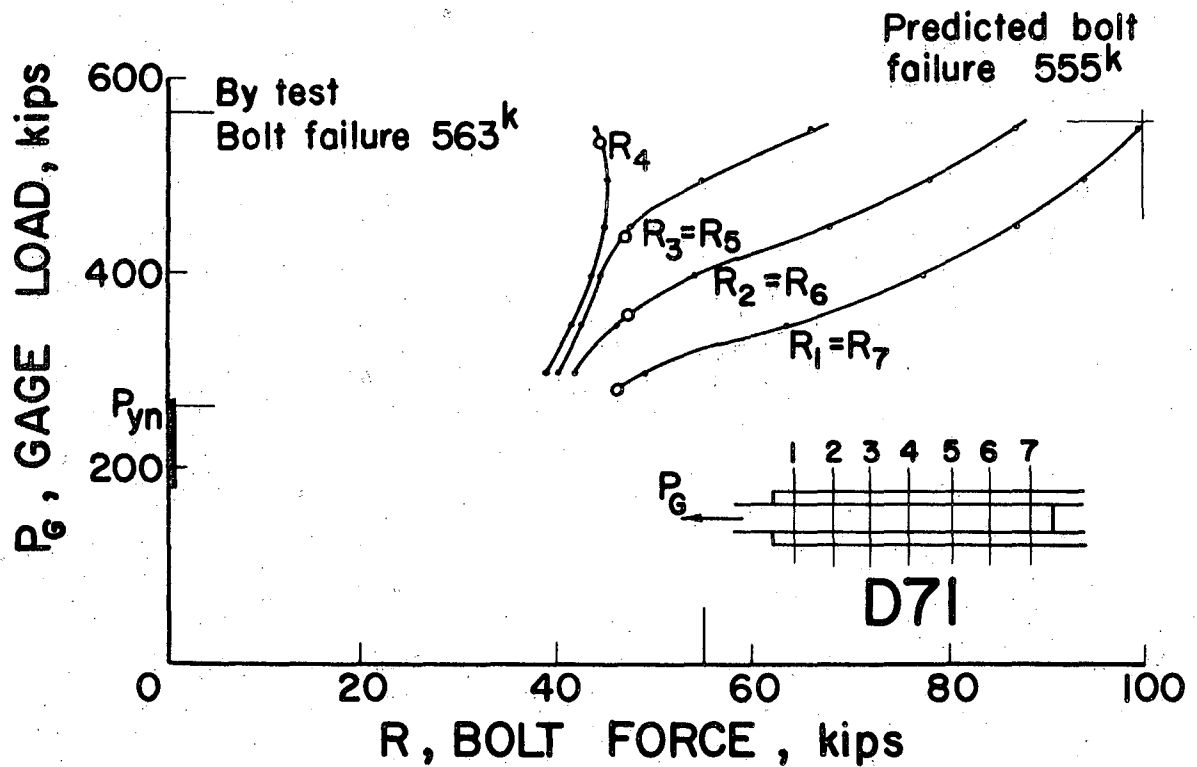
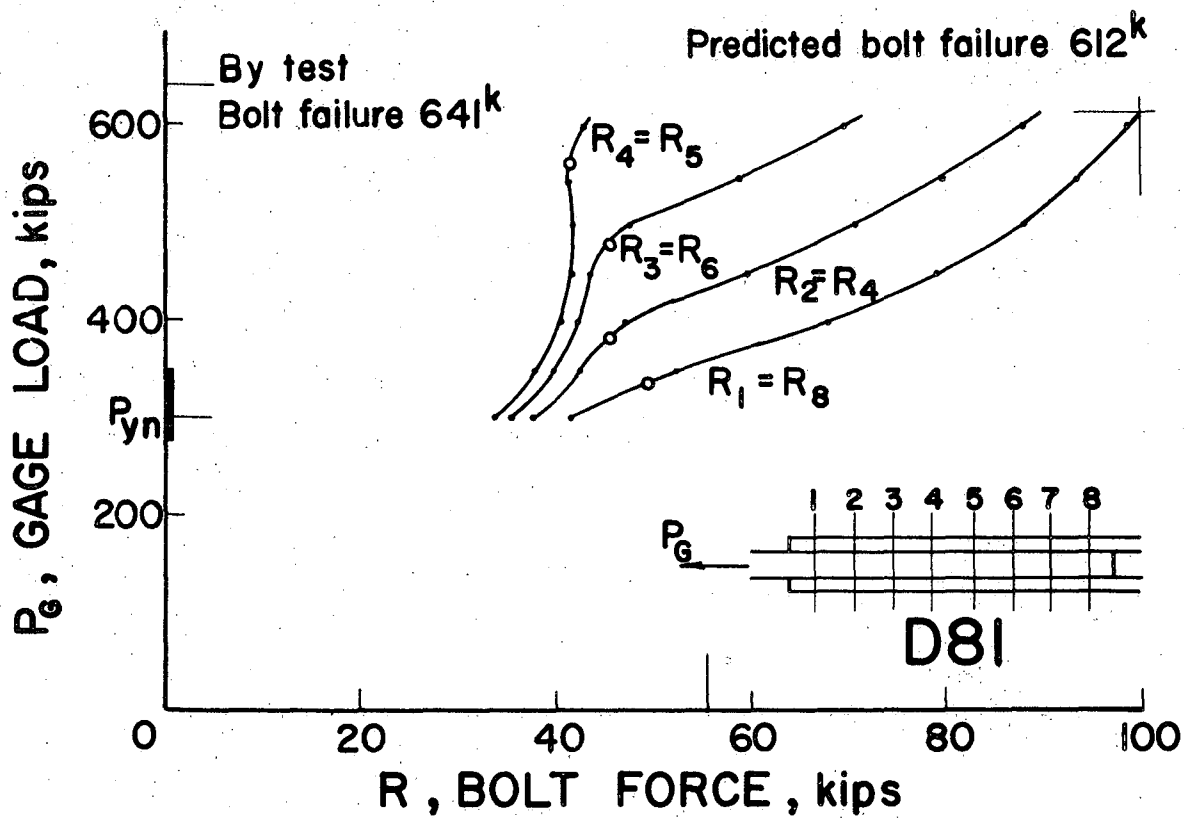


FIG. 4.2 JOINTS D81 AND D71, THEORETICAL BOLT FORCES

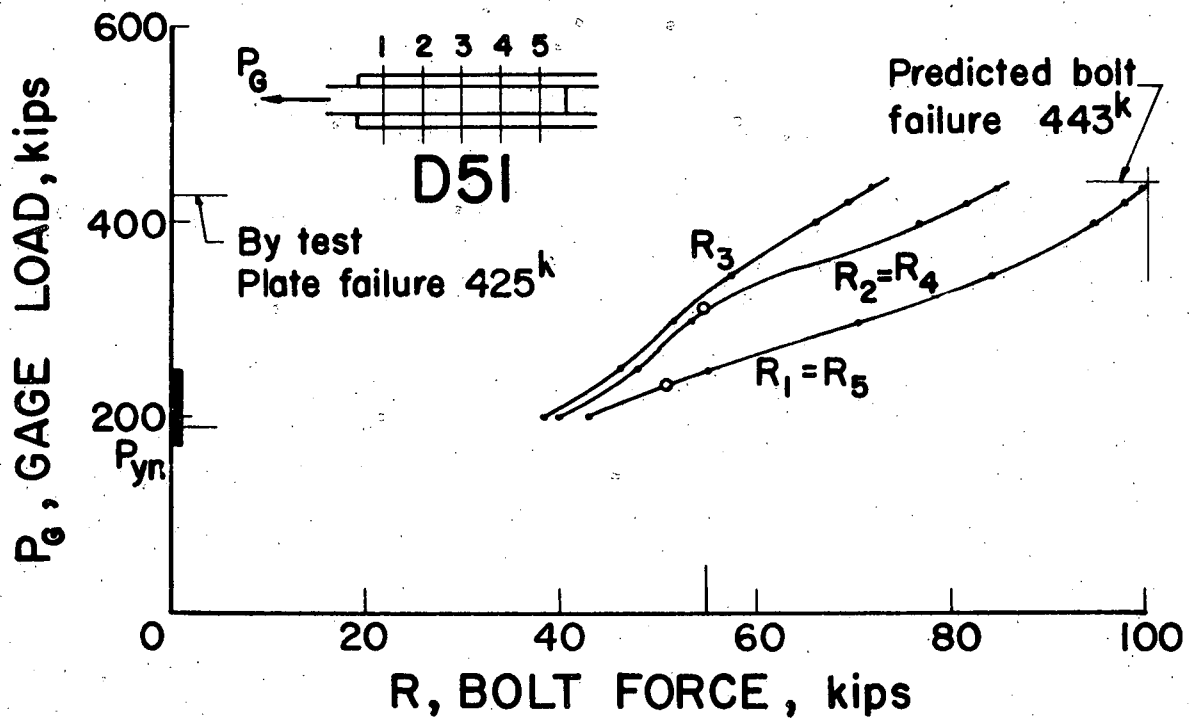
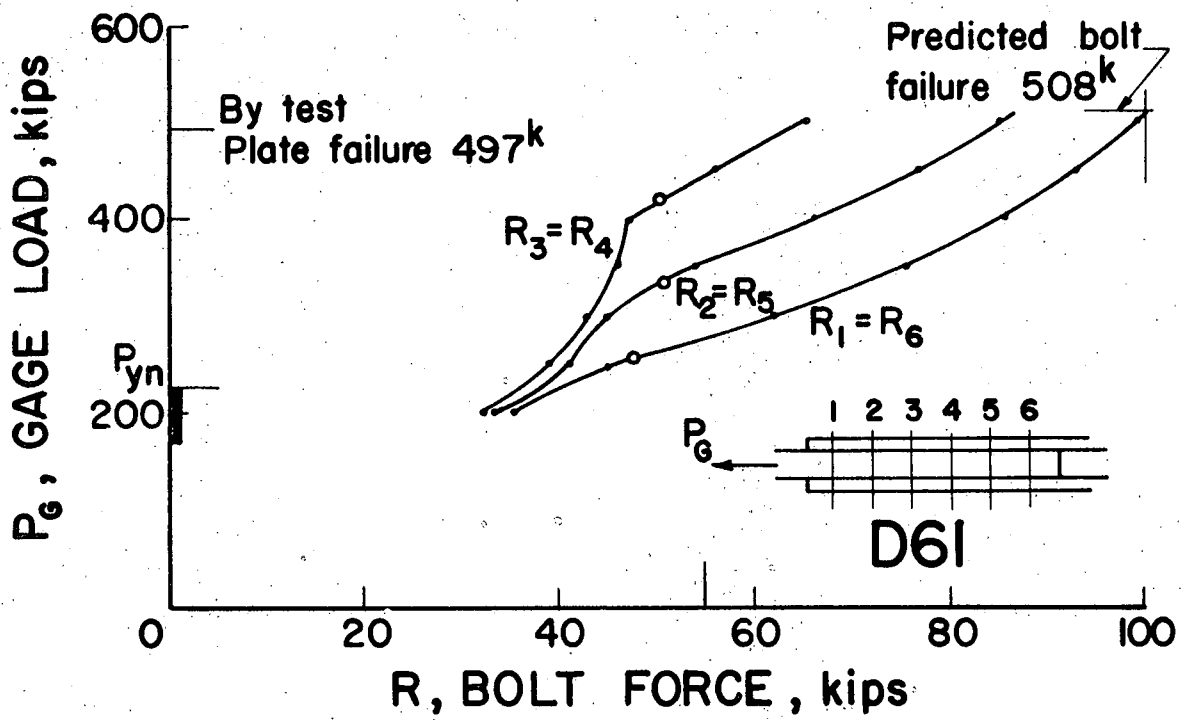


FIG. 4.3 JOINTS D61 AND D51, THEORETICAL BOLT FORCES

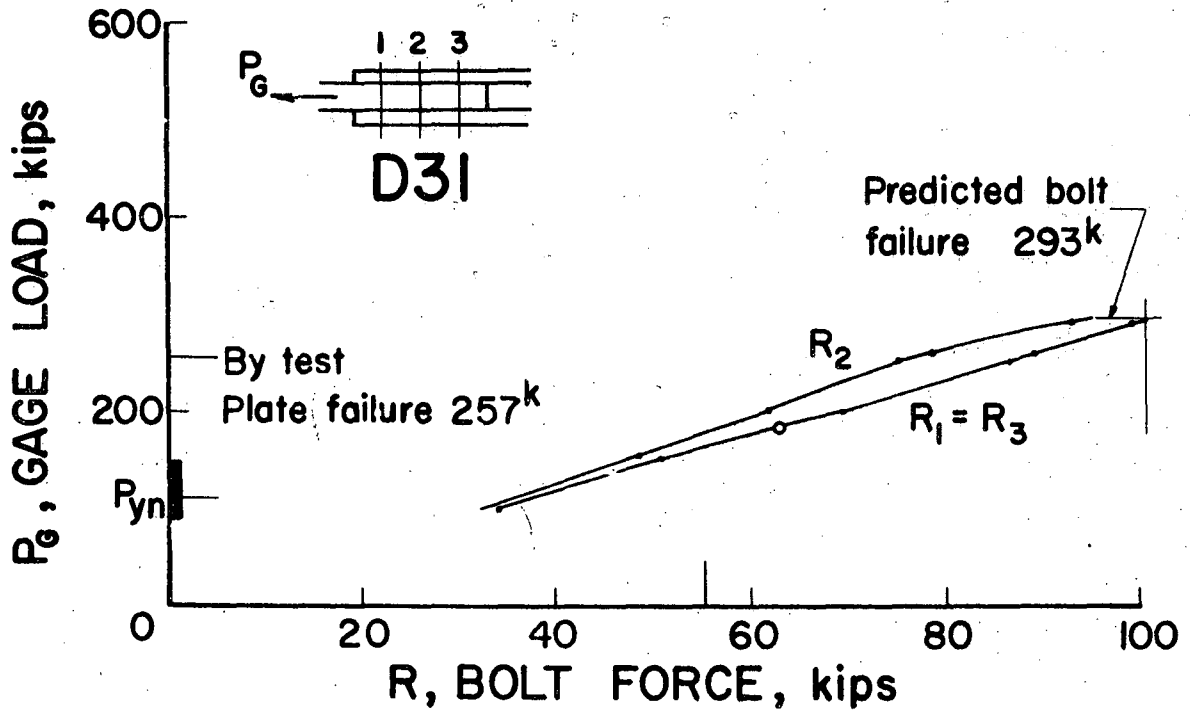
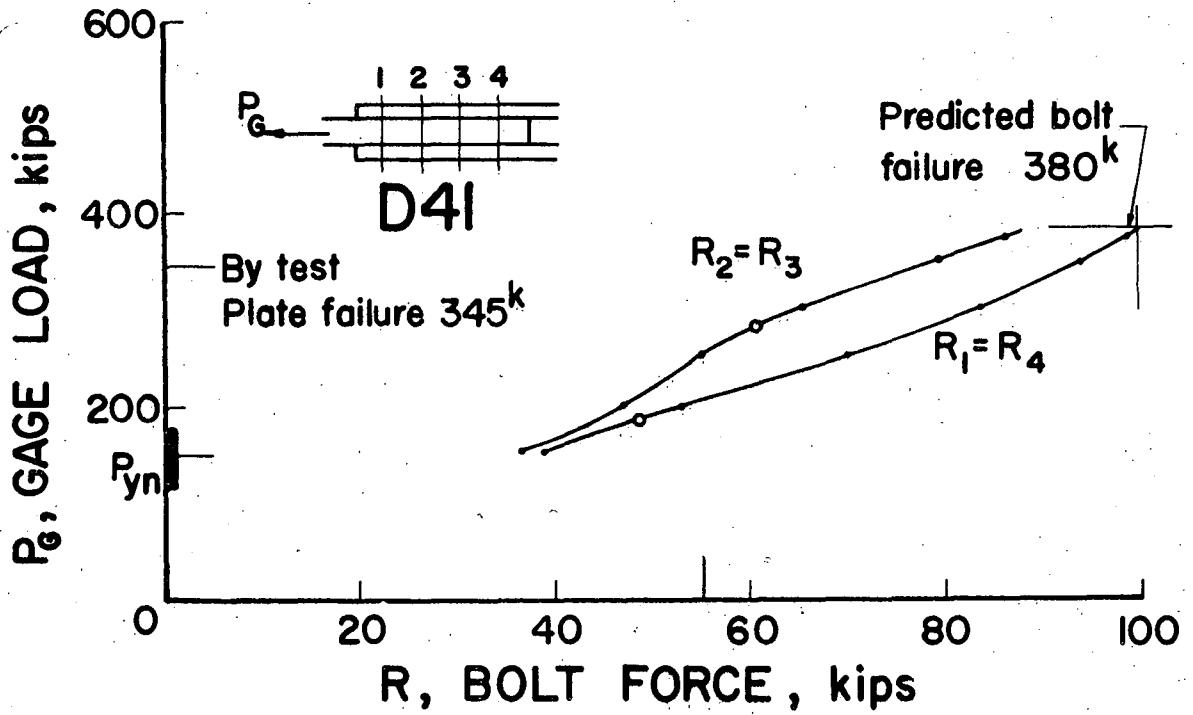


FIG. 4.4 JOINTS D41 AND D31, THEORETICAL BOLT FORCES

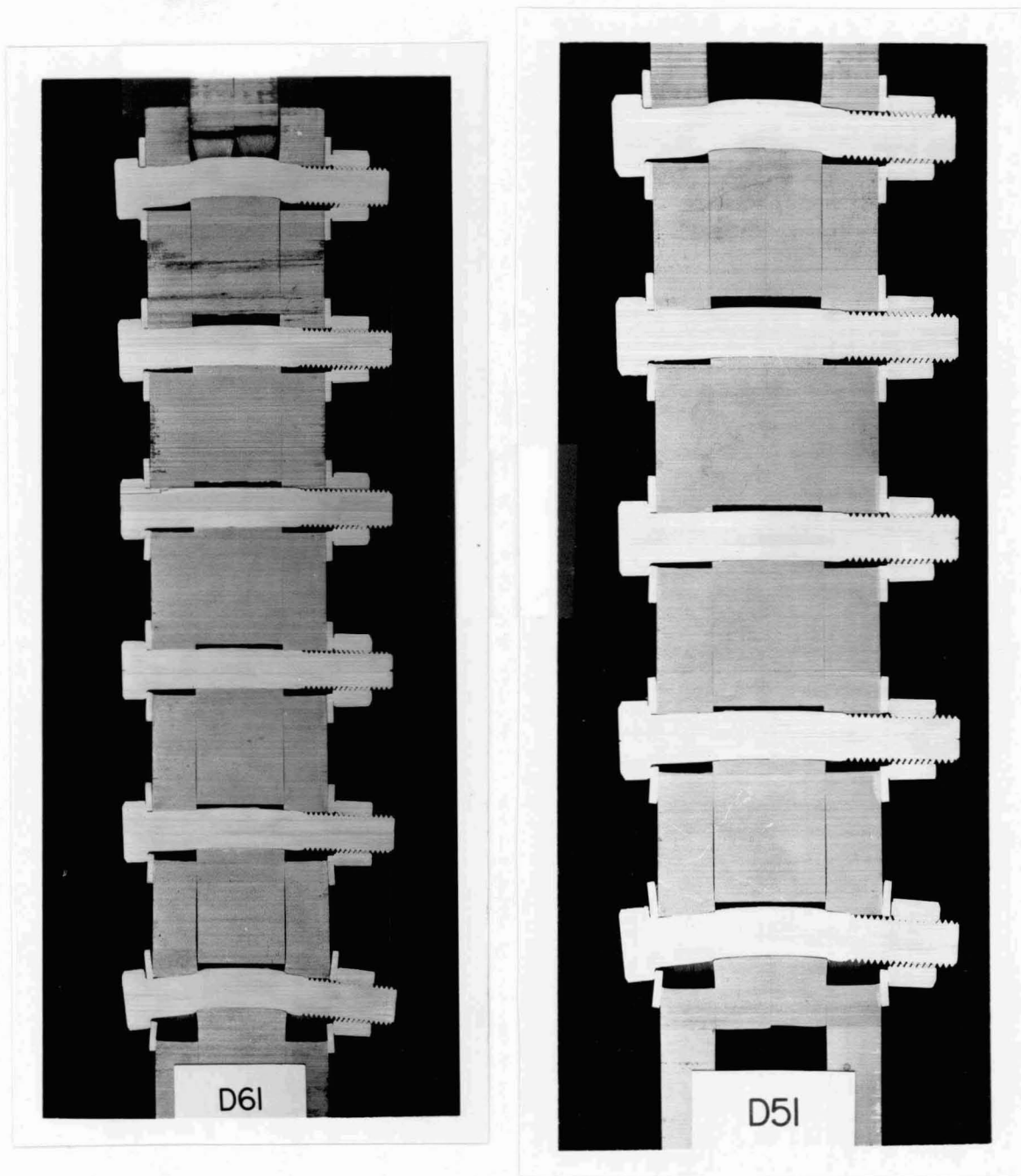


FIG. 4.5 SAWED SECTIONS OF JOINTS D61 AND D51

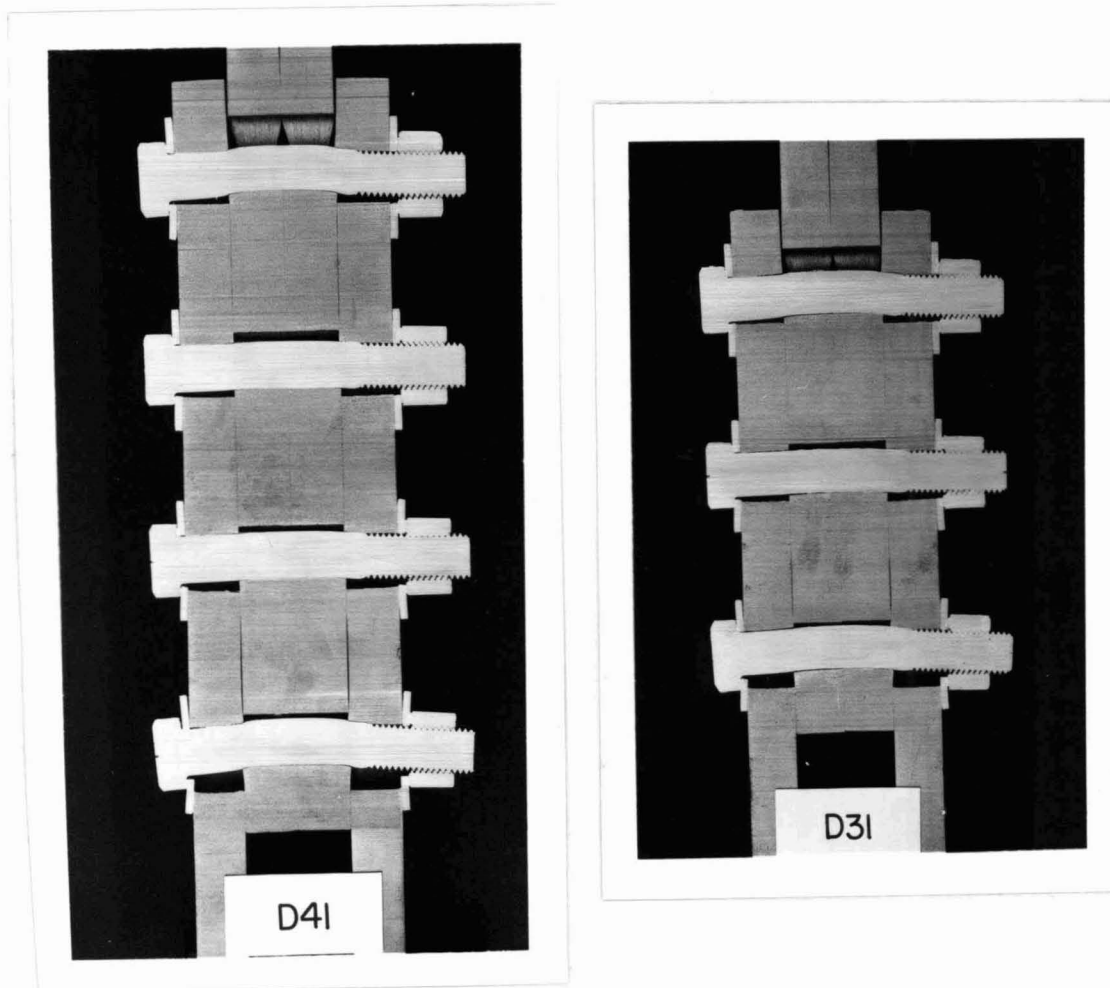


FIG. 4.6 SAWED SECTIONS OF JOINTS D41 AND D31

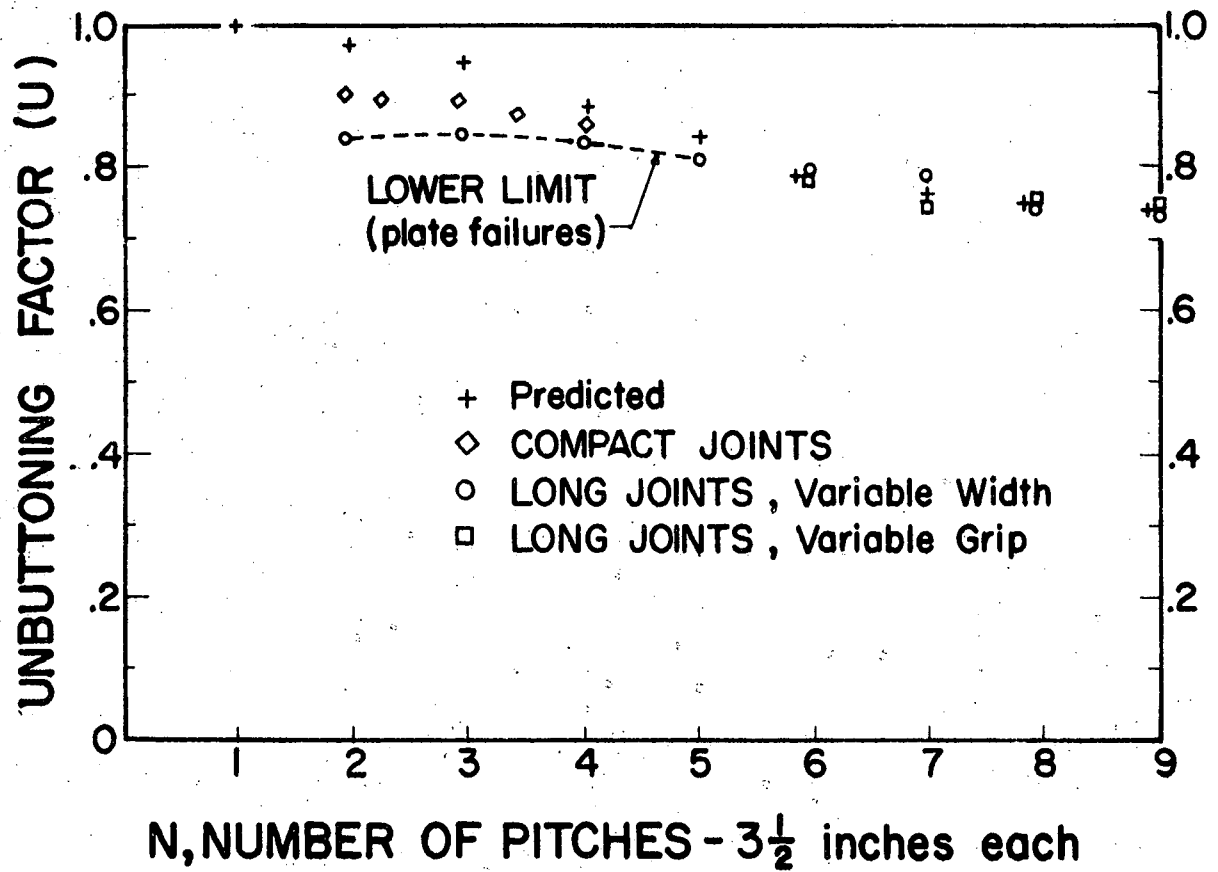


FIG. 4.7 UNBUTTONING FACTOR

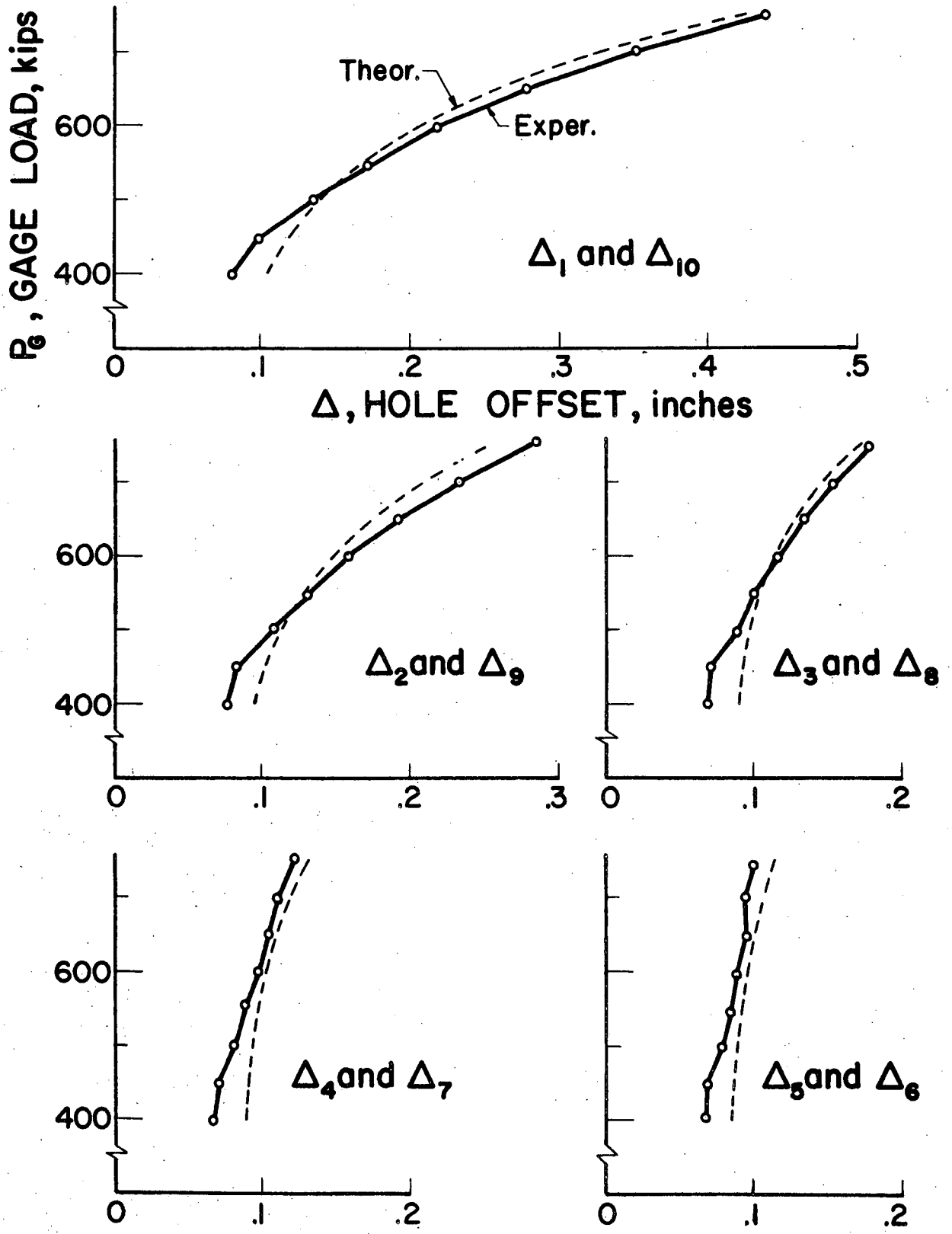


FIG. 4.8 JOINT D101, COMPARISON OF HOLE OFFSETS

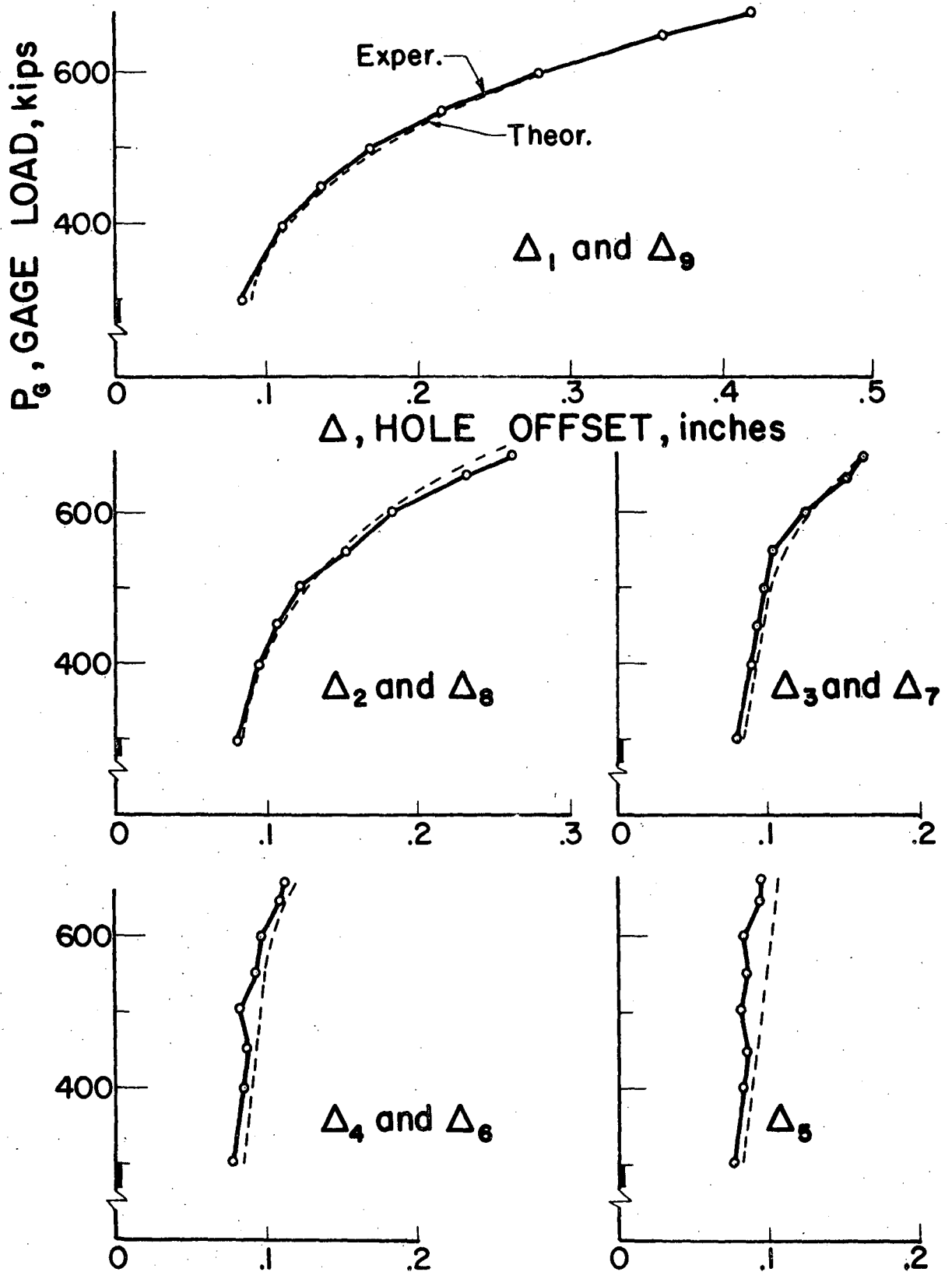


FIG. 4.9 JOINT D91, COMPARISON OF HOLE OFFSETS



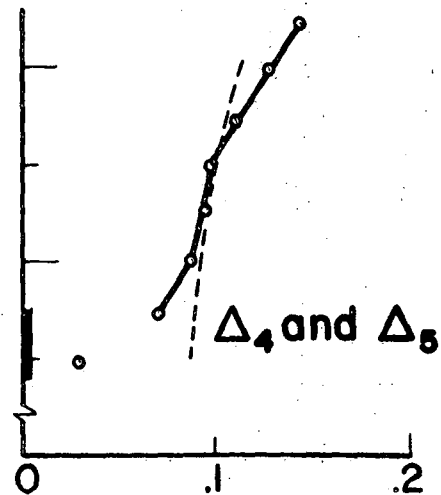
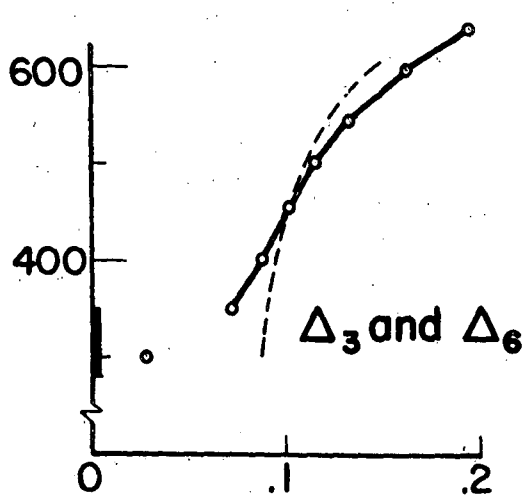
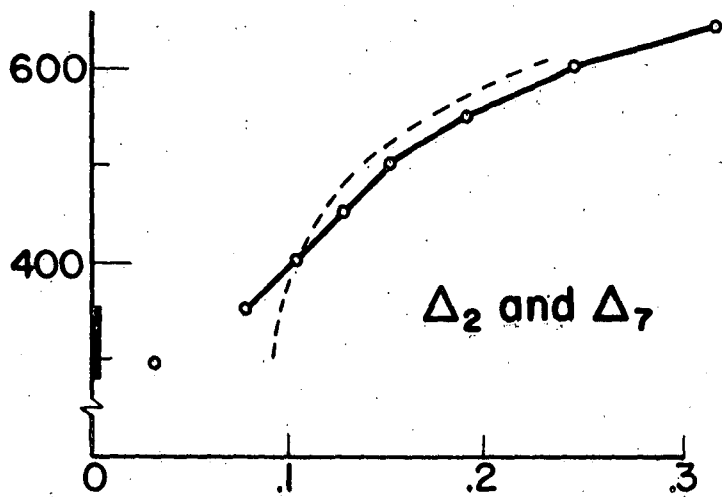
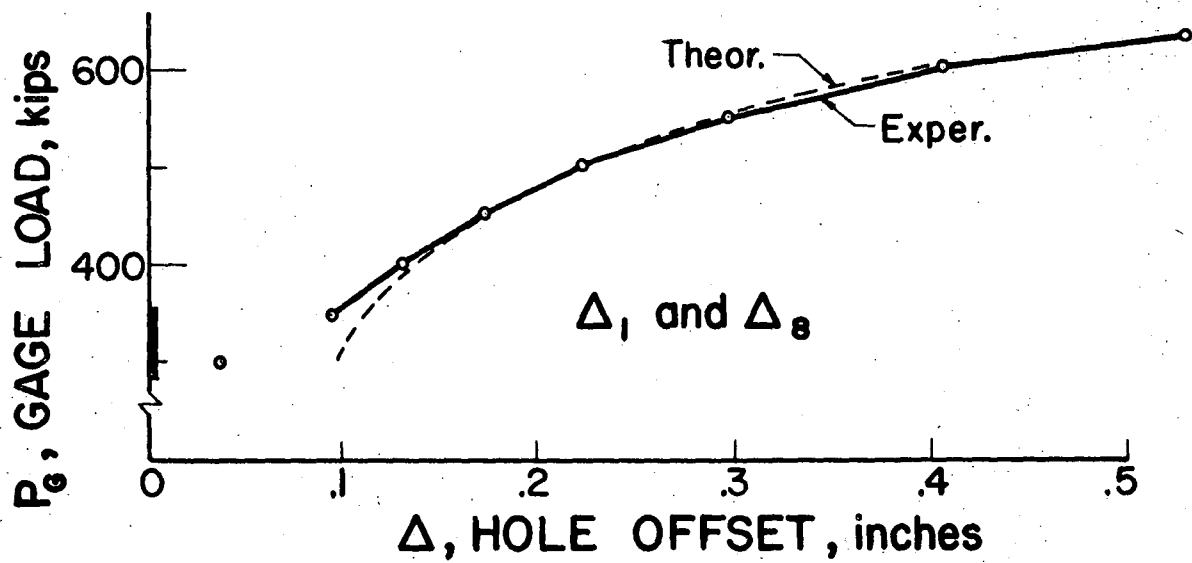


FIG. 4.10 JOINT D81, COMPARISON OF HOLE OFFSETS

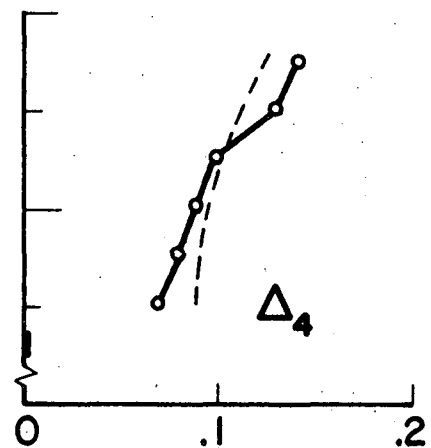
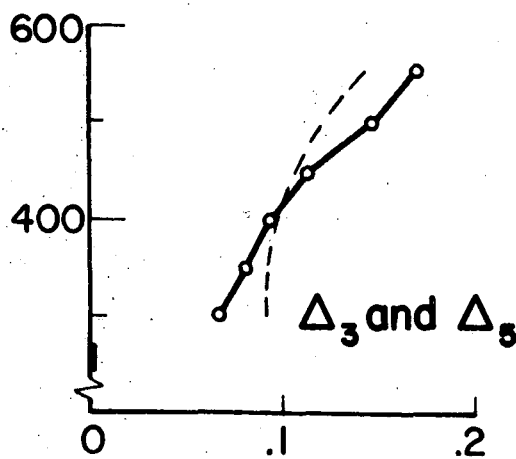
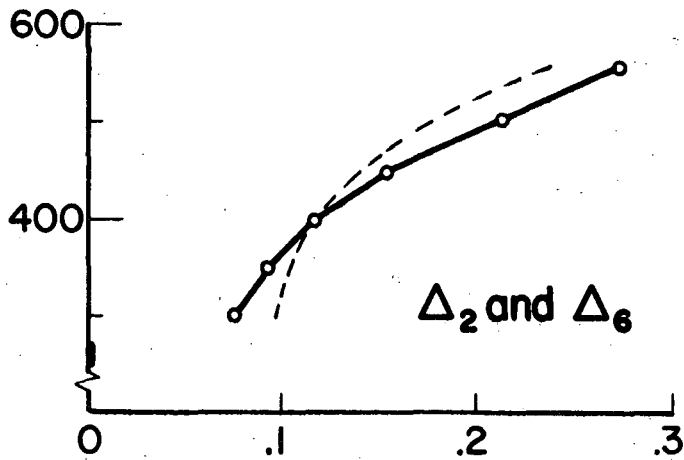
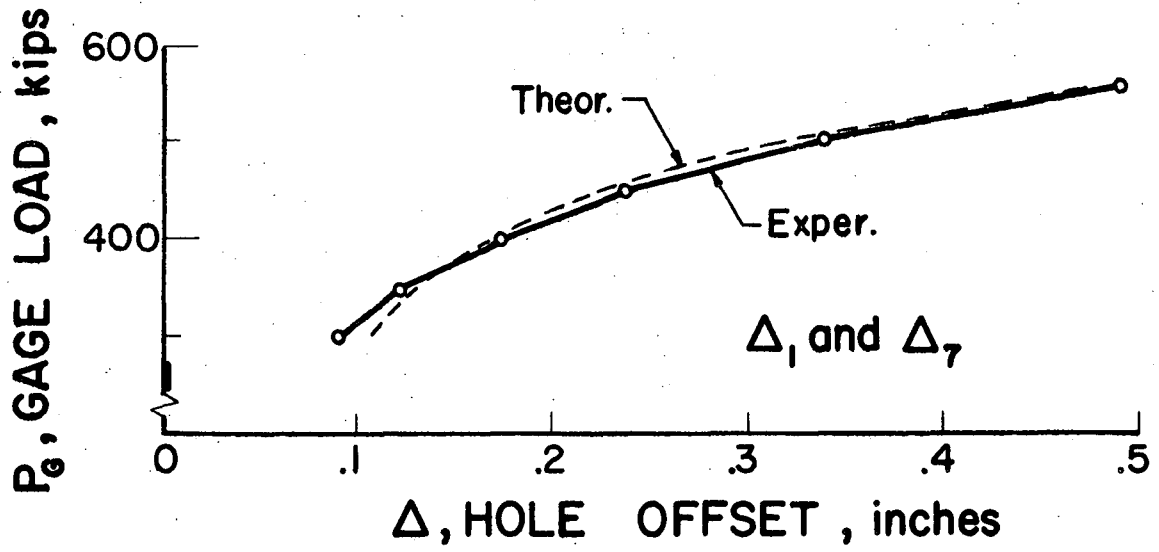


FIG. 4.11 JOINT D71, COMPARISON OF HOLE OFFSETS

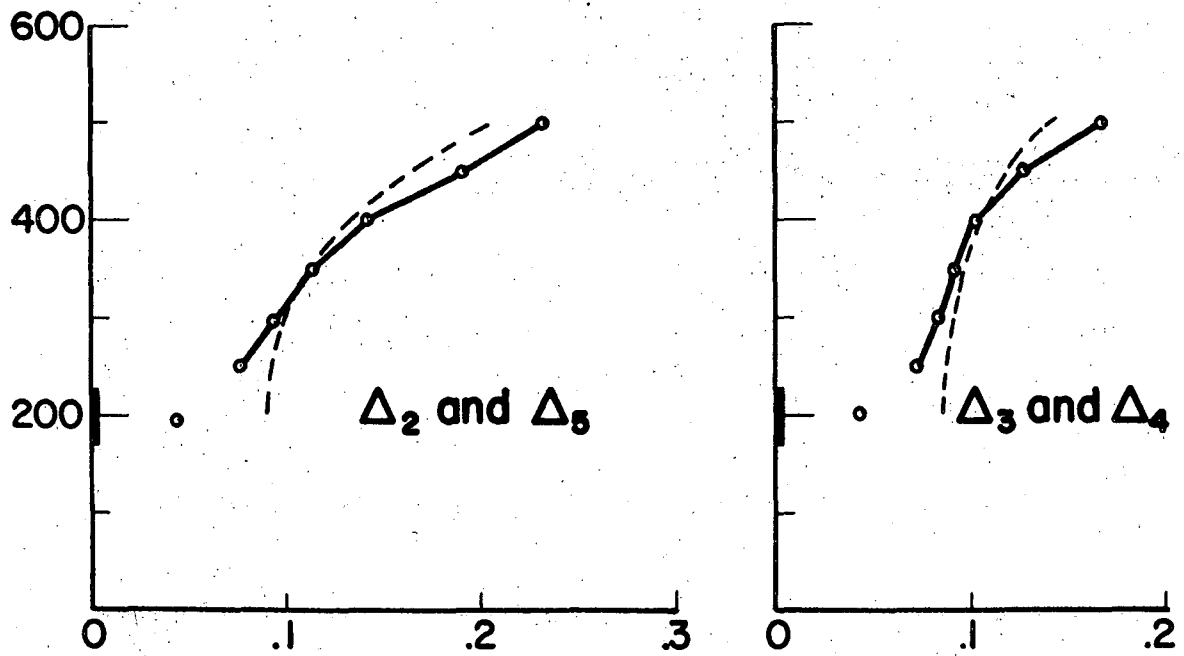
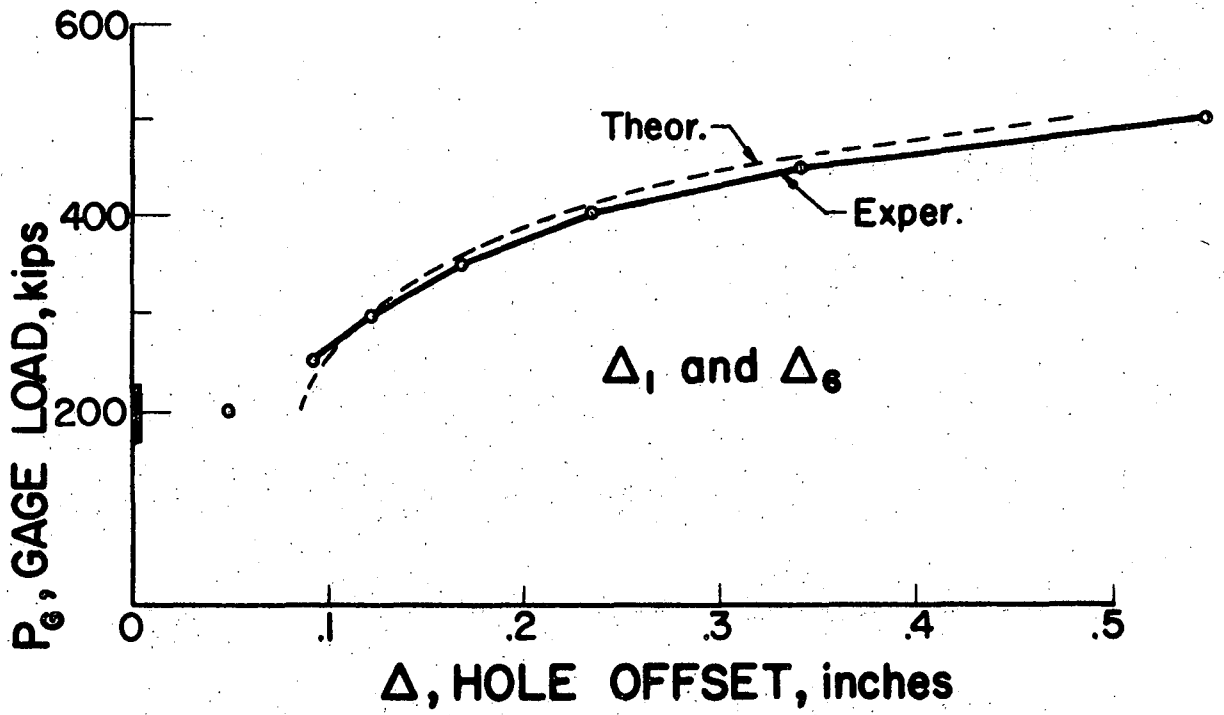


FIG. 4.12 JOINT D61, COMPARISON OF HOLE OFFSETS

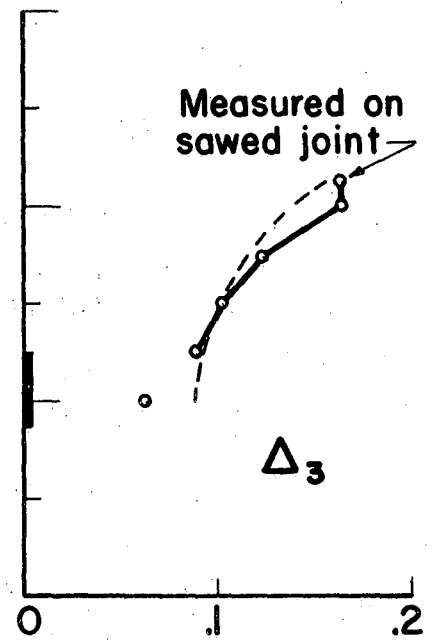
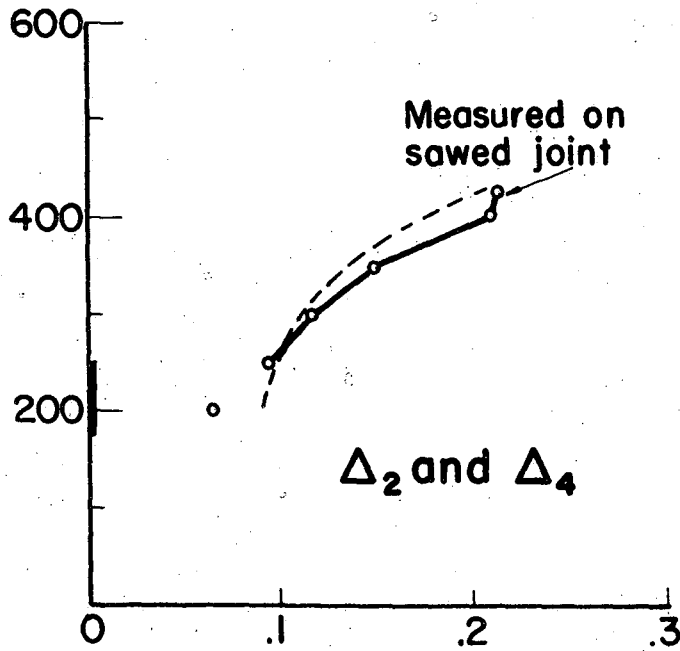
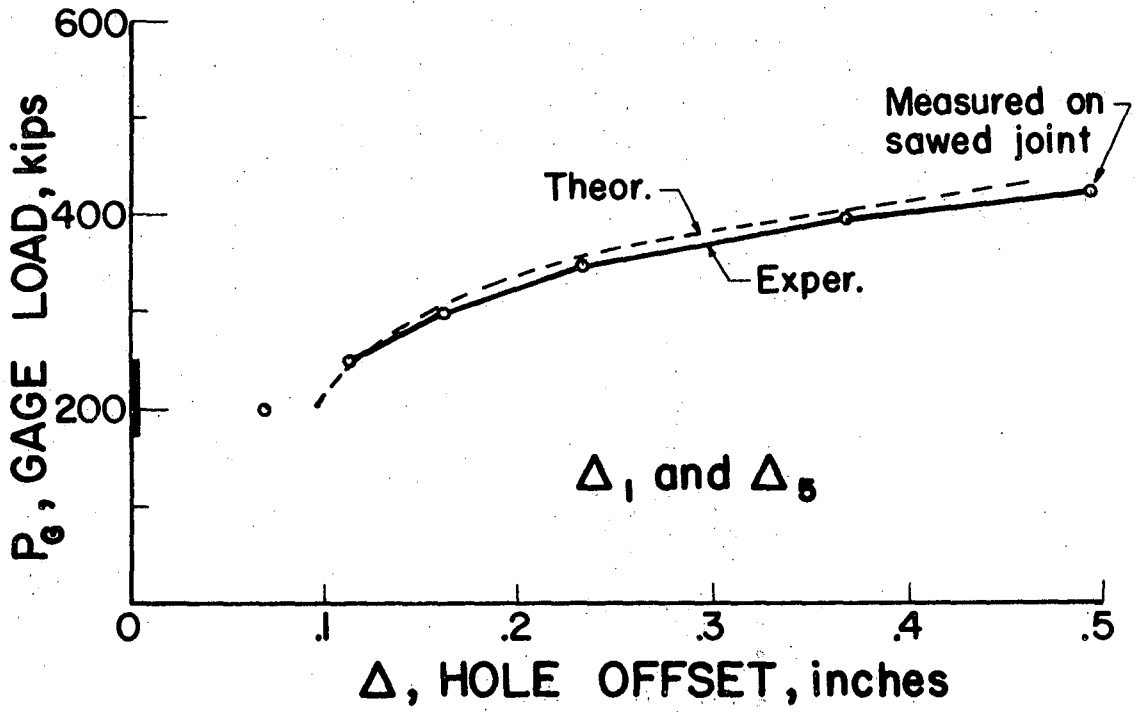


FIG. 4.13 JOINT D51, COMPARISON OF HOLE OFFSETS

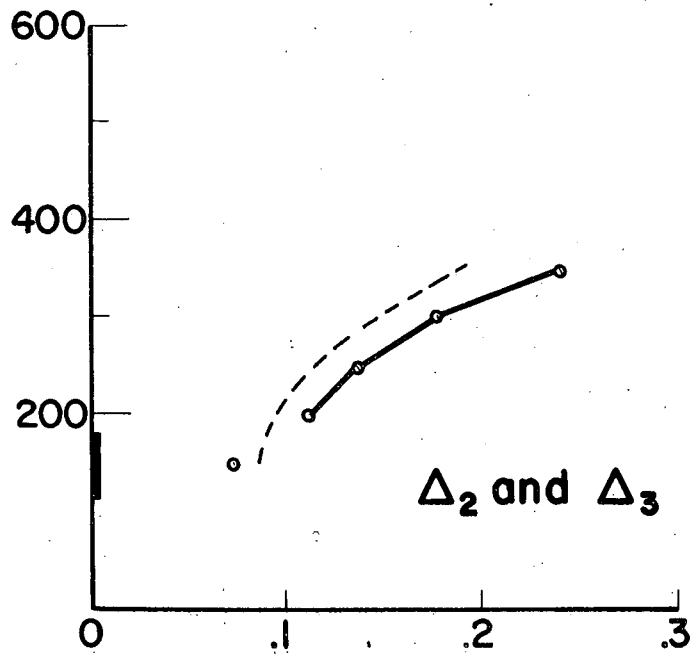
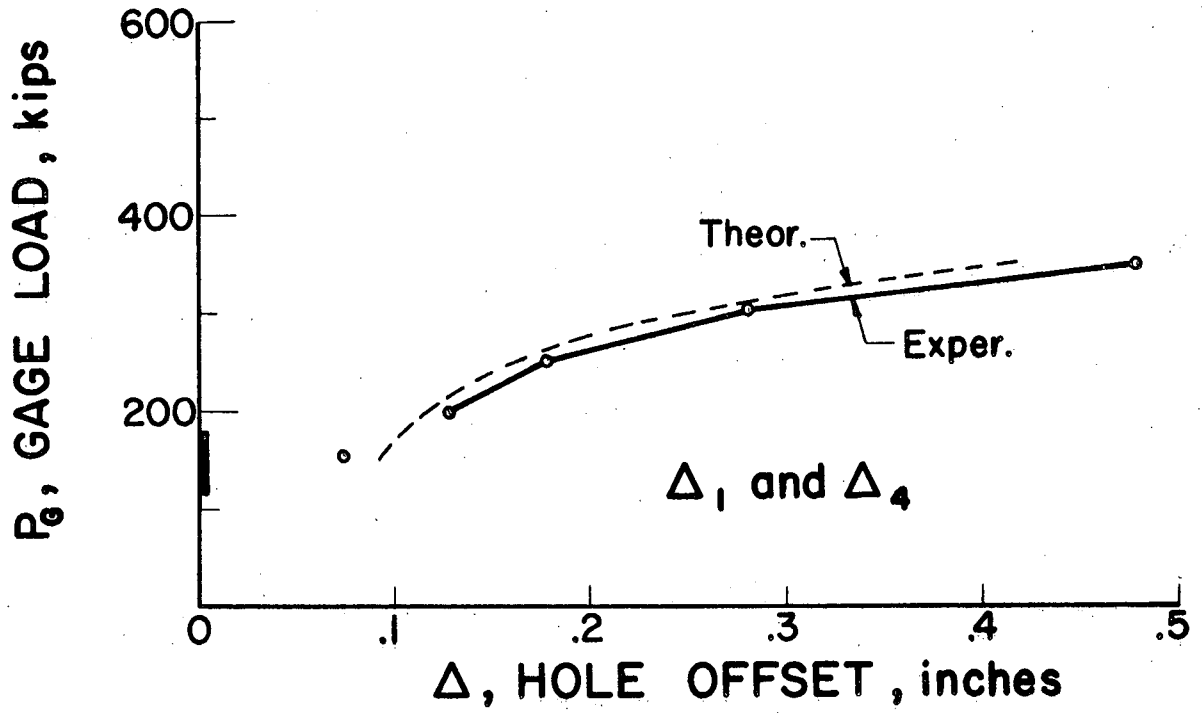


FIG. 4.14 JOINT D41, COMPARISON OF HOLE OFFSETS

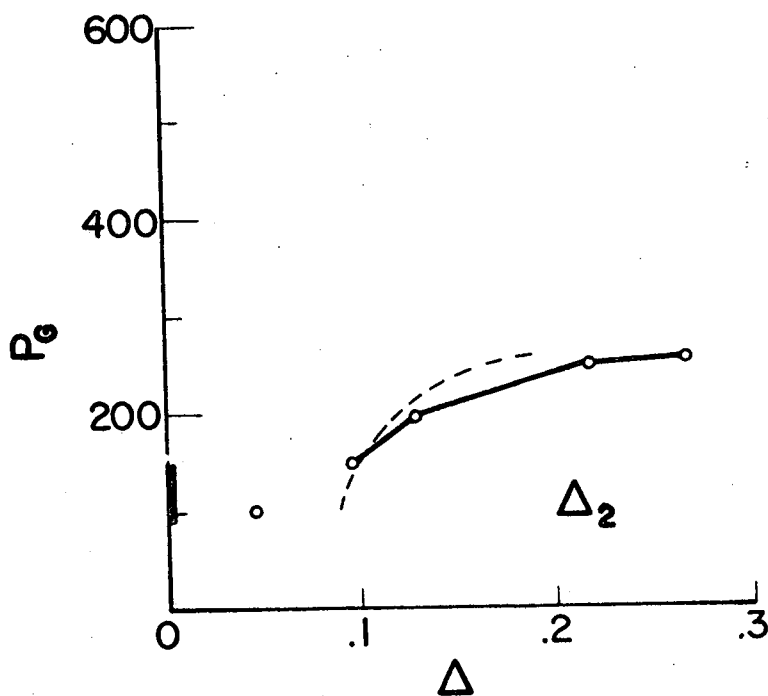
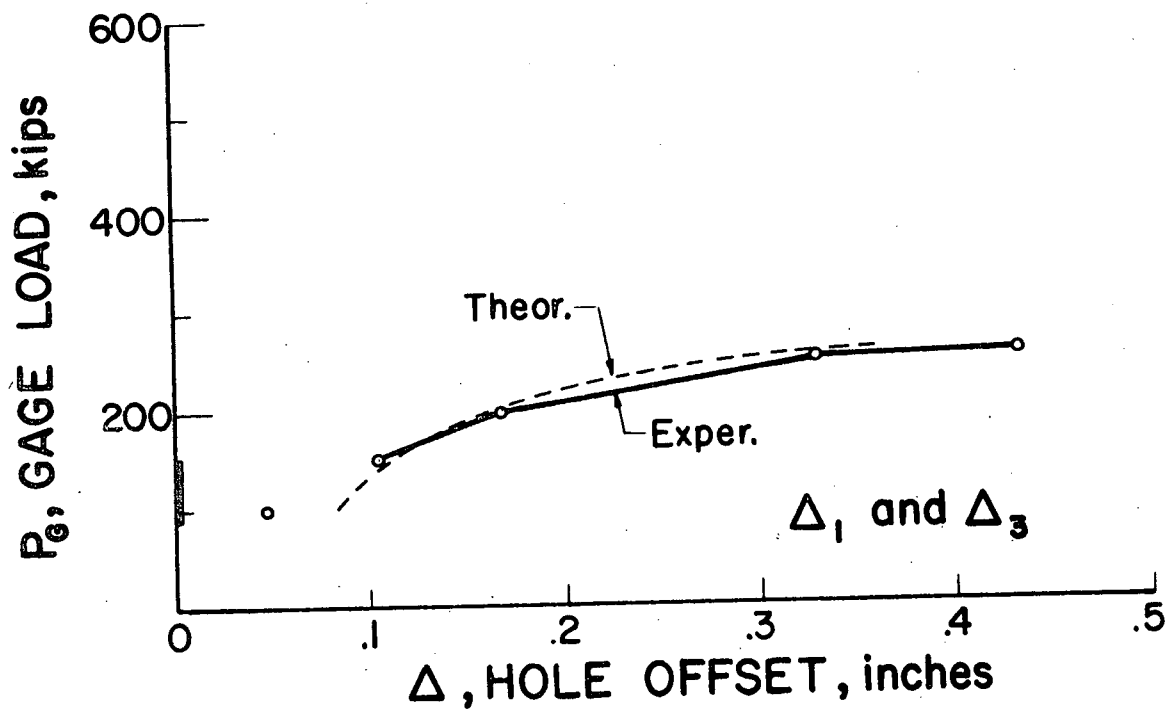


FIG. 4.15 JOINT D31, COMPARISON OF HOLE OFFSETS

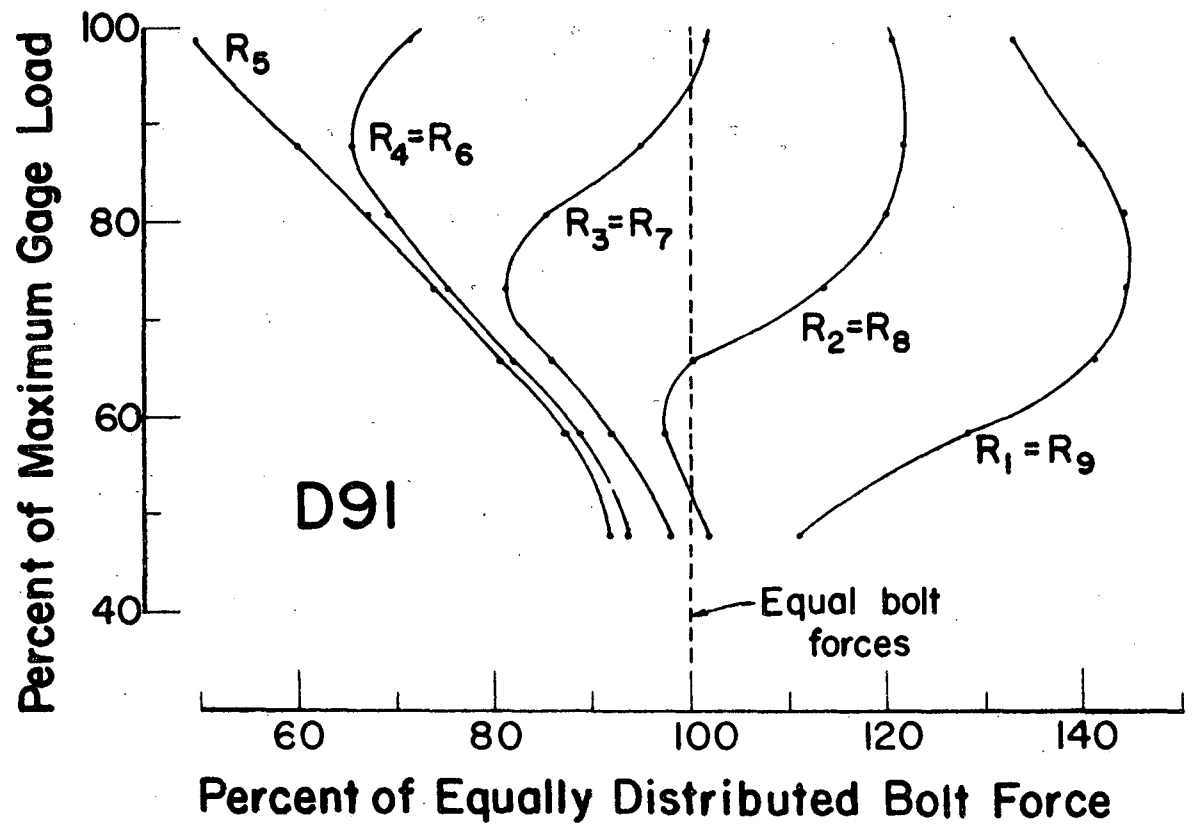
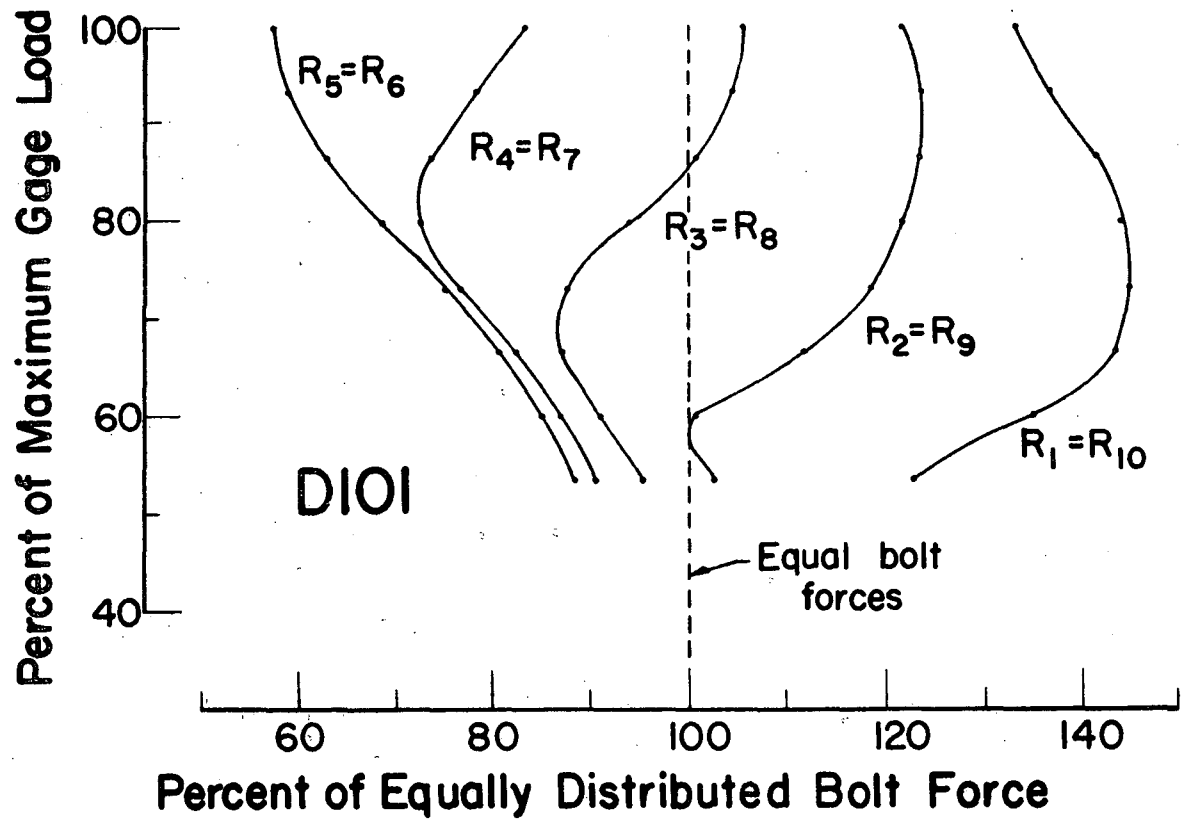


FIG. 4.16 JOINTS D101 AND D91, BOLT FORCE DISTRIBUTION

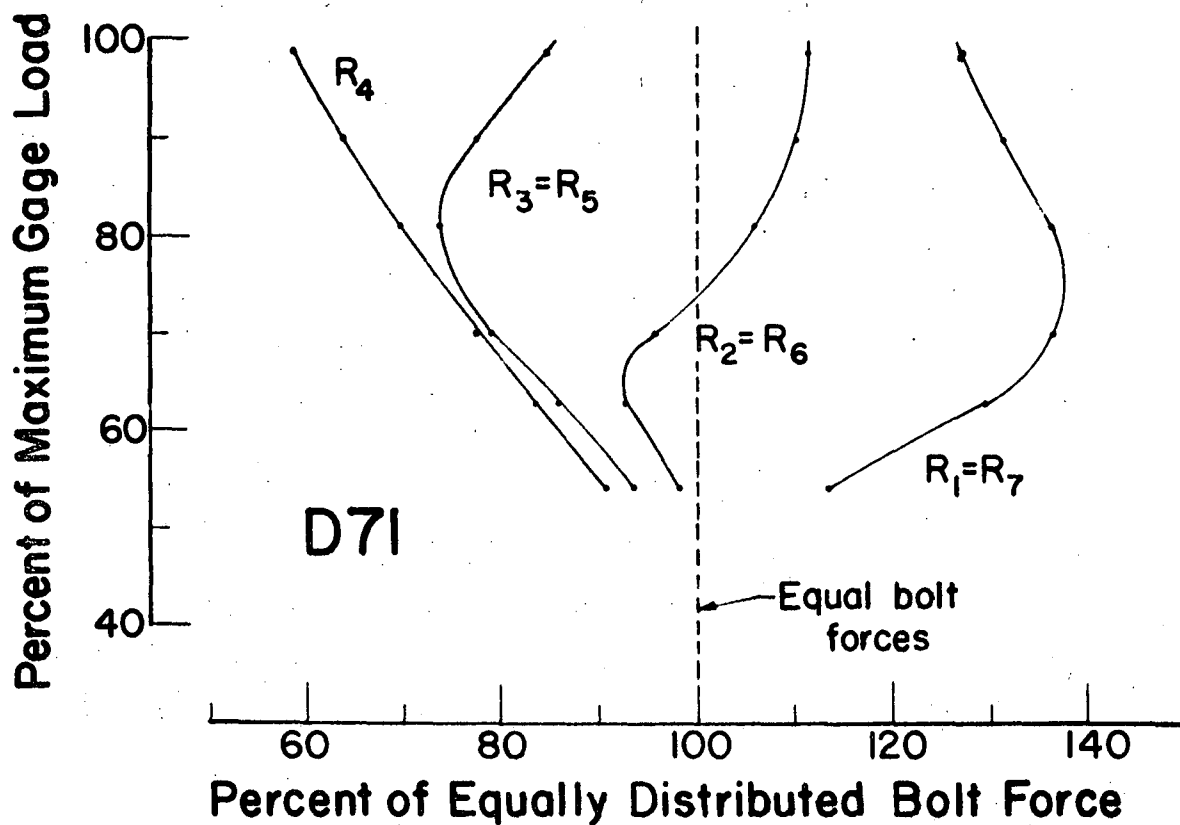
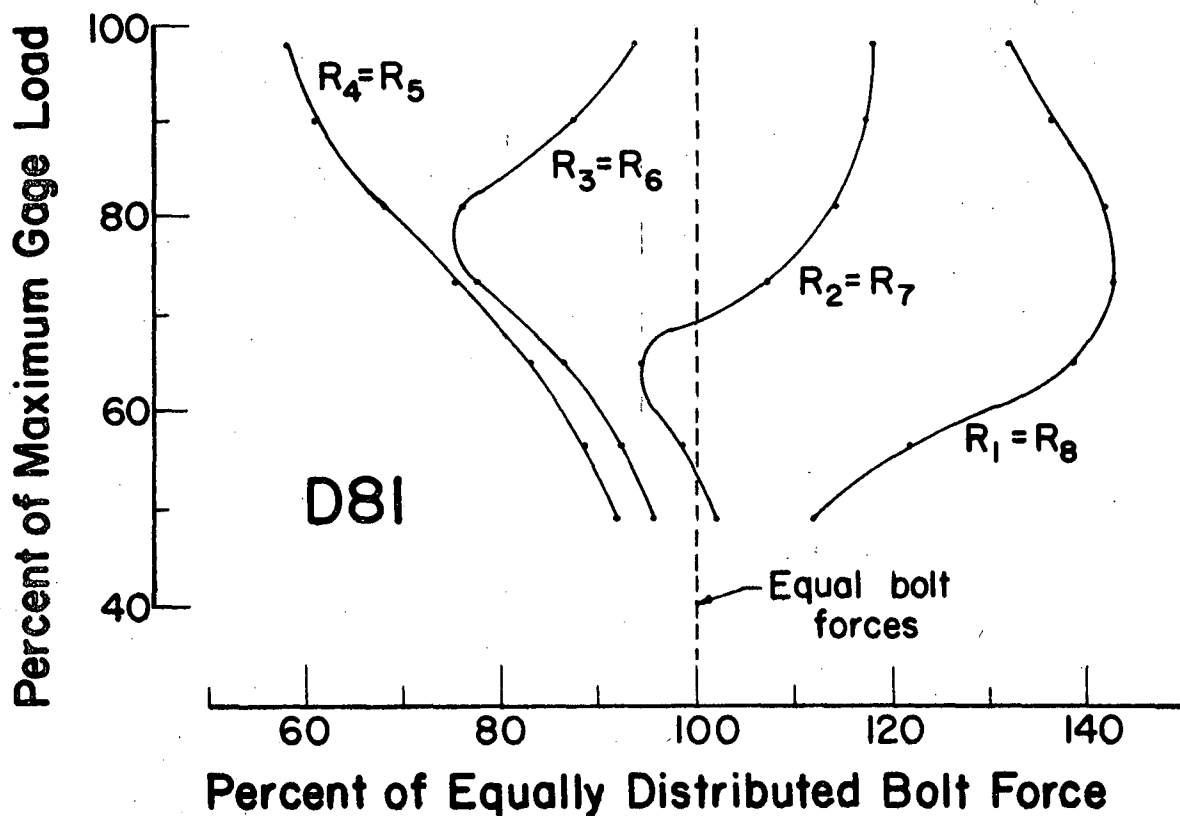


FIG. 4.17 JOINTS D81 AND D71, BOLT FORCE DISTRIBUTION



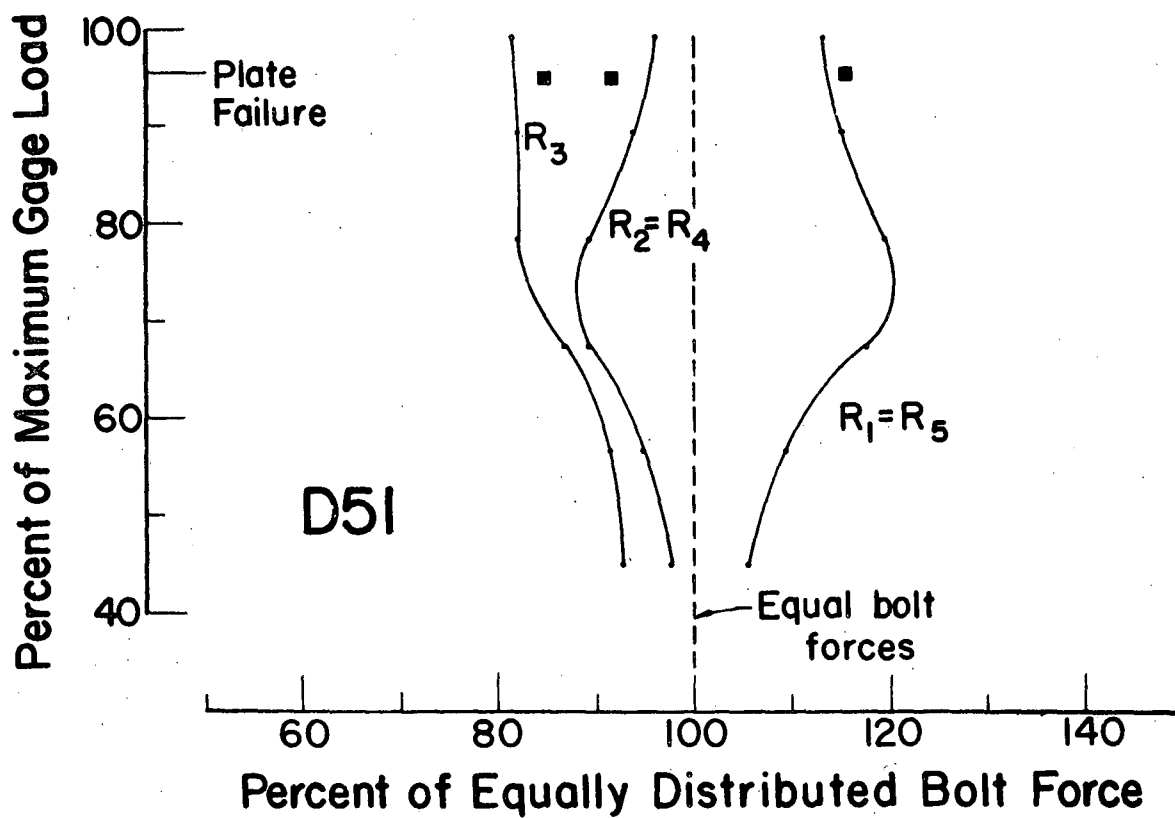
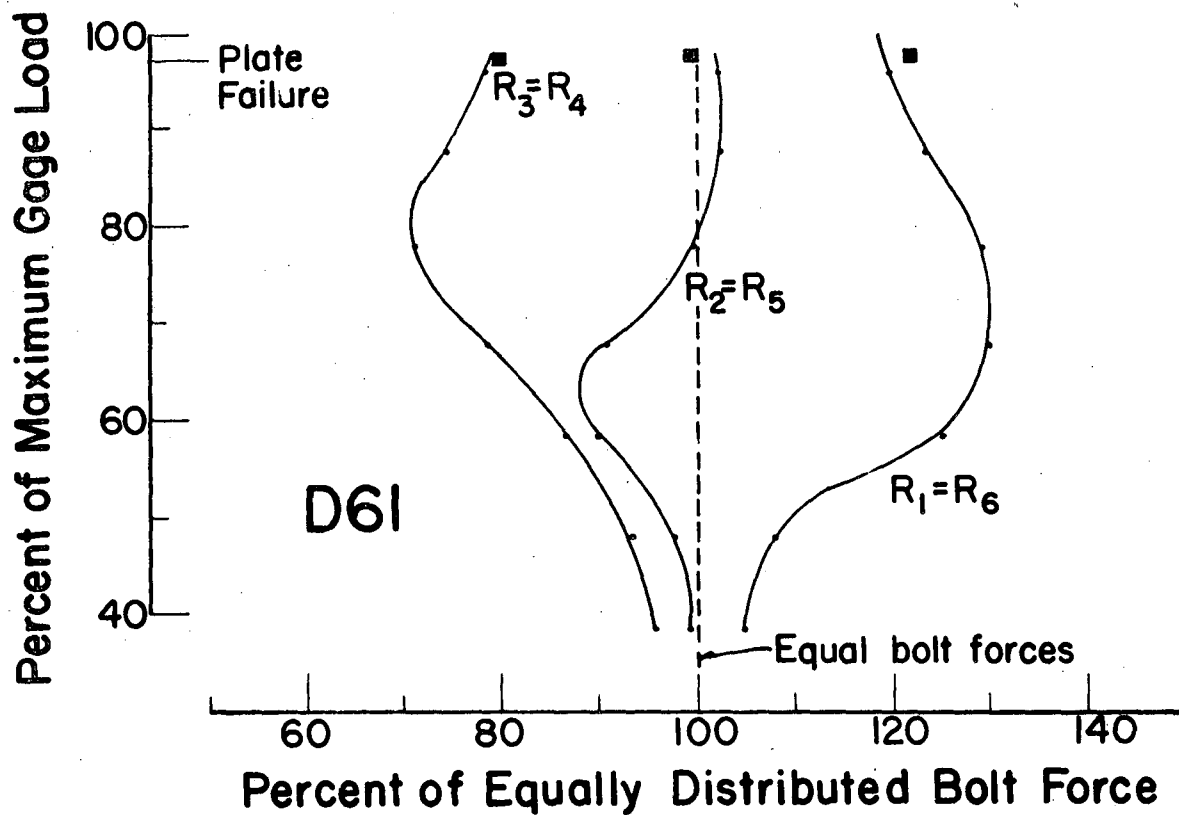


FIG. 4.18 JOINTS D61 AND D51, BOLT FORCE DISTRIBUTION

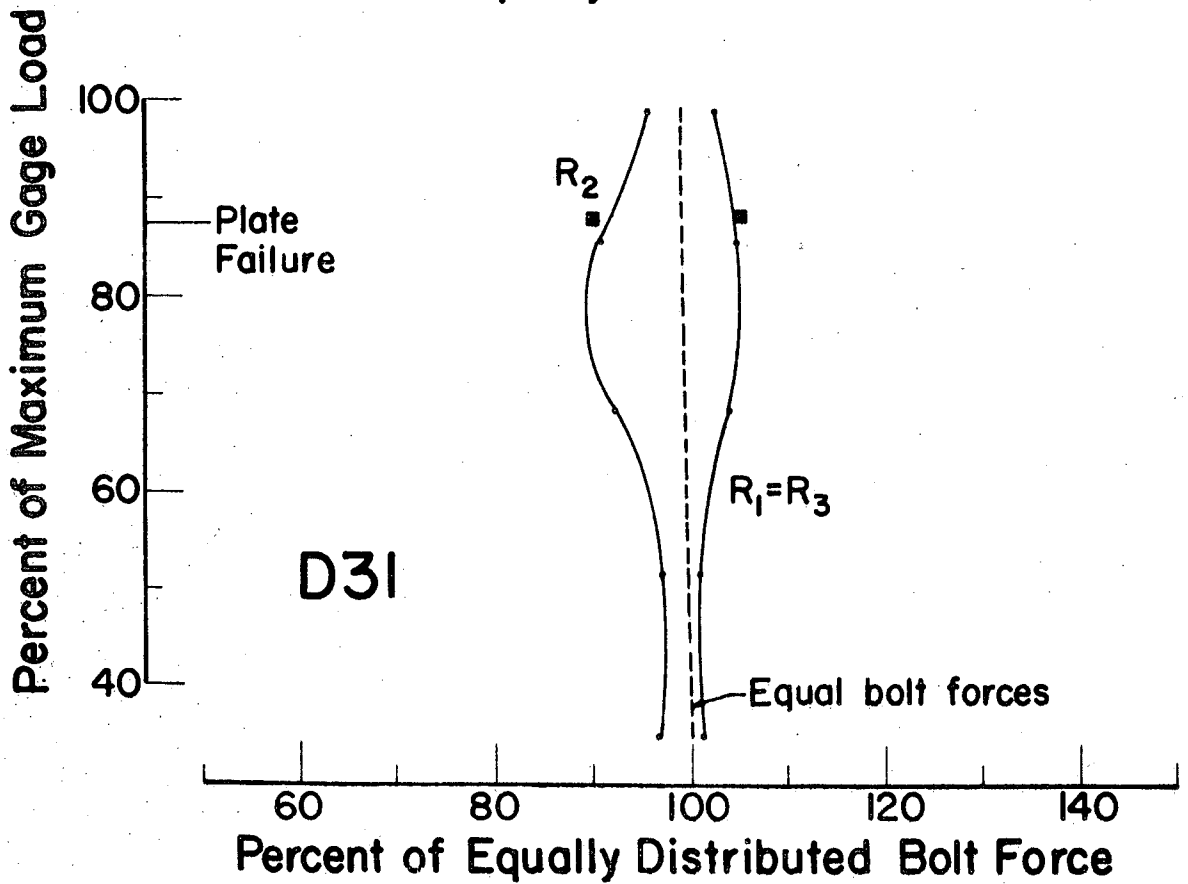
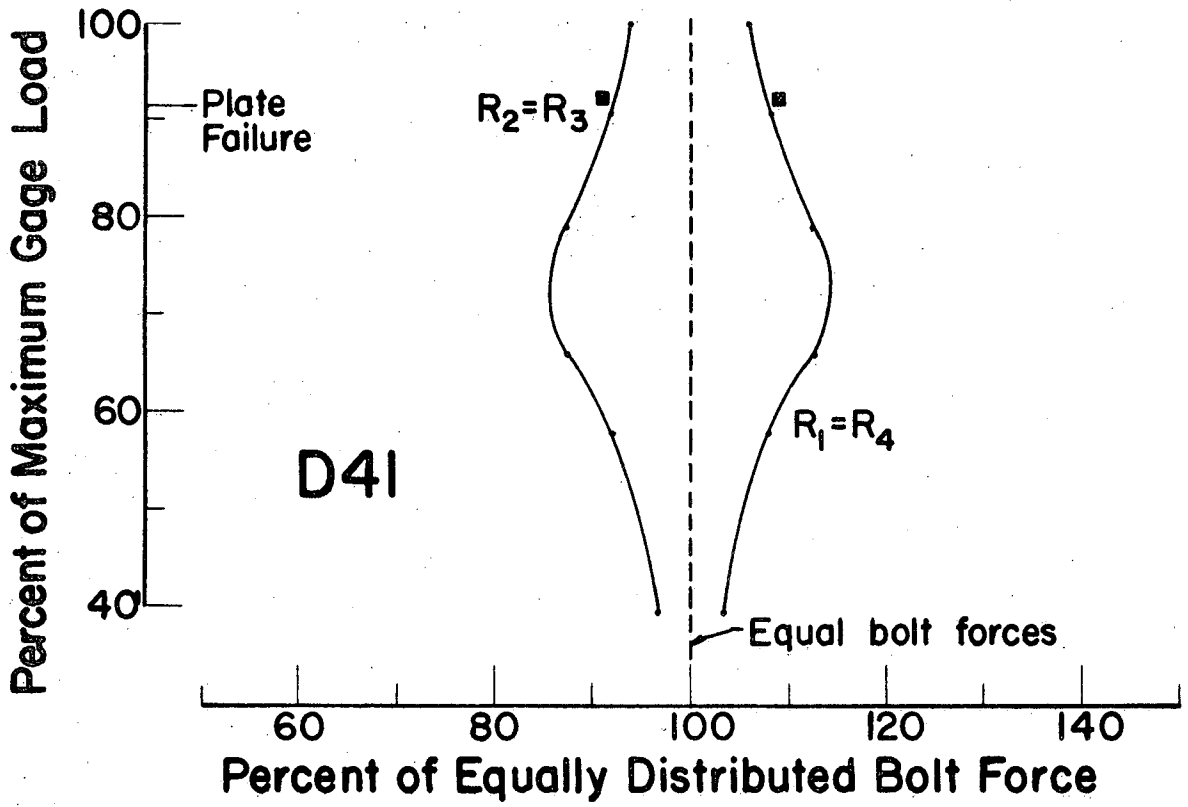


FIG. 4.19 JOINTS D41 AND D31, BOLT FORCE DISTRIBUTION

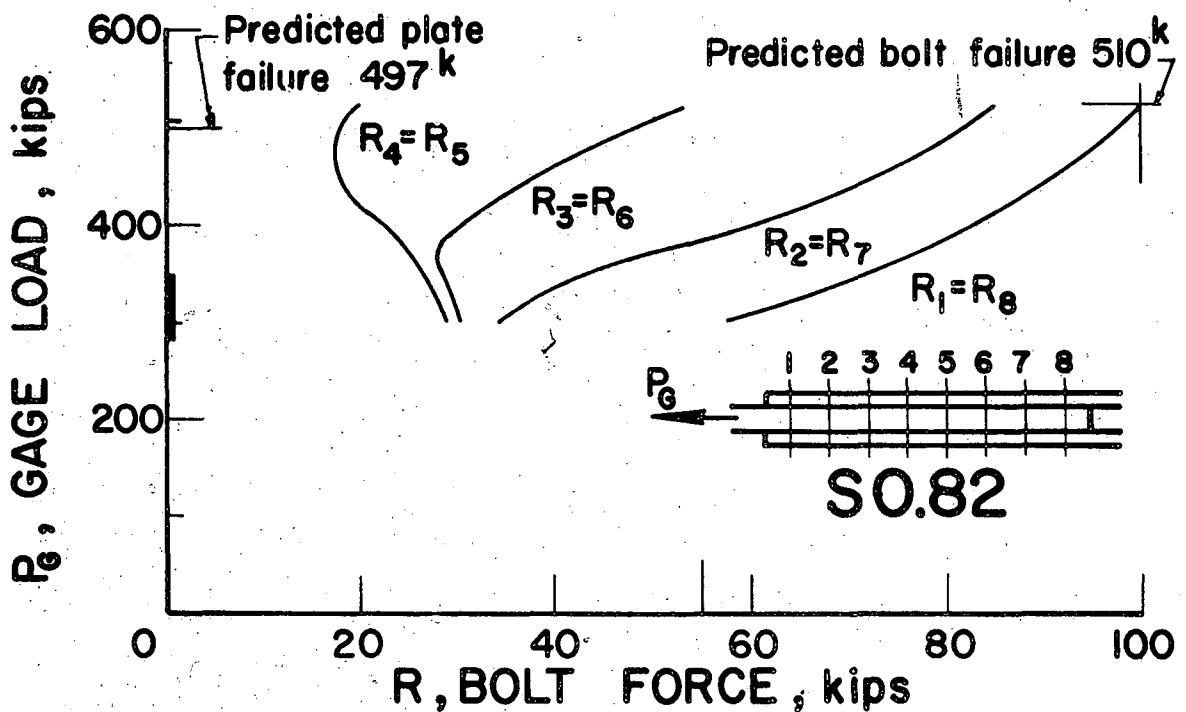
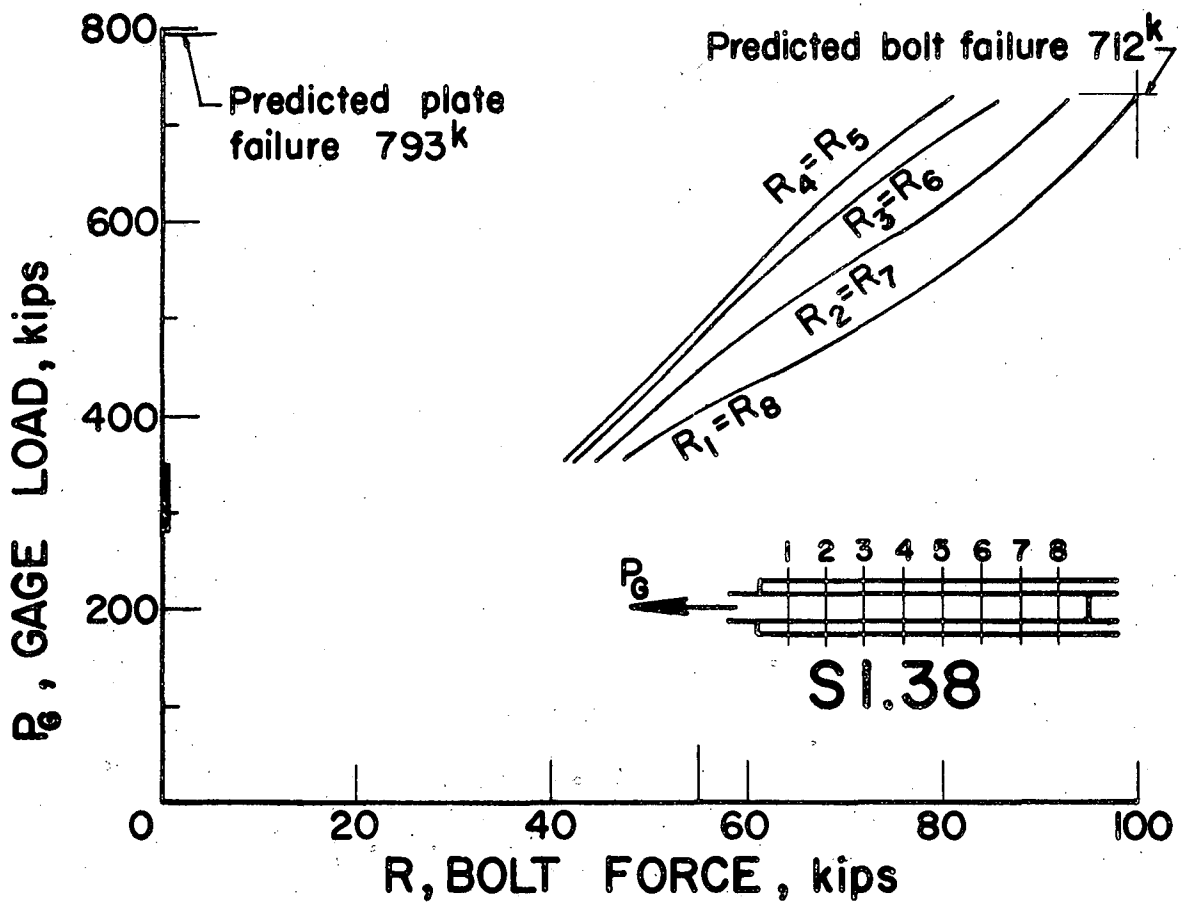


FIG. 5.1 JOINTS S1.38 AND S0.82, THEORETICAL BOLT FORCES

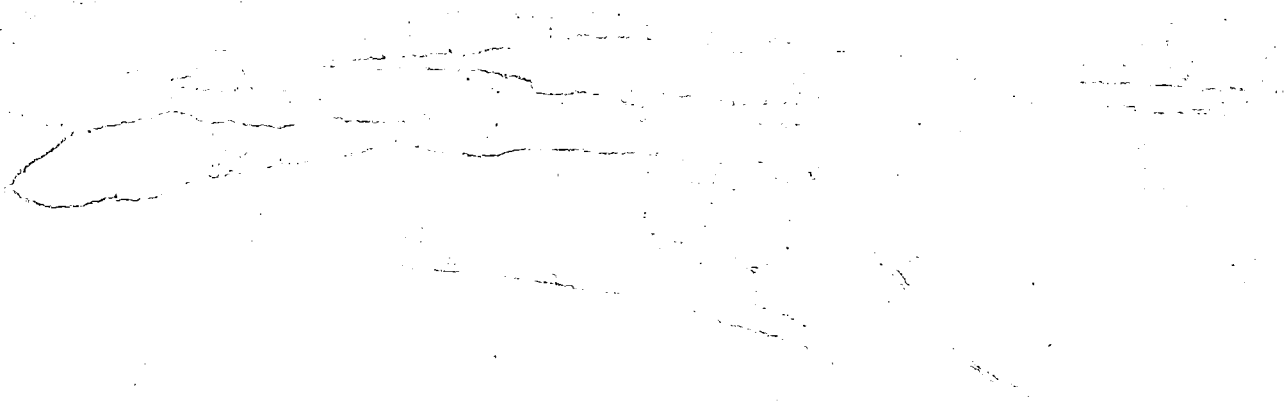
MIC 60-6518

52

Rumpf

(2/8)

Ret to OC



Page 175 - Fig. 5.1

To Mrs. Super in Dean Stout's office  
into L U Mail 4/7/61. Given to Charles  
at 10 AM

FBIZ ENGINEERING LABORATORY  
ADDRESS REPLY TO:

HYDRAULICS LAB' EXT. 338  
FBIZ E' G' OFFICE EXT. 338  
BETHLEHEM 1-2011  
PHONE

BETHLEHEM, PA  
DEPARTMENT OF CIVIL ENGINEERING AND MECHANICS  
LEHIGH UNIVERSITY

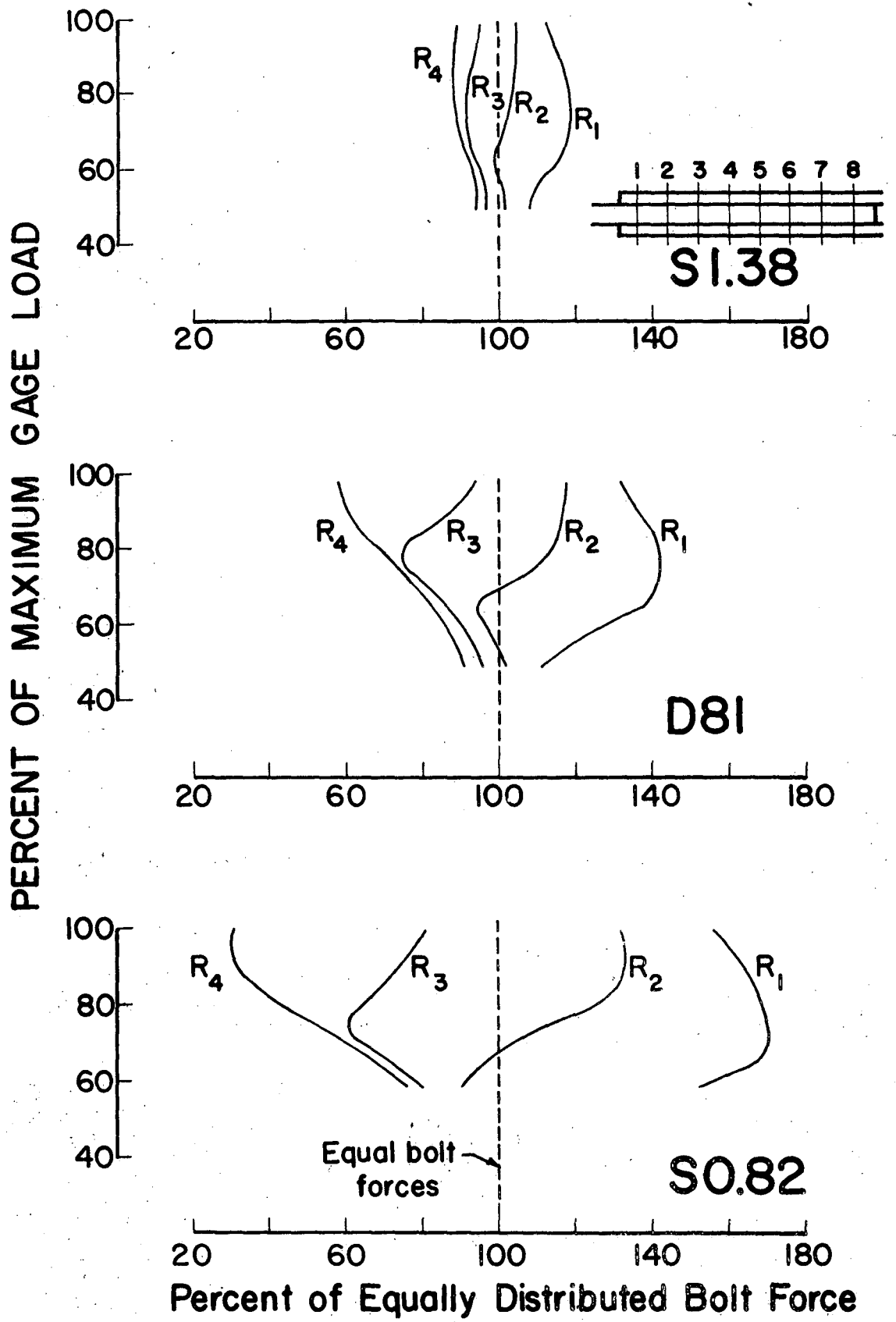


FIG. 5.2 EFFECT OF T/S RATIO ON BOLT FORCE DISTRIBUTION

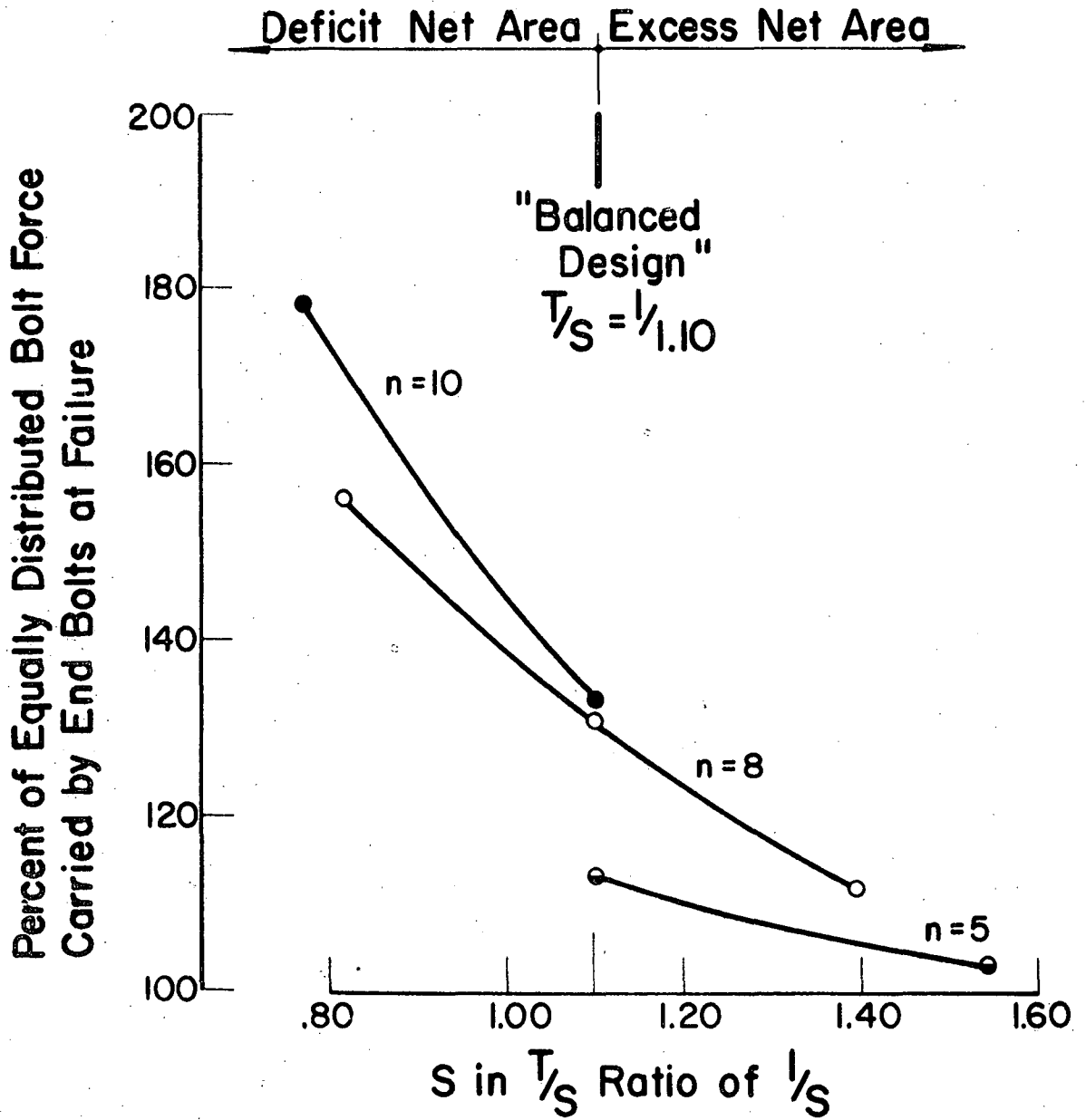


FIG. 5.3 EFFECT OF TENSION SHEAR RATIO ON LOAD CARRIED BY END BOLTS

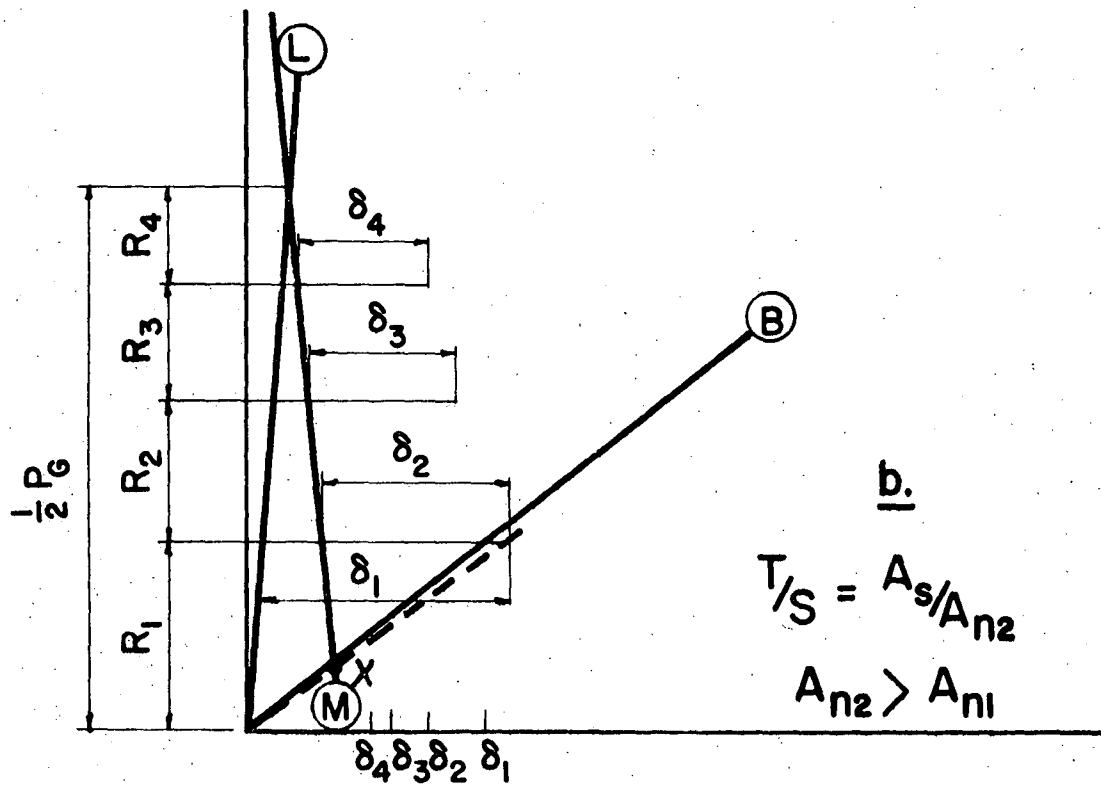
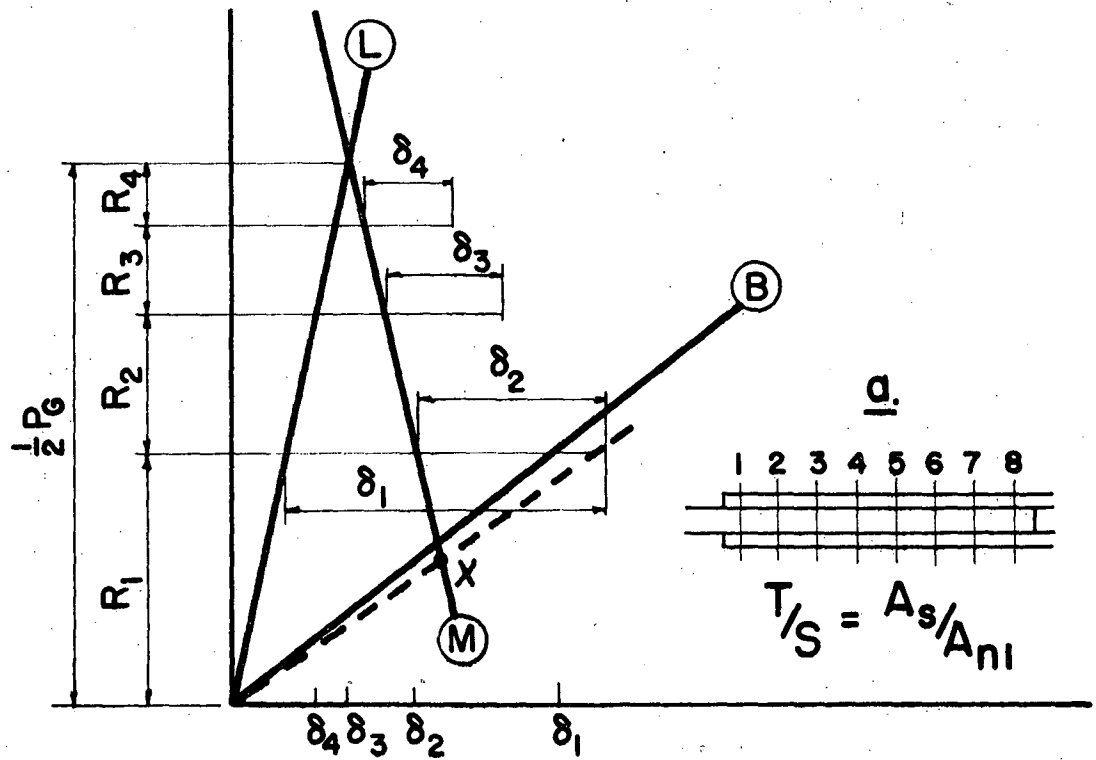


FIG. 5.4 EFFECT OF T/S RATIO IN ELASTIC RANGE



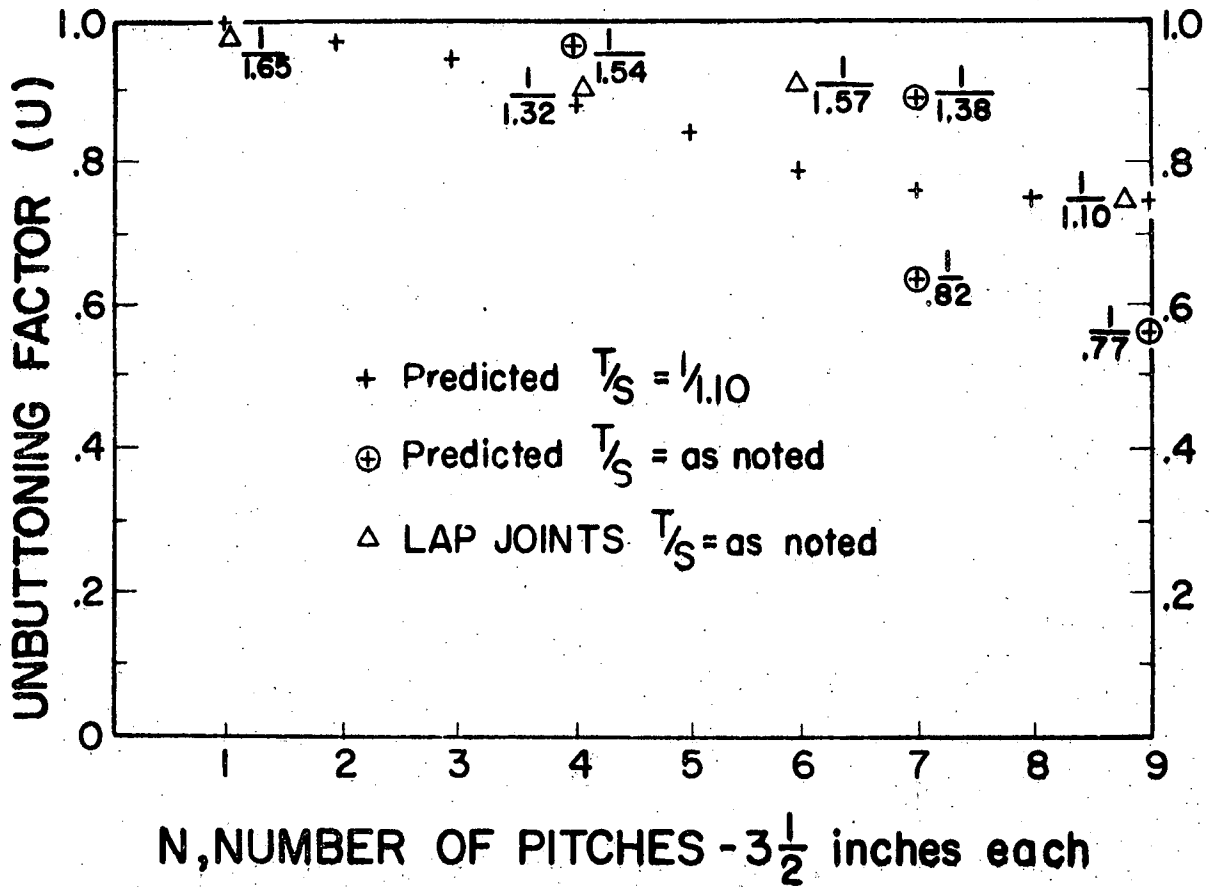


FIG. 5.5 UNBUTTONING FACTOR

## 9. REFERENCES

1. STEEL FASTENER COSTS COMPARED, Engineering News-Record, September 18, 1958
2. Foreman, R.T. and Rumpf, J.L.  
STATIC TENSION TESTS OF COMPACT BOLTED JOINTS, Proceedings of ASCE, Vol. 86, No. ST6, p. 73, June 1960
3. SPECIFICATIONS FOR STRUCTURAL JOINTS USING ASTM A325 BOLTS, Research Council on Riveted and Bolted Structural Joints of the Engineering Foundation, March 1960
4. SPECIFICATIONS FOR QUENCHED AND TEMPERED ALLOY STEEL BOLTS AND STUDS WITH SUITABLE NUTS AND PLAIN HARDENED WASHERS, A325-58T, American Society for Testing Materials
5. SPECIFICATIONS FOR STRUCTURAL RIVET STEEL, A141-58, American Society for Testing Materials
6. Schenker, L., Salmon, C.G., and Johnston, B.G.  
STRUCTURAL STEEL CONNECTIONS, AFSWP Report No. 352, University of Michigan, June 1954
7. Bendigo, R.A. and Rumpf J.L.  
STATIC TENSION TESTS OF LONG BOLTED JOINTS, Fritz Laboratory Report No. 271.8, Lehigh University, February 1960
8. Troelsch, H.W.  
DISTRIBUTION OF SHEAR IN WELDED CONNECTIONS, Transactions of ASCE, Vol. 99, pp. 409-436, 1934

9. Batho, C.  
RIVETED AND BOLTED CONNECTIONS, First Report  
of the Steel Structures Research Committee,  
H.M. Stationary Office, 1931
10. Steinhardt, O. and Möhler, K.  
VERSUCHE ZUR ANWENDUNG VORGESpanNTER SCHRAUBEN  
IM STAHLBAU, II. TEIL, Stahlbau-Verlags-GmbH.,  
Cologne, 1959
11. Rumpf, J.L.  
SHEAR RESISTANCE OF HIGH STRENGTH BOLTS, Fritz  
Laboratory Report No. 271.3, Lehigh University,  
December 1958
12. Bendigo, R.A.  
STATIC TENSION TESTS OF LONG BOLTED JOINTS,  
M.S. Thesis, Lehigh University, 1960
13. Arnovlevic, I.  
INANSPRUCHNAHME DER ANSCHLUSSNIETEN ELASTISCHER  
STÄBE, Zeitschrift für Architekten und  
Ingenieure, Vol. 14, Heft 2, p. 89, 1909
14. Batho, C.  
THE PARTITION OF LOAD IN RIVETED JOINTS, Journal  
of Franklin Institute, Vol. 182, p. 553, 1916
15. Findeisen, Cl.  
VERSUCHE ÜBER DIE BEANSPRUCHUNGEN IN DEN LASCHEN  
EINES GESTOSSENEN FLACHEISENS BEI VERWENDUNG  
ZYLINDRISCHER BOLZEN, Forschungsarbeiten des  
Vereines Deutscher Ingenieure, Heft 229, 1920
16. Bleich, F.  
THEORIE UND BERECHNUNG DER EISERNEN BRÜCKEN,  
Julius Springer, Berlin, 1924
17. Stüssi, F.  
ENTWURF UND BERECHNUNG VON STAHLBAUTEN,  
Julius Springer, Berlin, 1958

18. Hrennikoff, A.  
THE WORK OF RIVETS IN RIVETED JOINTS, Transactions of ASCE, Vol. 99, pp. 437-489, 1934
19. Vogt, F.  
LOAD DISTRIBUTION IN BOLTED OR RIVETED JOINTS IN LIGHT-ALLOY STRUCTURES, U.S. NACA Tech. Memo. No. 1135, 1947  
(Reprint of Royal Aircraft Establishment Rep. No. S.M.E. 3300, October 1944)
20. DeJonge, A.E.R.  
RIVETED JOINTS: A CRITICAL REVIEW OF THE LITERATURE COVERING THEIR DEVELOPMENT, ASME, New York, 1945
21. Francis, A.J.  
THE BEHAVIOR OF ALUMINIUM ALLOY RIVETED JOINTS, The Aluminium Development Association, Research Report No. 15, London, 1953
22. Vaserhelyi, D.D., Beano, S.Y., Madison, R.B., Lu, Z.A., and Vasishth, U.C.  
EFFECTS OF FABRICATION TECHNIQUES ON BOLTED JOINTS, Proceedings of ASCE, Vol. 85, No. ST3, p. 71, March 1959
23. Drew, F.P.  
TIGHTENING HIGH STRENGTH BOLTS, Proceedings of ASCE, Vol. 81, August 1955
24. Munse, W.H., Wright, D.T., and Newmark, N.M.  
LABORATORY TESTS OF HIGH TENSILE BOLTED STRUCTURAL JOINTS, Proceedings of ASCE, Vol. 80, Sep. 441, May 1954
25. Carter, J.W., McCalley, J.C., and Wyly, L.T.  
COMPARATIVE TEST OF A STRUCTURAL JOINT CONNECTED WITH HIGH STRENGTH BOLTS AND A STRUCTURAL JOINT CONNECTED WITH RIVETS AND HIGH STRENGTH BOLTS, AREA Bulletin 517, September-October 1954

26. Dörnen, K.  
UNTERSUCHUNG DER SCHUBSTEIFIGKEIT VON VERBINDUNGEN MIT VORGESPANNTEN (HOCHFESTEN) SCHRAUBEN IM STAHLBAU UND DIE DARAUSSICH ERGEBENDEN KONSTRUKTIVEN MASSNAHMEN, Dissertation T.H. Karlsruhe, 1955
27. Hansen, R.M. and Rumpf, J.L.  
SHEAR STRENGTH OF A325 BOLTS, Fritz Laboratory Report No. 271.10, Lehigh University, (unpublished)
28. Möhler, K.  
VERSUCHE MIT HV-VERBINDUNGEN, Veröffentlichungen des Deutschen Stahlbau-Verbandes, Stahlbau-Verlags-GmbH., Cologne, 1958
29. SPECIFICATIONS FOR STEEL FOR BRIDGES AND BUILDINGS, A7-58, American Society for Testing Materials
30. Ball, E.F. and Higgins, J.J.  
INSTALLATION AND TIGHTENING OF HIGH STRENGTH BOLTS, Proceedings of ASCE, Vol. 85, No. ST3, p. 117, March 1959
31. Wilson, W.M.  
Discussion of: Davis, R.E., Woodruff, G.B., and Davis, H.E.  
TENSION TESTS ON LARGE RIVETED JOINTS, Transactions of ASCE, Vol. 105, pp. 1264-1275, 1940
32. Schutz, F.W.  
EFFECTIVE NET SECTION OF RIVETED JOINTS, SRS #30, University of Illinois, September 1952
33. Marcin, S.T.  
LOAD DISTRIBUTION IN BOLTED JOINTS, Fritz Laboratory Report No. 271.13, Lehigh University, (unpublished)
34. Bendigo, R.A. and Rumpf, J.L.  
STATIC TENSION TESTS OF BOLTED LAP JOINTS, Fritz Laboratory Report No. 271.9, Lehigh University, (unpublished)

## V I T A

The author was born as the oldest child of Harry and Emma Rumpf on February 21, 1921.

He was awarded the degree of Bachelor of Science in Civil Engineering by Drexel Institute of Technology in 1943 and the degree of Master of Science in Civil Engineering by the University of Pennsylvania in 1954.

During World War II he served for a time as an instructor at The Engineer School, Ft. Belvoir, Virginia. For this duty he was awarded the Army Commendation Ribbon. Later he served as company commander in engineer combat and construction battalions rising to the rank of captain.

Prior to the war the author had several years of detailing experience with Belmont Iron Works, steel fabricators, and upon release from military service in 1946, he returned to that company as a structural engineer.

In 1947 he joined the faculty of Drexel Institute of Technology as Instructor in Civil Engineering where he

remained until 1956. During that time he specialized in the field of structural design. He advanced to the rank of Associate Professor.

In 1956 he became Instructor in Civil Engineering at Lehigh University and began work on his doctoral program. For the year 1957-58 he was a National Science Foundation Science Faculty Fellow, and he continued his studies at Lehigh on a full-time basis. For the last two years he has been Research Instructor and has acted as supervisor for the "Large Bolted Joints" project.

The author is a Registered Structural Engineer and prior to joining the faculty at Lehigh University he engaged in professional practice in addition to his teaching duties. Included in this work were; rating of three major Schuylkill River bridges, inspection of railroad bridges for the Philadelphia Suburban Transportation Company, design of industrial buildings, insurance investigations and expert witness duty.